

RECEIVED: September 1, 2015

REVISED: December 15, 2015

ACCEPTED: January 13, 2016

PUBLISHED: January 28, 2016

Search for invisible decays of a Higgs boson using vector-boson fusion in pp collisions at $\sqrt{s} = 8$ TeV with the ATLAS detector



The ATLAS collaboration

E-mail: atlas.publications@cern.ch

ABSTRACT: A search for a Higgs boson produced via vector-boson fusion and decaying into invisible particles is presented, using 20.3 fb^{-1} of proton-proton collision data at a centre-of-mass energy of 8 TeV recorded by the ATLAS detector at the LHC. For a Higgs boson with a mass of 125 GeV, assuming the Standard Model production cross section, an upper bound of 0.28 is set on the branching fraction of $H \rightarrow \text{invisible}$ at 95% confidence level, where the expected upper limit is 0.31. The results are interpreted in models of Higgs-portal dark matter where the branching fraction limit is converted into upper bounds on the dark-matter-nucleon scattering cross section as a function of the dark-matter particle mass, and compared to results from the direct dark-matter detection experiments.

KEYWORDS: Hadron-Hadron scattering, Higgs physics

ARXIV EPRINT: [1508.07869](https://arxiv.org/abs/1508.07869)

Contents

| | | |
|----------|---|-----------|
| 1 | Introduction | 1 |
| 2 | Detector | 3 |
| 3 | Simulation | 3 |
| 4 | Event selection | 5 |
| 5 | Background estimations | 7 |
| 5.1 | Data-driven estimation of the multijet background | 8 |
| 5.2 | Estimations of the $Z(\rightarrow \nu\nu)$ +jets and $W(\rightarrow \ell\nu)$ +jets backgrounds | 8 |
| 5.3 | Validation of data-driven estimations | 14 |
| 6 | Systematic uncertainties | 14 |
| 7 | Results | 15 |
| 8 | Model interpretation | 19 |
| 9 | Conclusions | 20 |
| | The ATLAS collaboration | 28 |

1 Introduction

Astrophysical observations provide strong evidence for dark matter (see ref. [1] and the references therein). Dark matter (DM) may be explained by the existence of weakly interacting massive particles (WIMP) [2, 3]. The observed Higgs boson with a mass of about 125 GeV [4, 5] might decay to dark matter or neutral long-lived massive particles [6–10], provided this decay is kinematically allowed. This is referred to as an invisible decay of the Higgs boson [11–18].

This paper presents a search for invisible decays of a Higgs boson produced via the vector-boson fusion (VBF) process. In the Standard Model (SM), the process $H \rightarrow ZZ \rightarrow 4\nu$ is an invisible decay of the Higgs boson, but the branching fraction (BF) is 0.1% [19, 20], which is below the sensitivity of the search presented in this paper. In addition to the VBF Higgs boson signal itself, there is a contribution to Higgs boson production from the gluon fusion plus 2-jets (ggF+2-jets) process, which is smaller than the VBF signal in the phase space of interest in this search. The ggF+2-jets contribution is treated as signal. The search is performed with a dataset corresponding to an integrated luminosity of 20.3 fb^{-1} of proton-proton collisions at $\sqrt{s} = 8 \text{ TeV}$, recorded by the ATLAS detector at the LHC [21].

The signature of this process is two jets with a large separation in pseudorapidity¹ and large missing transverse momentum² E_T^{miss} . The VBF process, in its most extreme topology (high dijet invariant mass for example), offers strong rejection against the QCD-initiated (W, Z) +jets (V +jets) backgrounds. The resulting selection has a significantly better signal-to-background ratio than selections targeting the ggF process.

The CMS Collaboration obtained an upper bound of 58% on the branching fraction of invisible Higgs boson decays using a combination of the VBF and ZH production modes [22]. Weaker limits were obtained using the $Z(\rightarrow \ell\ell)H + E_T^{\text{miss}}$ signature by both the ATLAS and CMS collaborations [22, 23], giving upper limits at 95% CL of 75% and 83% on the branching fraction of invisible Higgs boson decays, respectively. By combining the searches in the $Z(\rightarrow \ell\ell)H$ and $Z(\rightarrow b\bar{b})H$ channels, CMS obtained an upper limit of 81% [22]. Using the associated production with a vector boson, VH , where the vector-boson decays to jets and the Higgs boson to invisible particles, ATLAS set a 95% CL upper bound of 78% on the branching fraction of $H \rightarrow$ invisible [24]. Other searches for large E_T^{miss} in association with one or more jets were reported in refs. [25–28]. These searches are less sensitive to Higgs-mediated interactions than the search presented here, because they are primarily sensitive to the ggF process and have significantly larger backgrounds.

Assuming that the couplings of the Higgs boson to SM particles correspond to the SM values, global fits to measurements of cross sections times branching fractions of different channels allow the extraction of a limit on the Higgs boson’s branching fraction to invisible particles. The 95% CL upper limits on this branching fraction set by ATLAS and CMS are 23% and 21% respectively [29, 30]. There is an important complementarity between direct searches for invisible decays of Higgs bosons and indirect constraints on the sum of invisible and undetected decays. A simultaneous excess would confirm a signal, while a non-zero branching fraction of $H \rightarrow$ invisible in the global fit, but no excess in the searches for Higgs boson decays to invisible particles, would point toward other undetected decays or model assumptions as the source of the global fit result.

In the search presented in this paper, the events observed in data are consistent with the background estimations. An upper bound on the cross section times the branching fraction of the Higgs boson decays to invisible particles is computed using a maximum-likelihood fit to the data with the profile likelihood-ratio test statistic [31]. A constraint on the branching fraction alone is obtained assuming the SM VBF and ggF production cross sections, acceptances and efficiencies, for invisible decays of a Higgs boson with a mass $m_H = 125$ GeV.

In the context of models where dark matter couples to the SM particles primarily through the Higgs boson [32], limits on the branching fraction of invisible Higgs boson decays can be interpreted in WIMP-nucleon interaction models [33] and compared to experi-

¹ATLAS uses a right-handed coordinate system with its origin at the nominal interaction point (IP) in the centre of the detector and the z -axis along the beam direction. The x -axis points from the IP to the centre of the LHC ring, and the y -axis points upward. Cylindrical coordinates (r, ϕ) are used in the transverse plane, ϕ being the azimuthal angle around the beam direction. The pseudorapidity is defined as $\eta = -\ln \tan \theta/2$, where θ is the polar angle.

²The transverse momentum is the component of the momentum vector perpendicular to the beam axis.

ments which search for dark-matter particles via their direct interaction with the material of a detector [34–42]. The paper is organized as follows. The ATLAS detector is briefly described in section 2. The modelling of the signal and background is presented in section 3. The dataset, triggers, event reconstruction, and event selection are described in section 4. The background estimations are presented in section 5. In section 6, the systematic uncertainties are discussed. The results are shown in section 7, and model interpretations are given in section 8. Finally, concluding remarks are presented in section 9.

2 Detector

ATLAS is a multipurpose detector with a forward-backward symmetric cylindrical geometry, described in detail in ref. [21].

At small radii from the beamline, the inner detector, immersed in a 2 T magnetic field produced by a thin superconducting solenoid located directly inside the calorimeter, is made up of fine-granularity pixel and microstrip silicon detectors covering the range $|\eta| < 2.5$, and a gas-filled straw-tube transition-radiation tracker (TRT) in the range $|\eta| < 2$. The TRT complements the silicon tracker at larger radii and also provides electron identification based on transition radiation. The electromagnetic (EM) calorimeter is a lead/liquid-argon sampling calorimeter with an accordion geometry. The EM calorimeter is divided into a barrel section covering $|\eta| < 1.475$ and two end-cap sections covering $1.375 < |\eta| < 3.2$. For $|\eta| < 2.5$ it is divided into three layers in depth, which are finely segmented in η and ϕ . An additional thin presampler layer, covering $|\eta| < 1.8$, is used to correct for fluctuations in energy losses between the production vertex and the calorimeter. Hadronic calorimetry in the region $|\eta| < 1.7$ uses steel absorbers, and scintillator tiles as the active medium. Liquid-argon calorimetry with copper absorbers is used in the hadronic end-cap calorimeters, which cover the region $1.5 < |\eta| < 3.2$. A forward calorimeter using copper or tungsten absorbers with liquid argon completes the calorimeter coverage up to $|\eta| = 4.9$. The muon spectrometer (MS) measures the curvature of muon trajectories with $|\eta| < 2.7$, using three stations of precision drift tubes, with cathode strip chambers in the innermost layer for $|\eta| > 2.0$. The deflection is provided by a toroidal magnetic field with an integral of approximately 3 Tm and 6 Tm in the central and end-cap regions of the ATLAS detector, respectively. The MS is also instrumented with dedicated trigger chambers, namely resistive-plate chambers in the barrel and thin-gap chambers in the end-cap, covering $|\eta| < 2.4$.

3 Simulation

Simulated signal and background event samples are produced with Monte Carlo (MC) event generators, and passed through a GEANT4[43] simulation of the ATLAS detector [21, 44], or a fast simulation based on a parameterization of the response to the electromagnetic and hadronic showers in the ATLAS calorimeters [45] and a detailed simulation of other parts of the detector and the trigger system. The results based on the fast simulation are validated against fully simulated samples and the difference is found to be negligible. The simulated events are reconstructed with the same software as the data. Additional pp collisions in

the same and nearby bunch-crossings (pileup) are included by merging diffractive and non-diffractive pp collisions simulated with PYTHIA-8.165 [46]. The multiplicity distribution of these pileup collisions is re-weighted to agree with the distribution in the collision data.

Both the VBF and ggF signals are modelled using POWHEG-BOX [47–52] with CT10 parton distribution functions (PDFs) [53], and PYTHIA-8.165 simulating the parton shower, hadronization and underlying event.³ The VBF and ggF Higgs boson production cross sections and their uncertainties are taken from ref. [54]. The transverse momentum (p_T) distribution of the VBF-produced Higgs boson is re-weighted to reflect electroweak (EW) radiative corrections computed by HAWK-2.0 [55]. These EW corrections amount to 10–25% in the Higgs boson p_T range of 150–1000 GeV. The ggF contribution to the signal is re-weighted [56, 57] so that the p_T distribution of the Higgs boson in events with two or more associated jets matches that of the next-to-leading-order (NLO) ggF+2-jets calculation in POWHEG-BOX MiNLO [58], and the inclusive distributions in jets match that of the next-to-next-to-leading-order (NNLO) and next-to-next-to-leading-logarithm (NNLL) calculation in HRES-2.1 [59, 60]. The effects of finite quark masses are also included [52].

The $W(\rightarrow l\nu)$ +jets and $Z(\rightarrow \ell\ell)$ +jets processes are generated using SHERPA-1.4.5 [61] including leading-order (LO) matrix elements for up to five partons in the final state with CT10 PDFs and matching these matrix elements with the parton shower following the procedure in ref. [62]. The $W(\rightarrow l\nu)$ +jets and $Z(\rightarrow \ell\ell)$ +jets processes are divided into two components based on the number of electroweak vertices in the Feynman diagrams. Diagrams which have only two electroweak vertices contain jets that are produced via the strong interaction, and are labelled “QCD” Z +jets or W +jets. Diagrams which have four electroweak vertices contain jets that are produced via the electroweak interaction, and are labelled “EW” Z +jets or W +jets [63]. The MC predictions of the QCD components of W +jets and Z +jets are normalized to NNLO in FEWZ [64, 65], while the EW components are normalized to VBFNLO [66], including the jet p_T and dijet invariant mass requirements. The interference between the QCD and EW components of Z +jets and W +jets is evaluated with SHERPA-1.4.5 to be 7.5–18.0% of the size of the EW contribution depending on the signal regions. To account for this interference effect, the EW contribution is corrected with the estimated size of the interference term. Figure 1 shows Feynman diagrams for the signal and example vector-boson backgrounds. There are additional small backgrounds from $t\bar{t}$, single top, diboson and multijet production. The $t\bar{t}$ process is modelled using POWHEG-BOX, with PYTHIA-8.165 modelling the parton shower, hadronization and underlying event. Single-top production samples are generated with MC@NLO [67] for the s - and Wt -channel [68], while ACERMC-v3.8 [69] is used for single-top production in the t -channel. A top-quark mass of 172.5 GeV is used consistently. The AUET2C (AUET2B) [70] set of optimized parameters for the underlying event description is used for $t\bar{t}$ (single-top) processes, with CT10 (CTEQ6L1) [71] PDFs. Diboson samples WW , WZ and ZZ (with leptonic decays) are normalized at NLO and generated using HERWIG-6.5.20 [72] with CT10 PDFs, including the parton shower and hadronization, and

³The invisible decay of the Higgs boson is simulated by forcing the Higgs boson (with $m_H = 125$ GeV) to decay via $H \rightarrow ZZ^* \rightarrow 4\nu$.

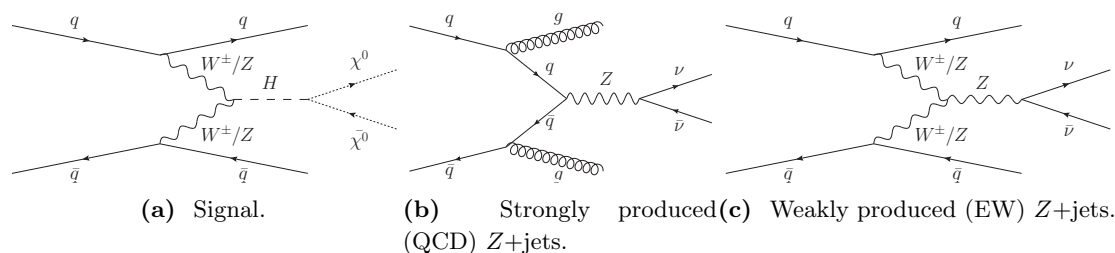


Figure 1. Example Feynman diagrams for the VBF $H(\rightarrow \text{invisible})$ signal and the vector-boson backgrounds.

Jimmy [73] to model the underlying event, whereas the WW , WZ , and $ZZ (\rightarrow \ell\ell qq, \nu\nu qq)$ processes are generated together with EW W +jets and Z +jets samples. Diboson WW , WZ and $ZZ (\rightarrow \ell\ell qq, \nu\nu qq)$ samples generated using SHERPA-1.4.5 with CT10 PDFs and normalized to NLO in QCD [74] are used as a cross-check. Multijet and γ +jet samples are generated using PYTHIA-8.165 with CT10 PDFs.

4 Event selection

The data used in this analysis were recorded with an E_T^{miss} trigger during periods when all ATLAS sub-detectors were operating under nominal conditions. The trigger consists of three levels of selections. The first two levels, L1 and L2, use as inputs coarse-spatial-granularity analog (L1) and digital (L2) sums of the measured energy. In the final level, calibrated clusters of cell energies in the calorimeter [75] are used. At each level, an increasingly stringent threshold is applied. The most stringent requirement is $E_T^{\text{miss}} \geq 80 \text{ GeV}$. Because of further corrections made in the offline reconstructed E_T^{miss} and the resolutions of the L1 and L2 calculations, this trigger is not fully efficient until the offline E_T^{miss} is greater than 150 GeV.

Jets are reconstructed from calibrated energy clusters [76, 77] using the anti- k_t algorithm [78] with radius parameter $R = 0.4$. Jets are corrected for pileup using the event-by-event jet-area subtraction method [79, 80] and calibrated to particle level by a multiplicative jet energy scale factor [76, 77]. The selected jets are required to have $p_T > 20 \text{ GeV}$ and $|\eta| < 4.5$. To discriminate against jets originating from minimum-bias interactions, selection criteria are applied to ensure that at least 50% of the jet's summed scalar track p_T , for jets within $|\eta| < 2.5$, is associated with tracks originating from the primary vertex, which is taken to be the vertex with the highest summed p_T^2 of associated tracks. Information about the tracks and clusters in the event is used to construct multivariate discriminators to veto events with b -jets and hadronic τ -jets. The requirements on these discriminators identify b -jets with 80% efficiency (estimated using $t\bar{t}$ events) [81–83], one-track jets from hadronic τ decays with 60% efficiency (measured with $Z \rightarrow \tau\tau$ events), and multiple-track jets from hadronic τ decays with 55% efficiency [84].

Electron candidates are reconstructed from clusters of energy deposits in the electromagnetic calorimeter matched to tracks in the inner detector [85]. Muon candidates are

| Requirement | SR1 | SR2a | SR2b |
|--------------------------------------|-----------------------------------|------------------------|-------------------------------|
| Leading Jet p_T | >75 GeV | >120 GeV | >120 GeV |
| Leading Jet Charge Fraction | N/A | $>10\%$ | $>10\%$ |
| Second Jet p_T | >50 GeV | >35 GeV | >35 GeV |
| m_{jj} | >1 TeV | $0.5 < m_{jj} < 1$ TeV | > 1 TeV |
| $\eta_{j1} \times \eta_{j2}$ | | <0 | |
| $ \Delta\eta_{jj} $ | >4.8 | >3 | $3 < \Delta\eta_{jj} < 4.8$ |
| $ \Delta\phi_{jj} $ | <2.5 | N/A | |
| Third Jet Veto p_T Threshold | 30 GeV | | |
| $ \Delta\phi_{j,E_T^{\text{miss}}} $ | >1.6 for j_1 , >1 otherwise | >0.5 | |
| E_T^{miss} | >150 GeV | >200 GeV | |

Table 1. Summary of the main kinematic requirements in the three signal regions.

reconstructed by requiring a match between a track in the inner detector and a track in the muon spectrometer [86].

The selection defines three orthogonal signal regions (SR), SR1, SR2a and SR2b. They are distinguished primarily by the selection requirements on the invariant mass m_{jj} of the two highest- p_T jets and their separation in pseudorapidity $\Delta\eta_{jj}$ as shown in table 1. The SR1 selection requires events to have two jets: one with $p_T > 75$ GeV and one with $p_T > 50$ GeV. The \vec{E}_T^{miss} is constructed as the negative vectorial sum of the transverse momenta of all calibrated objects (identified electrons, muons, photons, hadronic decays of τ -leptons, and jets) and an additional term for transverse energy in the calorimeter not included in any of these objects [87]. Events must have $E_T^{\text{miss}} > 150$ GeV in order to suppress the background from multijet events. To further suppress the multijet background, the two leading jets are required to have an azimuthal opening angle $|\Delta\phi_{jj}| < 2.5$ radians and an azimuthal opening angle with respect to the E_T^{miss} of $|\Delta\phi_{j,E_T^{\text{miss}}}| > 1.6$ radians for the leading jet and $|\Delta\phi_{j,E_T^{\text{miss}}}| > 1$ radian otherwise. In the VBF process, the forward jets tend to have large separations in pseudorapidity ($\Delta\eta_{jj}$), with correspondingly large dijet masses, and little hadronic activity between the two jets. To focus on the VBF production, the leading jets are required to be well-separated in pseudorapidity $|\Delta\eta_{jj}| > 4.8$, and have an invariant mass $m_{jj} > 1$ TeV. Events are rejected if any jet is identified as arising from the decay of a b -quark or a τ -lepton. The rejection of events with b -quarks suppresses top-quark backgrounds. Similarly, rejection of events with a τ -lepton suppresses the $W(\rightarrow \tau\nu)$ +jets background. Further, events are vetoed if they contain any reconstructed leptons passing the transverse momentum thresholds $p_T^e > 10$ GeV for electrons, $p_T^\mu > 5$ GeV for muons, or $p_T^\tau > 20$ GeV for τ -leptons. Finally, events with a third jet having $p_T > 30$ GeV and $|\eta| < 4.5$ are rejected. The SR2 selections are motivated by a search for new phenomena in final states with an energetic jet and large missing transverse momentum [25], and differ from those of SR1. First, the leading jet⁴ is required to have $p_T > 120$ GeV and $|\eta| < 2.5$.

⁴The ‘‘charge fraction’’ of this jet is defined as the ratio of the Σp_T of tracks associated to the jet to the

Additionally, the sub-leading jet is required to have $p_T > 35$ GeV, the $\Delta\phi_{jj}$ requirement is removed, the requirement on $\Delta\phi_{j,E_T^{\text{miss}}}$ is relaxed to $|\Delta\phi_{j,E_T^{\text{miss}}}| > 0.5$, and the E_T^{miss} requirement is tightened to $E_T^{\text{miss}} > 200$ GeV. A common threshold of $p_T = 7$ GeV is used to veto events with electrons and muons, and no τ -lepton veto is applied. Finally in SR2, the E_T^{miss} computation excludes the muon contribution and treats hadronic taus like jets (this allows the modelling of W +jets and Z +jets in the control regions and signal regions using the same E_T^{miss} variable as discussed in section 5). SR2 is further subdivided into SR2a with $500 < m_{jj} < 1000$ GeV, $\eta_{j1} \times \eta_{j2} < 0$, and $|\Delta\eta_{jj}| > 3$, and SR2b with $m_{jj} > 1000$ GeV, $\eta_{j1} \times \eta_{j2} < 0$ and $3 < |\Delta\eta_{jj}| < 4.8$.

5 Background estimations

In order to reduce the impact of theoretical and experimental uncertainties, the major backgrounds, $Z \rightarrow \nu\nu$ and $W \rightarrow \ell\nu$, are determined from measurements in a set of control samples consisting of $Z \rightarrow \ell\ell$ or $W \rightarrow \ell\nu$ events ($\ell = e/\mu$). In each of these control regions (CR), two additional jets are required, following the same requirements as the signal regions. The $Z \rightarrow \ell\ell$ control samples consist of events where the invariant mass of two same-flavour and opposite-sign leptons is consistent with the Z -boson mass, and so backgrounds in these control regions are small enough that they are taken from their MC predictions rather than from data-driven methods. In the $W \rightarrow \ell\nu$ control regions, the background from jets misidentified as leptons is more important, at least for the case of $W \rightarrow e\nu$. In SR1, the background from jets misidentified as leptons in the $W \rightarrow \ell\nu$ control regions is normalized using a fit that takes advantage of the distinctive shape of the transverse mass distribution

$$m_T = \sqrt{2p_T^\ell E_T^{\text{miss}} \left[1 - \cos(\Delta\phi_{\ell,E_T^{\text{miss}}}) \right]} \quad (5.1)$$

of the lepton and E_T^{miss} , and the charge asymmetry in W^+/W^- events. In SR2, the background from jets misidentified as leptons in the $W \rightarrow \ell\nu$ control regions is reduced by the requirements on m_T and E_T^{miss} as discussed in section 5.2.

In order to use the control regions rather than the MC predictions for setting the W +jets and Z +jets background normalizations, the MC predictions in each of the three signal regions and six corresponding $Z(\rightarrow ee/\mu\mu)$ +jets and $W(\rightarrow e\nu/\mu\nu)$ +jets control regions are scaled by free parameters k_i . There is one k_i for each signal region and the corresponding control regions. In SR1 for example, omitting factors that model systematic uncertainties, the expected number of events for $Z(\rightarrow \nu\nu)$ +jets in the signal region is $Z_{\text{SR1}} = k_1 Z_{\text{SR1}}^{\text{MC}}$, for $Z(\rightarrow \ell\ell)$ +jets in the $Z \rightarrow \ell\ell$ control region $Z_{\text{CR}} = k_1 Z_{\text{CR}}^{\text{MC}}$, and for $W(\rightarrow \ell\nu)$ +jets in the $W \rightarrow \ell\nu$ control region $W_{\text{CR}} = k_1 W_{\text{CR}}^{\text{MC}}$. The scale factors k_i are common for the Z +jets and W +jets background normalizations. The scale factors k_i are determined from the maximum Likelihood fit described in section 7. The $Z(\rightarrow \ell\ell)$ +jets and the $W(\rightarrow \ell\nu)$ +jets MC predictions thus affect the final estimates of $Z(\rightarrow \nu\nu)$ +jets

calibrated jet p_T ; this quantity must be at least 10% of the maximum fraction of the jet energy deposited in one calorimeter layer. The charged fraction requirement was shown to suppress fake jet backgrounds from beam-induced effects and cosmic-ray events [25].

and $W(\rightarrow \ell\nu)+\text{jets}$ in the signal region through an implicit dependence on the MC ratios $Z_{\text{SR}}/Z_{\text{CR}}$ and $Z_{\text{SR}}/W_{\text{CR}}$ for $Z(\rightarrow \nu\nu)+\text{jets}$, and $W_{\text{SR}}/W_{\text{CR}}$ for $W(\rightarrow \ell\nu)+\text{jets}$:

$$\begin{aligned} Z_{\text{SR}} &\sim (Z_{\text{SR}}/Z_{\text{CR}})^{\text{MC}} \times Z_{\text{CR}}^{\text{data}}, \\ Z_{\text{SR}} &\sim (Z_{\text{SR}}/W_{\text{CR}})^{\text{MC}} \times W_{\text{CR}}^{\text{data}}, \\ W_{\text{SR}} &\sim (W_{\text{SR}}/W_{\text{CR}})^{\text{MC}} \times W_{\text{CR}}^{\text{data}}. \end{aligned} \tag{5.2}$$

Unique estimates of the $Z(\rightarrow \nu\nu)+\text{jets}$ and $W(\rightarrow \ell\nu)+\text{jets}$ backgrounds in the signal region result from the simultaneous maximum likelihood fit to the control regions and signal region.

The multijet background is estimated from data-driven methods as presented in section 5.1. The data-driven normalizations for the $Z+\text{jets}$ and $W+\text{jets}$ backgrounds are described in section 5.2. The background estimations are validated in control regions with no signal contamination, and are in good agreement with observations in the validation control regions, as discussed in section 5.3. In SR1 and SR2, the smaller backgrounds of $t\bar{t}$, single top and dibosons are taken from their MC predictions.

Background contributions from the visible Higgs boson decay channels are suppressed by the signal region requirements described in section 4.

5.1 Data-driven estimation of the multijet background

Multijet events which have no prompt (from the primary interactions) neutrinos can pass the $E_{\text{T}}^{\text{miss}}$ selection due to instrumental effects such as the mis-measurement of the jet energy. Because of the very large rejection from the $E_{\text{T}}^{\text{miss}}$ requirement, it is not practical to simulate this background, so it is estimated using data-driven methods instead.

In the SR2 selections, the multijet background is estimated from data, using a jet smearing method as described in ref. [88], which relies on the assumption that the $E_{\text{T}}^{\text{miss}}$ of multijet events is dominated by fluctuations in the detector response to jets measured in the data. The estimated multijet background in SR2 is 24 ± 24 events (a 100% uncertainty is assigned to the estimate).

In SR1, the multijet background is estimated from data as follows. A control region is defined where the $\Delta\phi_{j,E_{\text{T}}^{\text{miss}}}$ requirement is inverted, so that the $E_{\text{T}}^{\text{miss}}$ vector is in the direction of a jet in the event. The resulting sample is dominated by multijet events. The signal region requirements on the leading and sub-leading jet p_{T} and on the $E_{\text{T}}^{\text{miss}}$ trigger are applied as described in section 4. The efficiency of each subsequent requirement is determined using this sample and assumed to apply to the signal region with the nominal $\Delta\phi_{j,E_{\text{T}}^{\text{miss}}}$ requirement. A systematic uncertainty is assessed based on the accuracy of this assumption in a control region with $|\Delta\eta_{jj}| < 3.8$ and in a control region with three jets. To account for the $\Delta\phi_{j,E_{\text{T}}^{\text{miss}}}$ requirement itself, the $\Delta\phi_{jj}$ requirement is inverted, requiring back-to-back jets in ϕ . This sample is also multijet-dominated. Combining all the efficiencies with the observed control region yield gives an estimate of 2 ± 2 events for the multijet background in SR1.

5.2 Estimations of the $Z(\rightarrow \nu\nu)+\text{jets}$ and $W(\rightarrow \ell\nu)+\text{jets}$ backgrounds

To estimate the $Z(\rightarrow \nu\nu)+\text{jets}$ background, both the $Z(\rightarrow ee/\mu\mu)+\text{jets}$ and $W(\rightarrow e\nu/\mu\nu)+\text{jets}$ control regions are employed. The $W+\text{jets}$ background is estimated using

$W(\rightarrow e\nu/\mu\nu)$ +jets control regions. In the $Z(\rightarrow ee)$ +jets control samples for SR1 and $W(\rightarrow \ell\nu)$ +jets control samples for SR1 or SR2, electrons and muons are required to be isolated. Electron isolation is not required in the SR2 $Z(\rightarrow ee)$ +jets control sample. For electrons, the normalized calorimeter isolation transverse energy, i.e. the ratio of the isolation transverse energy to lepton p_T , is required to be less than 0.28 (0.05) for SR1 (SR2), and the normalized track isolation is required to be less than 0.1 (0.05) within a cone $\Delta R = \sqrt{(\Delta\eta)^2 + (\Delta\phi)^2} = 0.3$ for SR1 (SR2). In the SR1 selections, muons must have a normalized calorimeter isolation less than 0.3 (or < 0.18 if $p_T < 25$ GeV) and a normalized track isolation less than 0.12 within $\Delta R = 0.3$, whereas in the SR2 selections, the scalar sum of the transverse momentum of tracks in a cone with radius 0.2 around the muon candidate is required to be less than 1.8 GeV. Electrons and muons are also required to point back to the primary vertex. The transverse impact parameter significance must be less than 3σ for both the electrons and muons, while the longitudinal impact parameter must be $< 0.4(1.0)$ mm for electrons (muons).

The $Z(\rightarrow ee/\mu\mu)$ +jets control regions are defined by selecting events containing two same-flavour, oppositely charged leptons with $p_T > 20$ GeV and $|m_{\ell\ell} - m_Z| < 25$ GeV, where $m_{\ell\ell}$ and m_Z are the dilepton invariant mass and the Z -boson mass, respectively. In the control sample corresponding to the SR1 selection, the leading lepton is required to have $p_T > 30$ GeV. Triggers requiring a single electron or muon with $p_T > 24$ GeV are used to select the control samples in SR1; in SR2, either a single-electron or E_T^{miss} trigger is used. The inefficiency of the triggers with respect to the offline requirements is negligible. In order to emulate the effect of the offline missing transverse momentum selection used in the signal region, the E_T^{miss} quantity is corrected by vectorially adding the electron (SR1 and SR2) and muon transverse momenta (SR1 only). All the $Z(\rightarrow ee/\mu\mu)$ +jets events are then required to pass the other signal region selections. Backgrounds from processes other than $Z(\rightarrow ee/\mu\mu)$ +jets are small in these control regions; the contributions from non- Z backgrounds are estimated from MC simulation. For $Z \rightarrow ee$ ($Z \rightarrow \mu\mu$), the non- Z background is at a level of 1.6% (0.9%) of the sample. There is 50% uncertainty (mainly due to the limited numbers of MC events) on the non- Z background contamination in the Z control regions. The observed yield in the SR1 Z control region, shown in table 2, is larger than the expected yield by 16% but is compatible within the combined statistical uncertainties of MC simulation and data. In the SR2 control regions, the observed and expected yields differ by 10% as shown in table 3 but are compatible within the total statistical and systematic uncertainties (see section 6). The emulated E_T^{miss} distributions for the Z control regions are shown in figures 2 and 3 for SR1 and SR2 respectively. Because the muon momentum is excluded from the E_T^{miss} definition in SR2, the “emulated” label is omitted from figure 3b.

The $W(\rightarrow e\nu/\mu\nu)$ +jets control regions are similarly defined by selecting events containing one lepton with transverse momentum $p_T > 30$ GeV (25 GeV) in the case of SR1 (SR2), and no additional leptons with $p_T > 20$ GeV. The E_T^{miss} is emulated in the same way as for the $Z \rightarrow ee/\mu\mu$ control region and events are required to pass the signal region selections on jets and E_T^{miss} . In SR1, the contributions of the three lepton flavours to the total $W \rightarrow \ell\nu$ background after all the requirements are 20% for $W \rightarrow e\nu$, 20% for $W \rightarrow \mu\nu$, and 60% for $W \rightarrow \tau\nu$. The equal contributions from $W \rightarrow e\nu$ and $W \rightarrow \mu\nu$

| Background | SR1 Z Control Regions | |
|------------------------------|---------------------------------|-------------------------------------|
| | $Z(\rightarrow ee)+\text{jets}$ | $Z(\rightarrow \mu\mu)+\text{jets}$ |
| QCD $Z \rightarrow \ell\ell$ | 10.4 ± 1.5 | 14.0 ± 1.5 |
| EW $Z \rightarrow \ell\ell$ | 7.4 ± 0.8 | 8.2 ± 0.8 |
| Other Backgrounds | 0.3 ± 0.2 | 0.2 ± 0.1 |
| Total | 18.1 ± 1.7 | 22.4 ± 1.7 |
| Data | 22 | 25 |

Table 2. Expected and observed yields for the SR1 $Z(\rightarrow ee/\mu\mu)+\text{jets}$ control sample in 20.3 fb^{-1} of 2012 data. Expected contributions are evaluated using MC simulation, and the uncertainties are statistical only.

| SR2 Z Control Regions | SR2a | | SR2b | |
|------------------------------|---------------------------------|-------------------------------------|---------------------------------|-------------------------------------|
| | $Z(\rightarrow ee)+\text{jets}$ | $Z(\rightarrow \mu\mu)+\text{jets}$ | $Z(\rightarrow ee)+\text{jets}$ | $Z(\rightarrow \mu\mu)+\text{jets}$ |
| QCD $Z \rightarrow \ell\ell$ | 116 ± 3 | 121 ± 4 | 26 ± 2 | 28 ± 2 |
| EW $Z \rightarrow \ell\ell$ | 17 ± 1 | 17 ± 1 | 16 ± 1 | 16 ± 2 |
| Other backgrounds | 8 ± 1 | 10 ± 2 | 2 ± 1 | 3 ± 1 |
| Total | 141 ± 3 | 148 ± 5 | 44 ± 3 | 47 ± 3 |
| Data | 159 | 139 | 33 | 38 |

Table 3. Expected and observed yields for the SR2 $Z(\rightarrow ee/\mu\mu)+\text{jets}$ control sample in 20.3 fb^{-1} of 2012 data. Expected contributions are evaluated using MC simulation, and the uncertainties are statistical only.

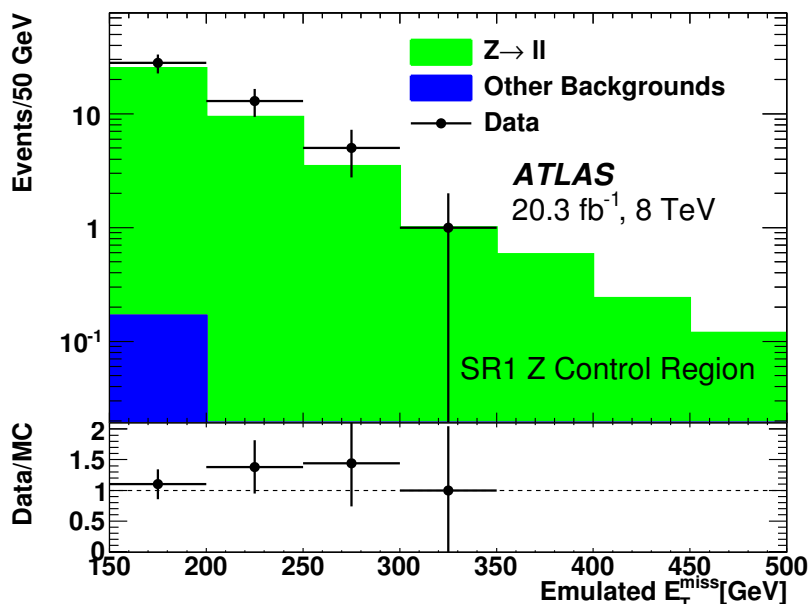


Figure 2. Data and MC distributions of the emulated E_T^{miss} (as described in the text) in the SR1 $Z(\rightarrow ee/\mu\mu)+\text{jets}$ control region.

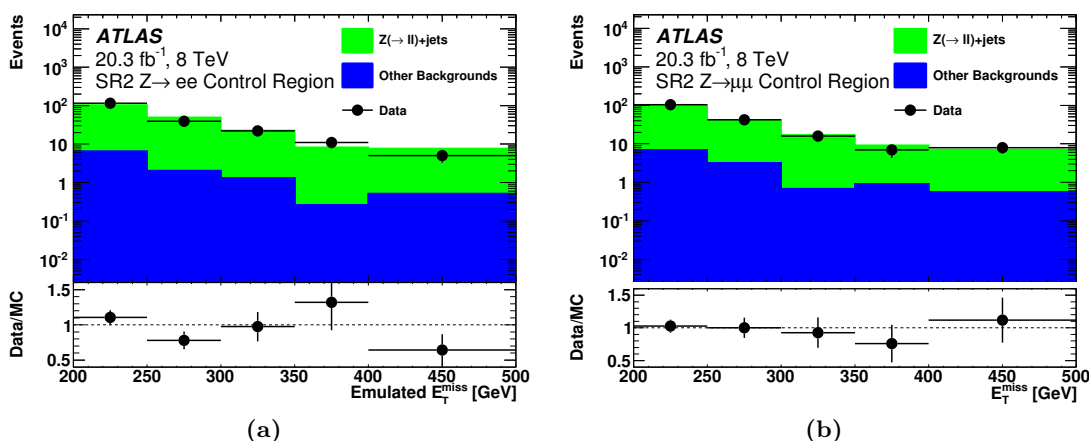


Figure 3. Data and MC distributions of the E_T^{miss} (as described in the text) in the SR2 Z +jets control regions (a) $Z(\rightarrow ee)$ +jets and (b) $Z(\rightarrow \mu\mu)$ +jets.

suggest that these are events where the lepton is below its p_T threshold or sufficiently far forward to escape the jet veto, and not events where the lepton is misidentified as a tag jet (since muons deposit little energy in the calorimeter and would therefore not be identified as a jet). This expectation is checked explicitly for the case of $W \rightarrow \tau\nu$, by using MC truth information about the direction of the τ -lepton to find the ΔR between the τ -lepton and the nearest reconstructed tag jet. The component with $\Delta R_{j,\tau} < 0.4$ is completely negligible after the signal region requirements, indicating that the lepton tends to be recoiling against the tag jets rather than being aligned with them. For SR1, four W control regions are considered using different charge samples for $W^+/W^- \rightarrow e\nu/\mu\nu$ since $W(\rightarrow \ell\nu)$ +jets is not charge symmetric as shown in table 4, whereas in SR2, only two control regions $W(\rightarrow e\nu/\mu\nu)$ +jets are used as shown in table 5.

In the $W(\rightarrow e\nu/\mu\nu)$ +jets control regions corresponding to the SR1 selection, a fit to the transverse mass defined in eq. (5.1) is used to estimate the multijet background. In order to obtain an explicit measurement and uncertainty for the background from multijets, no requirements are made on E_T^{miss} and m_T . Because the multijet background does not have a prompt neutrino, the E_T^{miss} tends to be lower and to point in the direction of the jet that was misidentified as a lepton. As a result, the multijet background tends to have significantly lower m_T than the W +jets contribution. Control samples modelling the jets misidentified as leptons in multijet events are constructed by selecting events that pass the W +jets control region selection, except for certain lepton identification criteria: for electrons, some of the EM calorimeter shower shape requirements are loosened and fully identified electrons are removed, while for muons, the transverse impact parameter (d_0) requirement which suppresses muons originating from heavy-flavour jets is reversed. To obtain the normalization of the multijet background in the W +jets control region, templates of the m_T distribution for processes with prompt leptons are taken from MC simulation. Shape templates for the backgrounds from multijet events are constructed by summing the observed yields in control samples obtained by inverting the lepton identification and d_0

| Background | SR1 W Control Regions | | | |
|------------------------------|-------------------------|------------------------|--------------------------|--------------------------|
| | $W^+ \rightarrow e\nu$ | $W^- \rightarrow e\nu$ | $W^+ \rightarrow \mu\nu$ | $W^- \rightarrow \mu\nu$ |
| QCD $W \rightarrow \ell\nu$ | 92.3 ± 7.2 | 55.1 ± 5.3 | 85.5 ± 7.0 | 43.8 ± 4.6 |
| EW $W \rightarrow \ell\nu$ | 99.4 ± 4.0 | 52.5 ± 2.9 | 81.9 ± 3.7 | 39.1 ± 2.5 |
| QCD $Z \rightarrow \ell\ell$ | 3.4 ± 0.6 | 4.4 ± 0.9 | 6.4 ± 1.1 | 5.0 ± 0.9 |
| EW $Z \rightarrow \ell\ell$ | 2.5 ± 0.3 | 2.9 ± 0.3 | 2.7 ± 0.3 | 3.2 ± 0.3 |
| Multijet | 28.0 ± 6.8 | 28.0 ± 6.8 | 1.6 ± 2.6 | 1.6 ± 2.6 |
| Other backgrounds | 4.0 ± 0.7 | 1.8 ± 0.4 | 3.2 ± 0.7 | 1.0 ± 0.3 |
| Total | 230 ± 11 | 145 ± 9 | 181 ± 8 | 93.7 ± 5.9 |
| Data | 225 | 141 | 182 | 98 |

Table 4. Expected and observed yields for the SR1 $W \rightarrow \ell\nu$ control sample, after all requirements in 20.3 fb^{-1} of 2012 data. The multijet background is estimated using the data-driven method described in the text; all other contributions are evaluated using MC simulation. Only the statistical uncertainties are shown.

| SR2 W Control Regions | SR2a | | SR2b | |
|------------------------------|-----------------------------------|-------------------------------------|-----------------------------------|-------------------------------------|
| | $W(\rightarrow e\nu)+\text{jets}$ | $W(\rightarrow \mu\nu)+\text{jets}$ | $W(\rightarrow e\nu)+\text{jets}$ | $W(\rightarrow \mu\nu)+\text{jets}$ |
| QCD $W \rightarrow \ell\nu$ | 595 ± 12 | 906 ± 15 | 122 ± 5 | 201 ± 7 |
| EW $W \rightarrow \ell\nu$ | 149 ± 5 | 214 ± 6 | 121 ± 4 | 184 ± 5 |
| QCD $Z \rightarrow \ell\ell$ | 5.8 ± 0.9 | 23 ± 1.6 | 1.6 ± 0.4 | 4.5 ± 0.6 |
| EW $Z \rightarrow \ell\ell$ | 0.4 ± 0.1 | 0.5 ± 0.2 | 2.0 ± 0.4 | 2.7 ± 0.8 |
| Multijet | 13 ± 3 | 0 ± 0 | 3 ± 1 | 0 ± 0 |
| Other backgrounds | 44 ± 4 | 78 ± 7 | 13 ± 2 | 19 ± 3 |
| Total | 807 ± 14 | 1222 ± 18 | 263 ± 7 | 411 ± 9 |
| Data | 783 | 1209 | 224 | 295 |

Table 5. Expected and observed yields for the SR2 $W(\rightarrow e\nu/\mu\nu)+\text{jets}$ control sample in 20.3 fb^{-1} of 2012 data. Expected contributions are evaluated using MC simulation, and the uncertainties are statistical only. The discrepancy in the $W(\rightarrow \mu\nu)+\text{jets}$ SR2b control region is due to a mis-modelling of the $W p_T$. The agreement improves when the systematic uncertainties (discussed in section 6) are included.

requirements, and subtracting the expected contributions from $W+\text{jets}$ and $Z+\text{jets}$ events using MC. Since the misidentified-jet samples are expected to be charge-symmetric, the same shape template and normalization factor is used to model both charge categories of a given lepton flavour (e or μ). To determine the $W(\rightarrow \ell\nu)+\text{jets}$ background normalization, a fit to the transverse mass m_T of the lepton and E_T^{miss} is used. The $W(\rightarrow \ell\nu)+\text{jets}$ contribution, however, is not charge symmetric, so the different charge samples are kept separate in the simultaneous fit to four m_T distributions, one for each lepton flavour and charge combination shown in figure 4. There are three free normalizations in the fit: one

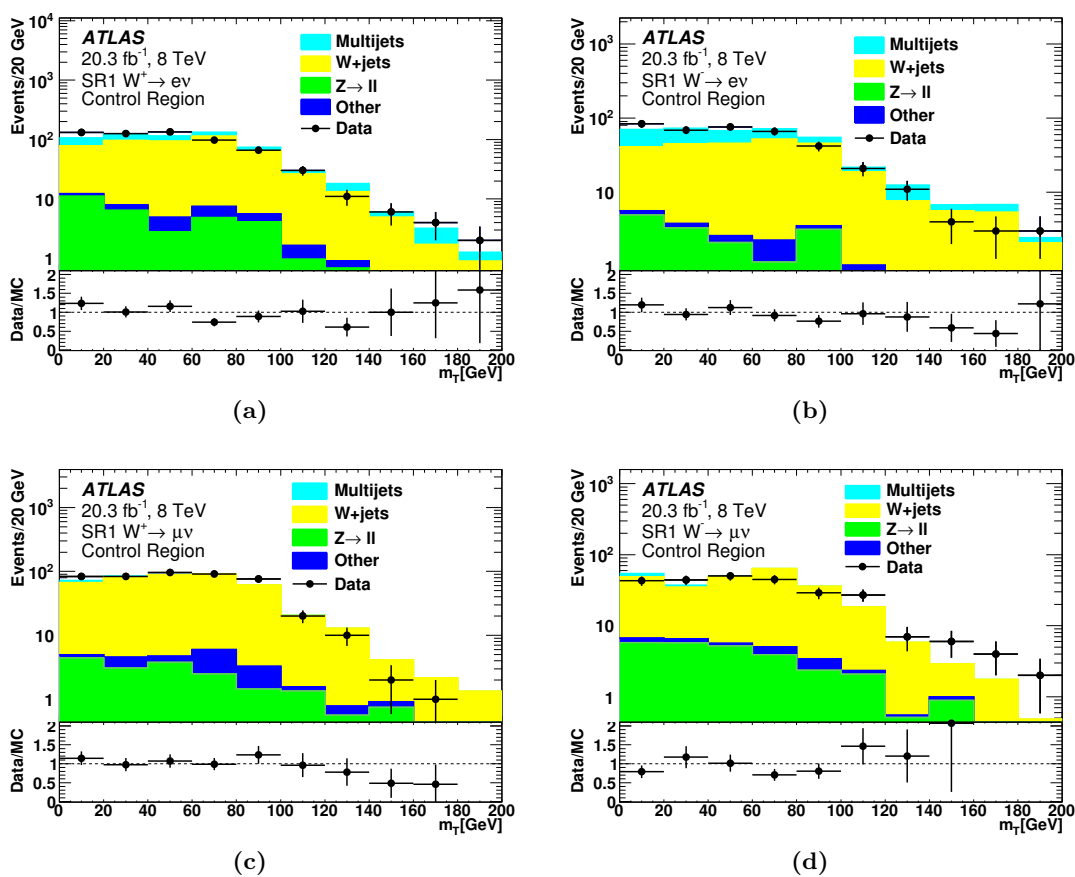


Figure 4. The transverse mass distributions used in the SR1 W +jets control regions after all requirements except for the $E_T^{\text{miss}} > 150$ GeV requirement: (a) $W^+ \rightarrow e^+\nu$, (b) $W^- \rightarrow e^-\nu$, (c) $W^+ \rightarrow \mu^+\nu$ and (d) $W^- \rightarrow \mu^-\nu$.

for events with a prompt lepton, one for events where a jet is misidentified as an electron, and one for events where a jet is misidentified as a muon. The normalization factor for the prompt leptons in the m_T fit is 0.95 ± 0.05 (stat).

In the $W \rightarrow e\nu$ control region corresponding to the SR2 selections, the background from multijet events is rejected by requiring that the E_T^{miss} (corrected by vectorially adding the electron transverse momentum) be larger than 25 GeV and that the transverse mass be in the range $40 < m_T < 100$ GeV. The selected electron is required to pass both the track and calorimeter isolation requirements. The tight requirements on electron isolation and E_T^{miss} greatly reduce the multijet background relative to the other backgrounds. The residual multijet background in the $W \rightarrow e\nu$ control region is at the level of 1% of the total control region background, with an uncertainty of 100%. For the $W \rightarrow \mu\nu$ control region corresponding to the SR2 selections, the selected muon is required to pass only the track isolation requirement and the transverse mass is required to be in the range $30 < m_T < 100$ GeV. An attempt is made to estimate the residual multijet background in the $W \rightarrow \mu\nu$ control region using a control sample with inverted muon isolation. The

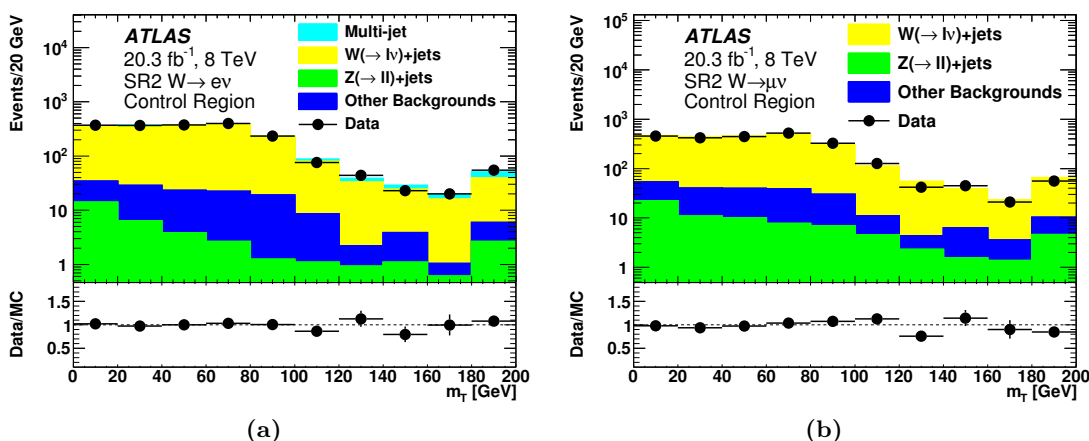


Figure 5. The transverse mass distributions in the SR2 W +jets control regions after all requirements: (a) $W \rightarrow e\nu$ and (b) $W \rightarrow \mu\nu$.

residual background from multijet events is negligible. Figure 5 shows the m_T distributions in the SR2 W +jets control regions.

5.3 Validation of data-driven estimations

To validate the background estimates for SR1, two signal-depleted neighbouring regions are defined by (1) reversing the veto against three-jet events and requiring that the third jet in the event has transverse momentum $p_T^{j3} > 40$ GeV, and (2) reversing both the jet veto with a $p_T^{j3} > 30$ GeV requirement and the jet rapidity gap with a $|\Delta\eta_{jj}| < 3.8$ requirement. Good agreement between expectation and observation is found in these validation regions, as shown in table 6.

6 Systematic uncertainties

The experimental uncertainties on the MC predictions for signals and backgrounds are dominated by uncertainties in the jet energy scale and resolution [76]. This includes effects such as the η dependence of the energy scale calibration and the dependence of the energy response on the jet flavour composition, where flavour refers to the gluon or light quark initiating the jet. Uncertainties related to the lepton identification in the control regions and lepton vetoes are negligible. Luminosity uncertainties [89] are applied to the signal and background yields that are obtained from MC simulation.

Theoretical uncertainties on the W +jets and Z +jets contributions to both the signal and control regions are assessed using SHERPA, and cross-checked with MCFM [74] and VBFNLO [66] for the EW and QCD processes respectively, and by a comparison between SHERPA and ALPGEN [90] for the latter process. In all cases, the uncertainties are determined by independently varying the factorization and renormalization scales by factors of 2 and 1/2, keeping their ratio within 0.5–2.0. The parton distribution function

| Process | 3-jet | 3-jet and $ \Delta\eta_{jj} < 3.8$ |
|--------------------------------------|-----------------|-------------------------------------|
| ggF signal | 6.2 ± 3.1 | - |
| VBF signal | 19.9 ± 1.4 | 4.7 ± 0.6 |
| $Z(\rightarrow \nu\nu)+\text{jets}$ | 97 ± 10 | 111 ± 10 |
| $W(\rightarrow \ell\nu)+\text{jets}$ | 78.5 ± 6.5 | 73 ± 10 |
| Multijet | 19.9 ± 21.8 | - |
| Other backgrounds | 2.2 ± 0.3 | 0.5 ± 0.1 |
| Total | 198 ± 25 | 185 ± 14 |
| Data | 212 | 195 |

Table 6. Expected and observed yields for the validation regions in 20.3fb^{-1} of data. 3-jet: reversal of the veto against three-jet events by requiring $p_T^{j3} > 40\text{ GeV}$; and 3-jet and $|\Delta\eta_{jj}| < 3.8$: requirements of both $|\Delta\eta_{jj}| < 3.8$ and $p_T^{j3} > 30\text{ GeV}$. Contributions from W +jets and Z +jets are normalized to data-driven estimates. The W +jets and Z +jets uncertainties include MC statistics from both the selected region and the corresponding control region, and the number of data events in the control regions. The other numbers are evaluated using MC simulation and their uncertainties indicate only statistical uncertainty.

uncertainties are evaluated with the CT10 error sets [53]. The uncertainty on the ggF yield due to the jet selection is evaluated using Stewart-Tackmann method [91]. Uncertainty in the p_T distribution of the Higgs boson in ggF is evaluated from scale variations in HRES following the re-weighting of the p_T distribution [59, 60] as mentioned in section 1. To assess the level of theoretical uncertainty on the jet veto, the variation in the predicted VBF cross section with respect to shifts in the renormalization and factorization scales as well as with respect to uncertainty in the parton-shower modelling is measured using POWHEG-BOX NLO generator matched to PYTHIA and to HERWIG. The effect of the parton shower on the QCD W +jets and Z +jets background estimations is obtained by comparing simulated samples with different parton shower models. As shown in table 7, where the main systematic uncertainties are summarized, using the MC predictions of $Z_{\text{SR}}/W_{\text{CR}}$ and $W_{\text{SR}}/W_{\text{CR}}$ ratios reduces the systematic uncertainties in the final Z +jets and W +jets background estimates. The $Z(\rightarrow \ell\ell)+\text{jets}/W(\rightarrow \ell\nu)+\text{jets}$ ratio is checked in data and MC, and no discrepancy larger than 10% is observed, consistent with the residual theory uncertainties on the $Z_{\text{SR}}/W_{\text{CR}}$ ratios shown in table 7.

7 Results

Figures 6 and 7 show the E_T^{miss} and the m_{jj} distributions after imposing the requirements of SR1 and SR2 respectively. There is good agreement between the data and the background expectations from the SM, and no statistically significant excess is observed in data. The limit on the branching fraction of $H \rightarrow \text{invisible}$ is computed using a maximum-likelihood fit to the yields in the signal regions and the $W(\rightarrow e\nu/\mu\nu)+\text{jets}$ and $Z(\rightarrow ee/\mu\mu)+\text{jets}$ control samples following the CL_S modified frequentist formalism [92] with

| Uncertainty | VBF | ggF | Z or W | $Z_{\text{SR}}/W_{\text{CR}}$ or $W_{\text{SR}}/W_{\text{CR}}$ |
|----------------------------|------------|------------|------------|--|
| Jet energy scale | 16 | 43 | 17–33 | 3–5 |
| | 9 | 12 | 0–11 | 1–4 |
| Jet energy resolution | Negligible | Negligible | Negligible | Negligible |
| | 3.1 | 3.2 | 0.2–7.6 | 0.5–5.8 |
| Luminosity | 2.8 | 2.8 | 2.8 | Irrelevant |
| QCD scale | 0.2 | 7.8 | 5–36 | 7.8–12 |
| | | | 7.5–21 | 1–2 |
| PDF | 2.3 | 7.5 | 3–5 | 1–2 |
| | 2.8 | | 0.1–2.6 | |
| Parton shower | 4.4 | 41 29 | 9–10 | 5 |
| Veto on third jet | | | Negligible | Negligible |
| Higgs boson p_{T} | Negligible | 9.7 | Irrelevant | Irrelevant |
| MC statistics | 2 | 46 | 2.3–6.4 | 3.3–6.6 |
| | 0.6 | 13 | 0.8–4.5 | |

Table 7. Detector and theory uncertainties (%) after all SR or CR selections. For each source of uncertainty, where relevant, the first and second rows correspond to the uncertainties in SR1 and SR2 respectively. The ranges of uncertainties in the Z or W column correspond to uncertainties in the Z +jets and W +jets MC yields in the SR or CR. The search uses the uncertainties in the ratios of SR to CR yields shown in the last column.

a profile likelihood-ratio test statistic [31]. Expected signal and background distributions in the signal and control regions are determined from MC predictions, with the exception of the multijet backgrounds, which use the data-driven methods described in section 5. Systematic uncertainties are parameterized as Gaussian constrained nuisance parameters. The nuisance parameter for each individual source of uncertainty is shared among the expected yields so that its correlated effect is taken into account. The relative weight of the $Z(\rightarrow ee/\mu\mu)$ +jets and $W(\rightarrow e\nu/\mu\nu)$ +jets in the control regions is determined by the maximization of the likelihood function.

One global likelihood function including all three signal regions and the six corresponding control regions is constructed with only the signal yields and correlated uncertainties coupling the search regions. The theoretical uncertainties are taken to be uncorrelated between the EW and QCD processes and uncorrelated with the scale uncertainty on the signal. The uncertainties which are treated as correlated between the regions are:

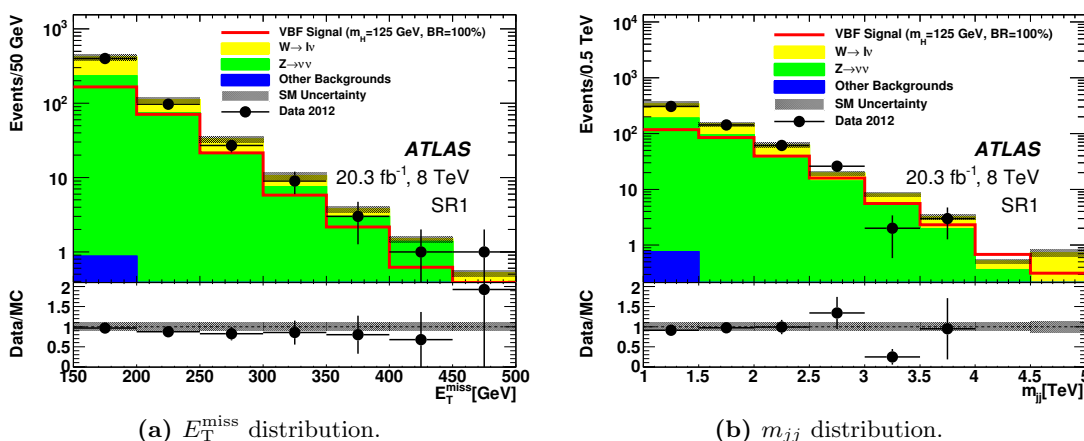


Figure 6. Data and MC distributions after all the requirements in SR1 for (a) E_T^{miss} and (b) the dijet invariant mass m_{jj} . The background histograms are normalized to the values in table 8. The VBF signal (red histogram) is normalized to the SM VBF Higgs boson production cross section with $\text{BF}(H \rightarrow \text{invisible}) = 100\%$.

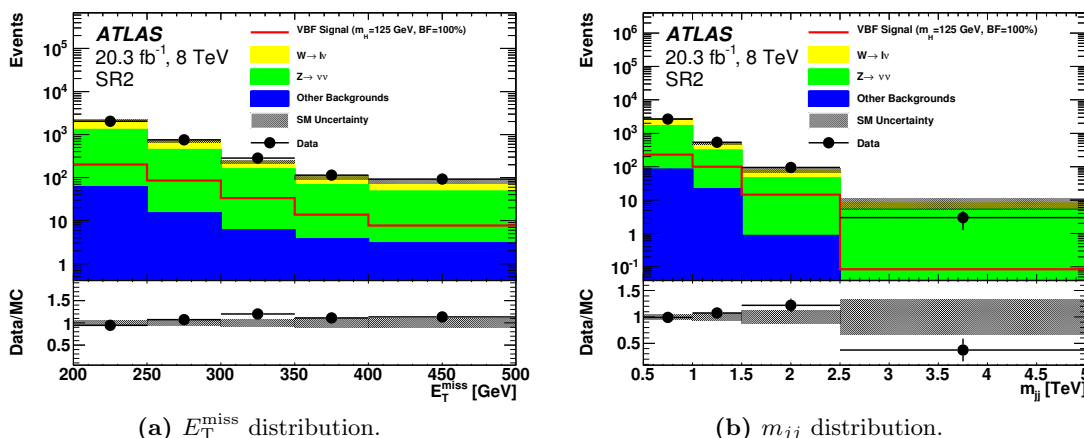


Figure 7. Data and MC distributions after all the requirements in SR2 for (a) E_T^{miss} and (b) the dijet invariant mass m_{jj} . The background histograms are normalized to the values in table 8. The VBF signal is normalized to the SM VBF Higgs boson production cross section with $\text{BF}(H \rightarrow \text{invisible}) = 100\%$.

- Uncertainty in the luminosity measurements. This impacts the predicted rates of the signals and the backgrounds that are estimated using MC simulation, namely ggF and VBF signals, and $t\bar{t}$, single top, and diboson backgrounds.
- Uncertainties in the absolute scale and resolution of the reconstructed jet energy.
- Uncertainties in the modelling of the parton shower.
- Uncertainties in renormalization and factorization scales.

| Signal region | SR1 | SR2a | SR2b |
|--------------------------------------|--------|----------|--------|
| Process | | | |
| ggF signal | 20±15 | 58±22 | 19±8 |
| VBF signal | 286±57 | 182±19 | 105±15 |
| $Z(\rightarrow \nu\nu)+\text{jets}$ | 339±37 | 1580±90 | 335±23 |
| $W(\rightarrow \ell\nu)+\text{jets}$ | 235±42 | 1010±50 | 225±16 |
| Multijet | 2±2 | 20±20 | 4±4 |
| Other backgrounds | 1±0.4 | 64±9 | 19±6 |
| Total background | 577±62 | 2680±130 | 583±34 |
| Data | 539 | 2654 | 636 |

Table 8. Estimates of the expected yields and their total uncertainties for SR1 and SR2 in 20.3 fb⁻¹ of 2012 data. The $Z(\rightarrow \nu\nu)+\text{jets}$, $W(\rightarrow \ell\nu)+\text{jets}$, and multijet background estimates are data-driven. The other backgrounds and the ggF and VBF signals are determined from MC simulation. The expected signal yields are shown for $m_H = 125$ GeV and are normalized to $\text{BF}(H \rightarrow \text{invisible}) = 100\%$. The $W+\text{jets}$ and $Z+\text{jets}$ statistical uncertainties result from the number of MC events in each signal and corresponding control region, and from the number of data events in the control region.

| Results | Expected | +1σ | -1σ | +2σ | -2σ | Observed |
|------------------|----------|------|------|------|------|----------|
| SR1 | 0.35 | 0.49 | 0.25 | 0.67 | 0.19 | 0.30 |
| SR2 | 0.60 | 0.85 | 0.43 | 1.18 | 0.32 | 0.83 |
| Combined Results | 0.31 | 0.44 | 0.23 | 0.60 | 0.17 | 0.28 |

Table 9. Summary of limits on $\text{BF}(H \rightarrow \text{invisible})$ for 20.3 fb⁻¹ of 8 TeV data in the individual search regions and their combination, assuming the SM cross section for $m_H = 125$ GeV.

Table 8 shows signal, background and data events after the global fit including the effects of systematic uncertainties, MC statistical uncertainties in the control and signal regions, and the data statistical uncertainties in the control regions. The post-fit values of the $Z+\text{jets}$ and $W+\text{jets}$ background normalization scale factors k_i , discussed in section 5, are 0.95 ± 0.21 , 0.87 ± 0.17 and 0.74 ± 0.12 for SR1, SR2a and SR2b and their control regions, respectively. As shown in table 8, the signal-to-background ratio is 0.53 in SR1, and 0.09 and 0.21 in SR2a and SR2b respectively, for $\text{BF}(H \rightarrow \text{invisible}) = 100\%$. Fits to the likelihood function are performed separately for each signal region and their combination, and the 95% CL limits on $\text{BF}(H \rightarrow \text{invisible})$ are shown in table 9.

The agreement between the data and the background expectations in SR1 is also expressed as a model-independent 95% CL upper limit on the fiducial cross section

$$\sigma_{\text{fid}} = \sigma \times \text{BF} \times \mathcal{A}, \tag{7.1}$$

$$= \frac{N}{\mathcal{L} \times \epsilon}, \tag{7.2}$$

where the acceptance \mathcal{A} is the fraction of events within the fiducial phase space defined at the MC truth level using the SR1 selections in section 4, N the accepted number of

| SR1 | Expected | +1 σ | -1 σ | +2 σ | -2 σ | Observed |
|-----------------------------|----------|-------------|-------------|-------------|-------------|----------|
| Fiducial cross section [fb] | 4.78 | 6.32 | 3.51 | 8.43 | 2.53 | 3.93 |

Table 10. Model-independent 95% CL upper limit on the fiducial cross section for non-SM processes σ_{fid} in SR1.

events, \mathcal{L} the integrated luminosity and ϵ the selection efficiency defined as the ratio of selected events to those in the fiducial phase space. Only the systematic uncertainties on the backgrounds and the integrated luminosity are taken into account in the upper limit on σ_{fid} , shown in table 10. In SR1, the acceptance and the event selection efficiency, estimated from simulated VBF $H \rightarrow ZZ \rightarrow 4\nu$ events, are $(0.89 \pm 0.04)\%$ and $(94 \pm 15)\%$ respectively. The uncertainties have been divided such that the theory uncertainties are assigned to the acceptance and the experiment uncertainties are assigned to the efficiency.

8 Model interpretation

In the Higgs-portal dark-matter scenario, a dark sector is coupled to the Standard Model via the Higgs boson [9, 10] by introducing a WIMP dark-matter singlet χ that only couples to the SM Higgs doublet. In this model, assuming that the dark-matter particle is lighter than half the Higgs boson mass, one would search for Higgs boson decays to undetected (invisible) dark-matter particles, e.g. $H \rightarrow \chi\chi$. The upper limits on the branching fraction to invisible particles directly determine the maximum allowed decay width to the invisible particles

$$\Gamma_H^{\text{inv}} = \frac{\text{BF}(H \rightarrow \text{invisible})}{1 - \text{BF}(H \rightarrow \text{invisible})} \times \Gamma_H, \quad (8.1)$$

where Γ_H is the SM decay width of the Higgs boson. Adopting the formulas from ref. [10], the decay width of the Higgs boson to the invisible particles can be written as

$$\Gamma_{H \rightarrow SS}^{\text{inv}} = \frac{\lambda_{HSS}^2 v^2 \beta_S}{64\pi m_H}, \quad (8.2)$$

$$\Gamma_{H \rightarrow VV}^{\text{inv}} = \frac{\lambda_{HVV}^2 v^2 m_H^3 \beta_V}{256\pi m_V^4} \left(1 - 4 \frac{m_V^2}{m_H^2} + 12 \frac{m_V^4}{m_H^4} \right), \quad (8.3)$$

$$\Gamma_{H \rightarrow ff}^{\text{inv}} = \frac{\lambda_{Hff}^2 v^2 m_H \beta_f^3}{32\pi \Lambda^2}, \quad (8.4)$$

for the scalar, vector and Majorana-fermion dark matter, respectively. The parameters λ_{HSS} , λ_{HVV} , λ_{Hff}/Λ are the corresponding coupling constants, v is the vacuum expectation value of the SM Higgs doublet, $\beta_\chi = \sqrt{1 - 4m_\chi^2/m_H^2}$ ($\chi = S, V, f$), and m_χ is the WIMP mass. In the Higgs-portal model, the Higgs boson is assumed to be the only mediator in the WIMP-nucleon scattering, and the WIMP-nucleon cross section can be written in a general spin-independent form. Inserting the couplings and masses for each spin scenario gives:

$$\sigma_{SN}^{\text{SI}} = \frac{\lambda_{HSS}^2}{16\pi m_H^4} \frac{m_N^4 f_N^2}{(m_S + m_N)^2}, \quad (8.5)$$

| | | |
|------------------------------------|--------------|------------------------|
| Vacuum expectation value | $v/\sqrt{2}$ | 174 GeV |
| Higgs boson mass | m_H | 125 GeV |
| Higgs boson width | Γ_H | 4.07 MeV |
| Nucleon mass | m_N | 939 MeV |
| Higgs-nucleon coupling form factor | f_N | $0.33^{+0.30}_{-0.07}$ |

Table 11. Parameters in the Higgs-portal dark-matter model.

$$\sigma_{VN}^{\text{SI}} = \frac{\lambda_{HVV}^2}{16\pi m_H^4} \frac{m_N^4 f_N^2}{(m_V + m_N)^2}, \tag{8.6}$$

$$\sigma_{fN}^{\text{SI}} = \frac{\lambda_{Hff}^2}{4\pi\Lambda^2 m_H^4} \frac{m_N^4 m_f^2 f_N^2}{(m_f + m_N)^2}, \tag{8.7}$$

where m_N is the nucleon mass, and f_N is the form factor associated to the Higgs boson-nucleon coupling and computed using lattice QCD [10]. The numerical values for all the parameters in the equations above are given in table 11.

The inferred 90% CL branching fraction limit for $H \rightarrow$ invisible, translated into an upper bound on the scattering cross section between nucleons and WIMP, is shown in figure 8 compared to the results from direct detection experiments. The WIMP-nucleon cross-section limits resulting from searches for invisible Higgs boson decays extend from low WIMP mass to half the Higgs boson mass, and are complementary to the results provided by direct detection experiments that have limited sensitivity to WIMP with mass of the order of 10 GeV and lower [34, 36–40, 42]. This is expected as the LHC has no limitations for the production of low-mass particles, whereas the recoil energies produced in the interactions of sub-relativistic WIMP with nuclei in the apparatus of a direct detection experiment are often below the sensitivity threshold for small WIMP masses. The aforementioned correlation between the branching fraction of Higgs boson decays to invisible particles and the WIMP-nucleon cross section is presented in the effective field theory framework, assuming that the new physics scale is $\mathcal{O}(\text{a few})$ TeV, well above the scale probed at SM Higgs boson mass. Adding a renormalizable mechanism for generating the fermion and vector WIMP masses could modify the correlation between the WIMP-nucleon cross section and the branching fraction of Higgs boson decays to invisible particles [93].

9 Conclusions

A search for Higgs boson decays to invisible particles is presented. The search uses data events with two forward jets and large missing transverse momentum, collected with the ATLAS detector from 20.3 fb^{-1} of pp collisions at $\sqrt{s} = 8 \text{ TeV}$ at the LHC. Assuming the SM production cross section, acceptance and efficiency for invisible decays of a Higgs boson with a mass of 125 GeV, a 95% CL upper bound is set on the $\text{BF}(H \rightarrow \text{invisible})$ at 0.28. The results are interpreted in the Higgs-portal dark-matter model where the 90% CL limit on the $\text{BF}(H \rightarrow \text{invisible})$ is converted into upper bounds on the dark-matter nucleon

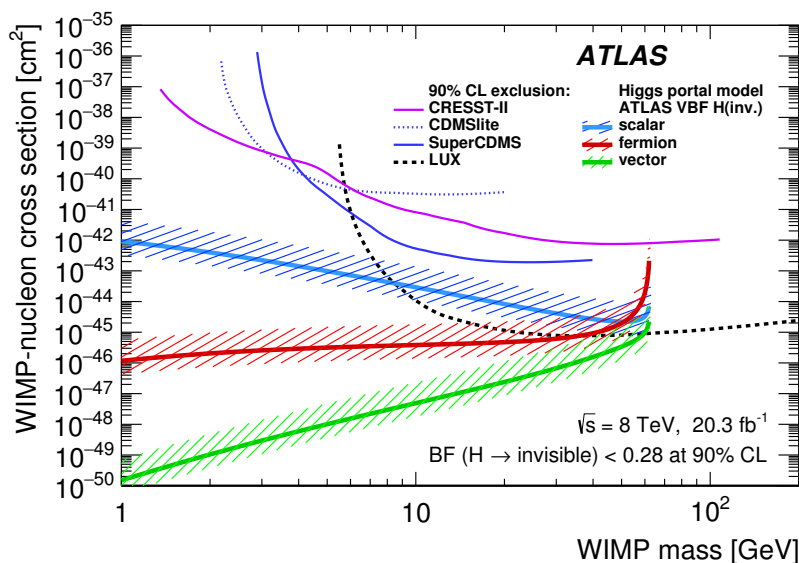


Figure 8. The WIMP-nucleon cross section as a function of the WIMP mass. The exclusion limits [34–38] of the direct detection experiments are compared to the ATLAS results from the $BF(H \rightarrow \text{invisible})$ limit in the Higgs-portal scenario, translated into the WIMP-nucleon cross section using the formulas from ref. [10]. The exclusion limits are shown at 90% CL. The error bands on the ATLAS results indicate the uncertainty coming from the different estimations of the Higgs-nucleon coupling form factor [94, 95].

scattering cross section as a function of the dark-matter particle mass. The ATLAS limits are complementary to the results from the direct dark-matter detection experiments.

Acknowledgments

We thank CERN for the very successful operation of the LHC, as well as the support staff from our institutions without whom ATLAS could not be operated efficiently.

We acknowledge the support of ANPCyT, Argentina; YerPhI, Armenia; ARC, Australia; BMWF, Austria; AHAS, Azerbaijan; SSTC, Belarus; CNPq and FAPESP, Brazil; NSERC, NRC and CFI, Canada; CERN; CONICYT, Chile; CAS, MOST and NSFC, China; COLCIENCIAS, Colombia; MSMT CR, MPO CR and VSC CR, Czech Republic; D NRF, DNSRC and Lundbeck Foundation, Denmark; ARTEMIS, European Union; IN2P3-CNRS, CEA-DSM/IRFU, France; GNAS, Georgia; BMBF, DFG, HGF, MPG and AvH Foundation, Germany; GSRT, Greece; ISF, MINERVA, GIF, DIP and Benoziyo Center, Israel; INFN, Italy; MEXT and JSPS, Japan; CNRST, Morocco; FOM and NWO, Netherlands; RCN, Norway; MNiSW, Poland; GRICES and FCT, Portugal; MERYYS (MECTS), Romania; MES of Russia and ROSATOM, Russian Federation; JINR; MSTD, Serbia; MSSR, Slovakia; ARRS and MVZT, Slovenia; DST/NRF, South Africa; MICINN, Spain; SRC and Wallenberg Foundation, Sweden; SER, SNSF and Cantons of Bern and Geneva, Switzerland; NSC, Taiwan; TAEK, Turkey; STFC, the Royal Society and Leverhulme Trust, United Kingdom; DOE and NSF, United States of America.

The crucial computing support from all WLCG partners is acknowledged gratefully, in particular from CERN and the ATLAS Tier-1 facilities at TRIUMF (Canada), NDGF (Denmark, Norway, Sweden), CC-IN2P3 (France), KIT/GridKA (Germany), INFN-CNAF (Italy), NL-T1 (Netherlands), PIC (Spain), ASGC (Taiwan), RAL (U.K.) and BNL (U.S.A.) and in the Tier-2 facilities worldwide.

Open Access. This article is distributed under the terms of the Creative Commons Attribution License ([CC-BY 4.0](https://creativecommons.org/licenses/by/4.0/)), which permits any use, distribution and reproduction in any medium, provided the original author(s) and source are credited.

References

- [1] D. Clowe et al., *A direct empirical proof of the existence of dark matter*, *Astrophys. J.* **648** (2006) L109 [[astro-ph/0608407](https://arxiv.org/abs/astro-ph/0608407)] [[INSPIRE](#)].
- [2] H. Goldberg, *Constraint on the photino mass from cosmology*, *Phys. Rev. Lett.* **50** (1983) 1419 [*Erratum ibid.* **103** (2009) 099905] [[INSPIRE](#)].
- [3] J.R. Ellis, J.S. Hagelin, D.V. Nanopoulos, K.A. Olive and M. Srednicki, *Supersymmetric relics from the big bang*, *Nucl. Phys. B* **238** (1984) 453 [[INSPIRE](#)].
- [4] ATLAS collaboration, *Observation of a new particle in the search for the standard model Higgs boson with the ATLAS detector at the LHC*, *Phys. Lett. B* **716** (2012) 1 [[arXiv:1207.7214](https://arxiv.org/abs/1207.7214)] [[INSPIRE](#)].
- [5] CMS collaboration, *Observation of a new boson at a mass of 125 GeV with the CMS experiment at the LHC*, *Phys. Lett. B* **716** (2012) 30 [[arXiv:1207.7235](https://arxiv.org/abs/1207.7235)] [[INSPIRE](#)].
- [6] I. Antoniadis, M. Tuckmantel and F. Zwirner, *Phenomenology of a leptonic goldstino and invisible Higgs boson decays*, *Nucl. Phys. B* **707** (2005) 215 [[hep-ph/0410165](https://arxiv.org/abs/hep-ph/0410165)] [[INSPIRE](#)].
- [7] N. Arkani-Hamed, S. Dimopoulos, G.R. Dvali and J. March-Russell, *Neutrino masses from large extra dimensions*, *Phys. Rev. D* **65** (2002) 024032 [[hep-ph/9811448](https://arxiv.org/abs/hep-ph/9811448)] [[INSPIRE](#)].
- [8] A. Datta, K. Huitu, J. Laamanen and B. Mukhopadhyaya, *Invisible Higgs in theories of large extra dimensions*, *Phys. Rev. D* **70** (2004) 075003 [[hep-ph/0404056](https://arxiv.org/abs/hep-ph/0404056)] [[INSPIRE](#)].
- [9] S. Kanemura, S. Matsumoto, T. Nabeshima and N. Okada, *Can WIMP dark matter overcome the nightmare scenario?*, *Phys. Rev. D* **82** (2010) 055026 [[arXiv:1005.5651](https://arxiv.org/abs/1005.5651)] [[INSPIRE](#)].
- [10] A. Djouadi, O. Lebedev, Y. Mambrini and J. Quevillon, *Implications of LHC searches for Higgs-portal dark matter*, *Phys. Lett. B* **709** (2012) 65 [[arXiv:1112.3299](https://arxiv.org/abs/1112.3299)] [[INSPIRE](#)].
- [11] R.E. Shrock and M. Suzuki, *Invisible decays of Higgs bosons*, *Phys. Lett. B* **110** (1982) 250 [[INSPIRE](#)].
- [12] D. Choudhury and D.P. Roy, *Signatures of an invisibly decaying Higgs particle at LHC*, *Phys. Lett. B* **322** (1994) 368 [[hep-ph/9312347](https://arxiv.org/abs/hep-ph/9312347)] [[INSPIRE](#)].
- [13] O.J.P. Eboli and D. Zeppenfeld, *Observing an invisible Higgs boson*, *Phys. Lett. B* **495** (2000) 147 [[hep-ph/0009158](https://arxiv.org/abs/hep-ph/0009158)] [[INSPIRE](#)].
- [14] H. Davoudiasl, T. Han and H.E. Logan, *Discovering an invisibly decaying Higgs at hadron colliders*, *Phys. Rev. D* **71** (2005) 115007 [[hep-ph/0412269](https://arxiv.org/abs/hep-ph/0412269)] [[INSPIRE](#)].

- [15] R.M. Godbole, M. Guchait, K. Mazumdar, S. Moretti and D.P. Roy, *Search for ‘invisible’ Higgs signals at LHC via associated production with gauge bosons*, *Phys. Lett. B* **571** (2003) 184 [[hep-ph/0304137](#)] [[INSPIRE](#)].
- [16] D. Ghosh, R. Godbole, M. Guchait, K. Mohan and D. Sengupta, *Looking for an invisible Higgs signal at the LHC*, *Phys. Lett. B* **725** (2013) 344 [[arXiv:1211.7015](#)] [[INSPIRE](#)].
- [17] G. Bélanger, B. Dumont, U. Ellwanger, J.F. Gunion and S. Kraml, *Status of invisible Higgs decays*, *Phys. Lett. B* **723** (2013) 340 [[arXiv:1302.5694](#)] [[INSPIRE](#)].
- [18] D. Curtin et al., *Exotic decays of the 125 GeV Higgs boson*, *Phys. Rev. D* **90** (2014) 075004 [[arXiv:1312.4992](#)] [[INSPIRE](#)].
- [19] LHC HIGGS CROSS SECTION WORKING GROUP collaboration, S. Dittmaier et al., *Handbook of LHC Higgs cross sections: 1. Inclusive observables*, CERN-2011-002, CERN, Geneva Switzerland (2011) [[arXiv:1101.0593](#)] [[INSPIRE](#)].
- [20] S. Dittmaier et al., *Handbook of LHC Higgs cross sections: 2. Differential distributions*, CERN-2012-002, CERN, Geneva Switzerland (2012) [[arXiv:1201.3084](#)] [[INSPIRE](#)].
- [21] ATLAS collaboration, *The ATLAS experiment at the CERN Large Hadron Collider*, 2008 *JINST* **3** S08003 [[INSPIRE](#)].
- [22] CMS collaboration, *Search for invisible decays of Higgs bosons in the vector boson fusion and associated ZH production modes*, *Eur. Phys. J. C* **74** (2014) 2980 [[arXiv:1404.1344](#)] [[INSPIRE](#)].
- [23] ATLAS collaboration, *Search for invisible decays of a Higgs boson produced in association with a Z boson in ATLAS*, *Phys. Rev. Lett.* **112** (2014) 201802 [[arXiv:1402.3244](#)] [[INSPIRE](#)].
- [24] ATLAS collaboration, *Search for invisible decays of the Higgs boson produced in association with a hadronically decaying vector boson in pp collisions at $\sqrt{s} = 8$ TeV with the ATLAS detector*, *Eur. Phys. J. C* **75** (2015) 337 [[arXiv:1504.04324](#)] [[INSPIRE](#)].
- [25] ATLAS collaboration, *Search for new phenomena in final states with an energetic jet and large missing transverse momentum in pp collisions at $\sqrt{s} = 8$ TeV with the ATLAS detector*, *Eur. Phys. J. C* **75** (2015) 299 [Erratum *ibid.* **C 75** (2015) 408] [[arXiv:1502.01518](#)] [[INSPIRE](#)].
- [26] CMS collaboration, *Search for dark matter, extra dimensions and unparticles in monojet events in proton-proton collisions at $\sqrt{s} = 8$ TeV*, *Eur. Phys. J. C* **75** (2015) 235 [[arXiv:1408.3583](#)] [[INSPIRE](#)].
- [27] ATLAS collaboration, *Search for dark matter in events with a hadronically decaying W or Z boson and missing transverse momentum in pp collisions at $\sqrt{s} = 8$ TeV with the ATLAS detector*, *Phys. Rev. Lett.* **112** (2014) 041802 [[arXiv:1309.4017](#)] [[INSPIRE](#)].
- [28] A. Djouadi, A. Falkowski, Y. Mambrini and J. Quevillon, *Direct detection of Higgs-portal dark matter at the LHC*, *Eur. Phys. J. C* **73** (2013) 2455 [[arXiv:1205.3169](#)] [[INSPIRE](#)].
- [29] ATLAS collaboration, *Constraints on new phenomena via Higgs boson couplings and invisible decays with the ATLAS detector*, *JHEP* **11** (2015) 206 [[arXiv:1509.00672](#)] [[INSPIRE](#)].
- [30] CMS collaboration, *Precise determination of the mass of the Higgs boson and tests of compatibility of its couplings with the standard model predictions using proton collisions at 7 and 8 TeV*, *Eur. Phys. J. C* **75** (2015) 212 [[arXiv:1412.8662](#)] [[INSPIRE](#)].

- [31] G. Cowan, K. Cranmer, E. Gross and O. Vitells, *Asymptotic formulae for likelihood-based tests of new physics*, *Eur. Phys. J. C* **71** (2011) 1554 [*Erratum ibid.* **C 73** (2013) 2501] [[arXiv:1007.1727](#)] [[INSPIRE](#)].
- [32] B. Patt and F. Wilczek, *Higgs-field portal into hidden sectors*, [hep-ph/0605188](#) [[INSPIRE](#)].
- [33] P.J. Fox, R. Harnik, J. Kopp and Y. Tsai, *Missing energy signatures of dark matter at the LHC*, *Phys. Rev. D* **85** (2012) 056011 [[arXiv:1109.4398](#)] [[INSPIRE](#)].
- [34] CRESST-II collaboration, G. Angloher et al., *Results on low mass WIMPs using an upgraded CRESST-II detector*, *Eur. Phys. J. C* **74** (2014) 3184 [[arXiv:1407.3146](#)] [[INSPIRE](#)].
- [35] SUPERCDMS collaboration, R. Agnese et al., *Search for low-mass weakly interacting massive particles using voltage-assisted calorimetric ionization detection in the SuperCDMS experiment*, *Phys. Rev. Lett.* **112** (2014) 041302 [[arXiv:1309.3259](#)] [[INSPIRE](#)].
- [36] SUPERCDMS collaboration, R. Agnese et al., *Search for low-mass weakly interacting massive particles with SuperCDMS*, *Phys. Rev. Lett.* **112** (2014) 241302 [[arXiv:1402.7137](#)] [[INSPIRE](#)].
- [37] XENON100 collaboration, E. Aprile et al., *Dark matter results from 225 live days of XENON100 data*, *Phys. Rev. Lett.* **109** (2012) 181301 [[arXiv:1207.5988](#)] [[INSPIRE](#)].
- [38] LUX collaboration, D.S. Akerib et al., *First results from the LUX dark matter experiment at the Sanford Underground Research Facility*, *Phys. Rev. Lett.* **112** (2014) 091303 [[arXiv:1310.8214](#)] [[INSPIRE](#)].
- [39] DAMA collaboration, R. Bernabei et al., *First results from DAMA/LIBRA and the combined results with DAMA/NaI*, *Eur. Phys. J. C* **56** (2008) 333 [[arXiv:0804.2741](#)] [[INSPIRE](#)].
- [40] C.E. Aalseth et al., *Maximum likelihood signal extraction method applied to 3.4 years of CoGeNT data*, [arXiv:1401.6234](#) [[INSPIRE](#)].
- [41] G. Angloher et al., *Results from 730 kg days of the CRESST-II dark matter search*, *Eur. Phys. J. C* **72** (2012) 1971 [[arXiv:1109.0702](#)] [[INSPIRE](#)].
- [42] CDMS collaboration, R. Agnese et al., *Silicon detector dark matter results from the final exposure of CDMS II*, *Phys. Rev. Lett.* **111** (2013) 251301 [[arXiv:1304.4279](#)] [[INSPIRE](#)].
- [43] GEANT4 collaboration, S. Agostinelli et al., *GEANT4: a simulation toolkit*, *Nucl. Instrum. Meth. A* **506** (2003) 250 [[INSPIRE](#)].
- [44] ATLAS collaboration, *The ATLAS simulation infrastructure*, *Eur. Phys. J. C* **70** (2010) 823 [[arXiv:1005.4568](#)] [[INSPIRE](#)].
- [45] ATLAS collaboration, *The simulation principle and performance of the ATLAS fast calorimeter simulation FastCaloSim*, [ATL-PHYS-PUB-2010-013](#), CERN, Geneva Switzerland (2010).
- [46] T. Sjöstrand, S. Mrenna and P.Z. Skands, *A brief introduction to PYTHIA 8.1*, *Comput. Phys. Commun.* **178** (2008) 852 [[arXiv:0710.3820](#)] [[INSPIRE](#)].
- [47] P. Nason, *A new method for combining NLO QCD with shower Monte Carlo algorithms*, *JHEP* **11** (2004) 040 [[hep-ph/0409146](#)] [[INSPIRE](#)].
- [48] S. Frixione, P. Nason and C. Oleari, *Matching NLO QCD computations with parton shower simulations: the POWHEG method*, *JHEP* **11** (2007) 070 [[arXiv:0709.2092](#)] [[INSPIRE](#)].

- [49] S. Alioli, P. Nason, C. Oleari and E. Re, *A general framework for implementing NLO calculations in shower Monte Carlo programs: the POWHEG BOX*, *JHEP* **06** (2010) 043 [[arXiv:1002.2581](#)] [[INSPIRE](#)].
- [50] S. Alioli, P. Nason, C. Oleari and E. Re, *NLO Higgs boson production via gluon fusion matched with shower in POWHEG*, *JHEP* **04** (2009) 002 [[arXiv:0812.0578](#)] [[INSPIRE](#)].
- [51] P. Nason and C. Oleari, *NLO Higgs boson production via vector-boson fusion matched with shower in POWHEG*, *JHEP* **02** (2010) 037 [[arXiv:0911.5299](#)] [[INSPIRE](#)].
- [52] E. Bagnaschi, G. Degrossi, P. Slavich and A. Vicini, *Higgs production via gluon fusion in the POWHEG approach in the SM and in the MSSM*, *JHEP* **02** (2012) 088 [[arXiv:1111.2854](#)] [[INSPIRE](#)].
- [53] H.-L. Lai et al., *New parton distributions for collider physics*, *Phys. Rev. D* **82** (2010) 074024 [[arXiv:1007.2241](#)] [[INSPIRE](#)].
- [54] LHC HIGGS CROSS SECTION WORKING GROUP collaboration, J.R. Andersen et al., *Handbook of LHC Higgs cross sections: 3. Higgs properties*, CERN-2013-004, CERN, Geneva Switzerland (2013) [[arXiv:1307.1347](#)] [[INSPIRE](#)].
- [55] M. Ciccolini, A. Denner and S. Dittmaier, *Electroweak and QCD corrections to Higgs production via vector-boson fusion at the LHC*, *Phys. Rev. D* **77** (2008) 013002 [[arXiv:0710.4749](#)] [[INSPIRE](#)].
- [56] ATLAS collaboration, *Measurement of Higgs boson production in the diphoton decay channel in pp collisions at center-of-mass energies of 7 and 8 TeV with the ATLAS detector*, *Phys. Rev. D* **90** (2014) 112015 [[arXiv:1408.7084](#)] [[INSPIRE](#)].
- [57] ATLAS collaboration, *Observation and measurement of Higgs boson decays to WW* with the ATLAS detector*, *Phys. Rev. D* **92** (2015) 012006 [[arXiv:1412.2641](#)] [[INSPIRE](#)].
- [58] K. Hamilton, P. Nason and G. Zanderighi, *MINLO: Multi-scale Improved NLO*, *JHEP* **10** (2012) 155 [[arXiv:1206.3572](#)] [[INSPIRE](#)].
- [59] D. de Florian, G. Ferrera, M. Grazzini and D. Tommasini, *Transverse-momentum resummation: Higgs boson production at the Tevatron and the LHC*, *JHEP* **11** (2011) 064 [[arXiv:1109.2109](#)] [[INSPIRE](#)].
- [60] M. Grazzini and H. Sargsyan, *Heavy-quark mass effects in Higgs boson production at the LHC*, *JHEP* **09** (2013) 129 [[arXiv:1306.4581](#)] [[INSPIRE](#)].
- [61] T. Gleisberg et al., *Event generation with SHERPA 1.1*, *JHEP* **02** (2009) 007 [[arXiv:0811.4622](#)] [[INSPIRE](#)].
- [62] S. Höche, F. Krauss, S. Schumann and F. Siegert, *QCD matrix elements and truncated showers*, *JHEP* **05** (2009) 053 [[arXiv:0903.1219](#)] [[INSPIRE](#)].
- [63] ATLAS collaboration, *Measurement of the electroweak production of dijets in association with a Z-boson and distributions sensitive to vector boson fusion in proton-proton collisions at $\sqrt{s} = 8$ TeV using the ATLAS detector*, *JHEP* **04** (2014) 031 [[arXiv:1401.7610](#)] [[INSPIRE](#)].
- [64] K. Melnikov and F. Petriello, *Electroweak gauge boson production at hadron colliders through $O(\alpha_s^2)$* , *Phys. Rev. D* **74** (2006) 114017 [[hep-ph/0609070](#)] [[INSPIRE](#)].

- [65] C. Anastasiou, L.J. Dixon, K. Melnikov and F. Petriello, *High precision QCD at hadron colliders: electroweak gauge boson rapidity distributions at NNLO*, *Phys. Rev. D* **69** (2004) 094008 [[hep-ph/0312266](#)] [[INSPIRE](#)].
- [66] K. Arnold et al., *VBFNLO: a parton level Monte Carlo for processes with electroweak bosons*, *Comput. Phys. Commun.* **180** (2009) 1661 [[arXiv:0811.4559](#)] [[INSPIRE](#)].
- [67] S. Frixione, E. Laenen, P. Motylinski and B.R. Webber, *Single-top production in MC@NLO*, *JHEP* **03** (2006) 092 [[hep-ph/0512250](#)] [[INSPIRE](#)].
- [68] S. Frixione, E. Laenen, P. Motylinski, B.R. Webber and C.D. White, *Single-top hadroproduction in association with a W boson*, *JHEP* **07** (2008) 029 [[arXiv:0805.3067](#)] [[INSPIRE](#)].
- [69] B.P. Kersevan and E. Richter-Was, *The Monte Carlo event generator AcerMC version 1.0 with interfaces to PYTHIA 6.2 and HERWIG 6.3*, *Comput. Phys. Commun.* **149** (2003) 142 [[hep-ph/0201302](#)] [[INSPIRE](#)].
- [70] ATLAS collaboration, *ATLAS tunes of PYTHIA 6 and PYTHIA 8 for MC11*, [ATL-PHYS-PUB-2011-009](#), CERN, Geneva Switzerland (2011).
- [71] J. Pumplin, D.R. Stump, J. Huston, H.L. Lai, P.M. Nadolsky and W.K. Tung, *New generation of parton distributions with uncertainties from global QCD analysis*, *JHEP* **07** (2002) 012 [[hep-ph/0201195](#)] [[INSPIRE](#)].
- [72] G. Corcella et al., *HERWIG 6: an event generator for hadron emission reactions with interfering gluons (including supersymmetric processes)*, *JHEP* **01** (2001) 010 [[hep-ph/0011363](#)] [[INSPIRE](#)].
- [73] J.M. Butterworth, J.R. Forshaw and M.H. Seymour, *Multiparton interactions in photoproduction at HERA*, *Z. Phys. C* **72** (1996) 637 [[hep-ph/9601371](#)] [[INSPIRE](#)].
- [74] J.M. Campbell, R.K. Ellis and C. Williams, *Vector boson pair production at the LHC*, *JHEP* **07** (2011) 018 [[arXiv:1105.0020](#)] [[INSPIRE](#)].
- [75] ATLAS collaboration, *Calorimeter clustering algorithms: description and performance*, [ATL-LARG-PUB-2008-002](#), CERN, Geneva Switzerland (2008).
- [76] ATLAS collaboration, *Jet energy measurement and its systematic uncertainty in proton-proton collisions at $\sqrt{s} = 7$ TeV with the ATLAS detector*, *Eur. Phys. J. C* **75** (2015) 17 [[arXiv:1406.0076](#)] [[INSPIRE](#)].
- [77] ATLAS collaboration, *Jet energy measurement with the ATLAS detector in proton-proton collisions at $\sqrt{s} = 7$ TeV*, *Eur. Phys. J. C* **73** (2013) 2304 [[arXiv:1112.6426](#)] [[INSPIRE](#)].
- [78] M. Cacciari, G.P. Salam and G. Soyez, *The anti- k_t jet clustering algorithm*, *JHEP* **04** (2008) 063 [[arXiv:0802.1189](#)] [[INSPIRE](#)].
- [79] M. Cacciari, G.P. Salam and G. Soyez, *The catchment area of jets*, *JHEP* **04** (2008) 005 [[arXiv:0802.1188](#)] [[INSPIRE](#)].
- [80] M. Cacciari and G.P. Salam, *Pileup subtraction using jet areas*, *Phys. Lett. B* **659** (2008) 119 [[arXiv:0707.1378](#)] [[INSPIRE](#)].
- [81] ATLAS collaboration, *Commissioning of the ATLAS high-performance b-tagging algorithms in the 7 TeV collision data*, [ATLAS-CONF-2011-102](#), CERN, Geneva Switzerland (2011).

- [82] ATLAS collaboration, *Calibration of b-tagging using dileptonic top pair events in a combinatorial likelihood approach with the ATLAS experiment*, [ATLAS-CONF-2014-004](#), CERN, Geneva Switzerland (2014).
- [83] ATLAS collaboration, *Calibration of the performance of b-tagging for c and light-flavour jets in the 2012 ATLAS data*, [ATLAS-CONF-2014-046](#), CERN, Geneva Switzerland (2014).
- [84] ATLAS collaboration, *Identification and energy calibration of hadronically decaying tau leptons with the ATLAS experiment in pp collisions at $\sqrt{s} = 8$ TeV*, *Eur. Phys. J. C* **75** (2015) 303 [[arXiv:1412.7086](#)] [[INSPIRE](#)].
- [85] ATLAS collaboration, *Electron performance measurements with the ATLAS detector using the 2010 LHC proton-proton collision data*, *Eur. Phys. J. C* **72** (2012) 1909 [[arXiv:1110.3174](#)] [[INSPIRE](#)].
- [86] ATLAS collaboration, *Measurement of the muon reconstruction performance of the ATLAS detector using 2011 and 2012 LHC proton-proton collision data*, *Eur. Phys. J. C* **74** (2014) 3130 [[arXiv:1407.3935](#)] [[INSPIRE](#)].
- [87] ATLAS collaboration, *Performance of missing transverse momentum reconstruction in ATLAS studied in proton-proton collisions recorded in 2012 at 8 TeV*, [ATLAS-CONF-2013-082](#), CERN, Geneva Switzerland (2013).
- [88] ATLAS collaboration, *Search for squarks and gluinos with the ATLAS detector in final states with jets and missing transverse momentum using 4.7 fb^{-1} of $\sqrt{s} = 7$ TeV proton-proton collision data*, *Phys. Rev. D* **87** (2013) 012008 [[arXiv:1208.0949](#)] [[INSPIRE](#)].
- [89] ATLAS collaboration, *Improved luminosity determination in pp collisions at $\sqrt{s} = 7$ TeV using the ATLAS detector at the LHC*, *Eur. Phys. J. C* **73** (2013) 2518 [[arXiv:1302.4393](#)] [[INSPIRE](#)].
- [90] M.L. Mangano, M. Moretti, F. Piccinini, R. Pittau and A.D. Polosa, *ALPGEN, a generator for hard multiparton processes in hadronic collisions*, *JHEP* **07** (2003) 001 [[hep-ph/0206293](#)] [[INSPIRE](#)].
- [91] I.W. Stewart and F.J. Tackmann, *Theory uncertainties for Higgs and other searches using jet bins*, *Phys. Rev. D* **85** (2012) 034011 [[arXiv:1107.2117](#)] [[INSPIRE](#)].
- [92] A.L. Read, *Presentation of search results: the CL_s technique*, *J. Phys. G* **28** (2002) 2693 [[INSPIRE](#)].
- [93] S. Baek, P. Ko and W.-I. Park, *Invisible Higgs decay width vs. dark matter direct detection cross section in Higgs portal dark matter models*, *Phys. Rev. D* **90** (2014) 055014 [[arXiv:1405.3530](#)] [[INSPIRE](#)].
- [94] R.D. Young and A.W. Thomas, *Octet baryon masses and sigma terms from an SU(3) chiral extrapolation*, *Phys. Rev. D* **81** (2010) 014503 [[arXiv:0901.3310](#)] [[INSPIRE](#)].
- [95] MILC collaboration, D. Toussaint and W. Freeman, *The strange quark condensate in the nucleon in 2 + 1 flavor QCD*, *Phys. Rev. Lett.* **103** (2009) 122002 [[arXiv:0905.2432](#)] [[INSPIRE](#)].

The ATLAS collaboration

G. Aad⁸⁵, B. Abbott¹¹³, J. Abdallah¹⁵¹, O. Abdinov¹¹, R. Aben¹⁰⁷, M. Abolins⁹⁰, O.S. AbouZeid¹⁵⁸, H. Abramowicz¹⁵³, H. Abreu¹⁵², R. Abreu¹¹⁶, Y. Abulaiti^{146a,146b}, B.S. Acharya^{164a,164b,a}, L. Adamczyk^{38a}, D.L. Adams²⁵, J. Adelman¹⁰⁸, S. Adomeit¹⁰⁰, T. Adye¹³¹, A.A. Affolder⁷⁴, T. Agatonovic-Jovin¹³, J. Agricola⁵⁴, J.A. Aguilar-Saavedra^{126a,126f}, S.P. Ahlen²², F. Ahmadov^{65,b}, G. Aielli^{133a,133b}, H. Akerstedt^{146a,146b}, T.P.A. Åkesson⁸¹, A.V. Akimov⁹⁶, G.L. Alberghi^{20a,20b}, J. Albert¹⁶⁹, S. Albrand⁵⁵, M.J. Alconada Verzini⁷¹, M. Aleksa³⁰, I.N. Aleksandrov⁶⁵, C. Alexa^{26a}, G. Alexander¹⁵³, T. Alexopoulos¹⁰, M. Alhroob¹¹³, G. Alimonti^{91a}, L. Alio⁸⁵, J. Alison³¹, S.P. Alkire³⁵, B.M.M. Allbrooke¹⁴⁹, P.P. Allport⁷⁴, A. Aloisio^{104a,104b}, A. Alonso³⁶, F. Alonso⁷¹, C. Alpigiani⁷⁶, A. Altheimer³⁵, B. Alvarez Gonzalez³⁰, D. Álvarez Piqueras¹⁶⁷, M.G. Alvigi^{104a,104b}, B.T. Amadio¹⁵, K. Amako⁶⁶, Y. Amaral Coutinho^{24a}, C. Amelung²³, D. Amidei⁸⁹, S.P. Amor Dos Santos^{126a,126c}, A. Amorim^{126a,126b}, S. Amoroso⁴⁸, N. Amram¹⁵³, G. Amundsen²³, C. Anastopoulos¹³⁹, L.S. Ancu⁴⁹, N. Andari¹⁰⁸, T. Andeen³⁵, C.F. Anders^{58b}, G. Anders³⁰, J.K. Anders⁷⁴, K.J. Anderson³¹, A. Andreazza^{91a,91b}, V. Andrei^{58a}, S. Angelidakis⁹, I. Angelozzi¹⁰⁷, P. Anger⁴⁴, A. Angerami³⁵, F. Anghinolfi³⁰, A.V. Anisenkov^{109,c}, N. Anjos¹², A. Annovi^{124a,124b}, M. Antonelli⁴⁷, A. Antonov⁹⁸, J. Antos^{144b}, F. Anulli^{132a}, M. Aoki⁶⁶, L. Aperio Bella¹⁸, G. Arabidze⁹⁰, Y. Arai⁶⁶, J.P. Araque^{126a}, A.T.H. Arce⁴⁵, F.A. Arduh⁷¹, J-F. Arguin⁹⁵, S. Argyropoulos⁶³, M. Arik^{19a}, A.J. Armbruster³⁰, O. Arnaez³⁰, V. Arnal⁸², H. Arnold⁴⁸, M. Arratia²⁸, O. Arslan²¹, A. Artamonov⁹⁷, G. Artoni²³, S. Asai¹⁵⁵, N. Asbah⁴², A. Ashkenazi¹⁵³, B. Åsman^{146a,146b}, L. Asquith¹⁴⁹, K. Assamagan²⁵, R. Astalos^{144a}, M. Atkinson¹⁶⁵, N.B. Atlay¹⁴¹, K. Augsten¹²⁸, M. Aourousseau^{145b}, G. Avolio³⁰, B. Axen¹⁵, M.K. Ayoub¹¹⁷, G. Azuelos^{95,d}, M.A. Baak³⁰, A.E. Baas^{58a}, M.J. Baca¹⁸, C. Bacci^{134a,134b}, H. Bachacou¹³⁶, K. Bachas¹⁵⁴, M. Backes³⁰, M. Backhaus³⁰, P. Bagiachi^{132a,132b}, P. Bagnaia^{132a,132b}, Y. Bai^{33a}, T. Bain³⁵, J.T. Baines¹³¹, O.K. Baker¹⁷⁶, E.M. Baldin^{109,c}, P. Balek¹²⁹, T. Balestri¹⁴⁸, F. Balli⁸⁴, W.K. Balunas¹²², E. Banas³⁹, Sw. Banerjee¹⁷³, A.A.E. Bannoura¹⁷⁵, H.S. Bansil¹⁸, L. Barak³⁰, E.L. Barberio⁸⁸, D. Barberis^{50a,50b}, M. Barbero⁸⁵, T. Barillari¹⁰¹, M. Barisonzi^{164a,164b}, T. Barklow¹⁴³, N. Barlow²⁸, S.L. Barnes⁸⁴, B.M. Barnett¹³¹, R.M. Barnett¹⁵, Z. Barnovska⁵, A. Baroncelli^{134a}, G. Barone²³, A.J. Barr¹²⁰, F. Barreiro⁸², J. Barreiro Guimarães da Costa⁵⁷, R. Bartoldus¹⁴³, A.E. Barton⁷², P. Bartos^{144a}, A. Basalae¹²³, A. Bassalat¹¹⁷, A. Basye¹⁶⁵, R.L. Bates⁵³, S.J. Batista¹⁵⁸, J.R. Batley²⁸, M. Battaglia¹³⁷, M. Bauge^{132a,132b}, F. Bauer¹³⁶, H.S. Bawa^{143,e}, J.B. Beacham¹¹¹, M.D. Beattie⁷², T. Beau⁸⁰, P.H. Beauchemin¹⁶¹, R. Beccherle^{124a,124b}, P. Bechtel²¹, H.P. Beck^{17,f}, K. Becker¹²⁰, M. Becker⁸³, M. Beckingham¹⁷⁰, C. Becot¹¹⁷, A.J. Beddall^{19b}, A. Beddall^{19b}, V.A. Bednyakov⁶⁵, C.P. Bee¹⁴⁸, L.J. Beemster¹⁰⁷, T.A. Beeraman³⁰, M. Begel²⁵, J.K. Behr¹²⁰, C. Belanger-Champagne⁸⁷, W.H. Bell⁴⁹, G. Bella¹⁵³, L. Bellagamba^{20a}, A. Bellerive²⁹, M. Bellomo⁸⁶, K. Belotskiy⁹⁸, O. Beltramello³⁰, O. Benary¹⁵³, D. Bencheikroun^{135a}, M. Bender¹⁰⁰, K. Bendtz^{146a,146b}, N. Benekos¹⁰, Y. Benhammou¹⁵³, E. Benhar Noccioli⁴⁹, J.A. Benitez Garcia^{159b}, D.P. Benjamin⁴⁵, J.R. Bensinger²³, S. Bentvelsen¹⁰⁷, L. Beresford¹²⁰, M. Beretta⁴⁷, D. Berge¹⁰⁷, E. Bergeas Kuutmann¹⁶⁶, N. Berger⁵, F. Berghaus¹⁶⁹, J. Beringer¹⁵, C. Bernard²², N.R. Bernard⁸⁶, C. Bernius¹¹⁰, F.U. Bernlochner²¹, T. Berry⁷⁷, P. Berta¹²⁹, C. Bertella⁸³, G. Bertoli^{146a,146b}, F. Bertolucci^{124a,124b}, C. Bertsche¹¹³, D. Bertsche¹¹³, M.I. Besana^{91a}, G.J. Besjes³⁶, O. Bessidskaia Bylund^{146a,146b}, M. Bessner⁴², N. Besson¹³⁶, C. Betancourt⁴⁸, S. Bethke¹⁰¹, A.J. Bevan⁷⁶, W. Bhimji¹⁵, R.M. Bianchi¹²⁵, L. Bianchini²³, M. Bianco³⁰, O. Biebel¹⁰⁰, D. Biedermann¹⁶, S.P. Bieniek⁷⁸, M. Biglietti^{134a}, J. Bilbao De Mendizabal⁴⁹, H. Bilokon⁴⁷, M. Bindi⁵⁴, S. Binet¹¹⁷, A. Bingul^{19b}, C. Bini^{132a,132b}, S. Biondi^{20a,20b}, C.W. Black¹⁵⁰, J.E. Black¹⁴³, K.M. Black²², D. Blackburn¹³⁸, R.E. Blair⁶, J.-B. Blanchard¹³⁶, J.E. Blanco⁷⁷,

T. Blazek^{144a}, I. Bloch⁴², C. Blocker²³, W. Blum^{83,*}, U. Blumenschein⁵⁴, G.J. Bobbink¹⁰⁷, V.S. Bobrovnikov^{109,c}, S.S. Bocchetta⁸¹, A. Bocci⁴⁵, C. Bock¹⁰⁰, M. Boehler⁴⁸, J.A. Bogaerts³⁰, D. Bogavac¹³, A.G. Bogdanchikov¹⁰⁹, C. Bohm^{146a}, V. Boisvert⁷⁷, T. Bold^{38a}, V. Boldea^{26a}, A.S. Boldyrev⁹⁹, M. Bomben⁸⁰, M. Bona⁷⁶, M. Boonekamp¹³⁶, A. Borisov¹³⁰, G. Borisso⁷², S. Borroni⁴², J. Bortfeldt¹⁰⁰, V. Bortolotto^{60a,60b,60c}, K. Bos¹⁰⁷, D. Boscherini^{20a}, M. Bosman¹², J. Boudreau¹²⁵, J. Bouffard², E.V. Bouhova-Thacker⁷², D. Boumediene³⁴, C. Bourdarios¹¹⁷, N. Bousson¹¹⁴, A. Boveia³⁰, J. Boyd³⁰, I.R. Boyko⁶⁵, I. Bozic¹³, J. Bracini¹⁸, A. Brandt⁸, G. Brandt⁵⁴, O. Brandt^{58a}, U. Bratzler¹⁵⁶, B. Brau⁸⁶, J.E. Brau¹¹⁶, H.M. Braun^{175,*}, S.F. Brazzale^{164a,164c}, W.D. Breaden Madden⁵³, K. Brendlinger¹²², A.J. Brennan⁸⁸, L. Brenner¹⁰⁷, R. Brenner¹⁶⁶, S. Bressler¹⁷², K. Bristow^{145c}, T.M. Bristow⁴⁶, D. Britton⁵³, D. Britzger⁴², F.M. Brochu²⁸, I. Brock²¹, R. Brock⁹⁰, J. Bronner¹⁰¹, G. Brooijmans³⁵, T. Brooks⁷⁷, W.K. Brooks^{32b}, J. Brosamer¹⁵, E. Brost¹¹⁶, J. Brown⁵⁵, P.A. Bruckman de Renstrom³⁹, D. Bruncko^{144b}, R. Bruneliere⁴⁸, A. Bruni^{20a}, G. Bruni^{20a}, M. Bruschi^{20a}, N. Brusino²¹, L. Bryngemark⁸¹, T. Buanes¹⁴, Q. Buat¹⁴², P. Buchholz¹⁴¹, A.G. Buckley⁵³, S.I. Buda^{26a}, I.A. Budagov⁶⁵, F. Buehrer⁴⁸, L. Bugge¹¹⁹, M.K. Bugge¹¹⁹, O. Bulekov⁹⁸, D. Bullock⁸, H. Burckhart³⁰, S. Burdin⁷⁴, C.D. Burgard⁴⁸, B. Burghgrave¹⁰⁸, S. Burke¹³¹, I. Burmeister⁴³, E. Busato³⁴, D. Büscher⁴⁸, V. Büscher⁸³, P. Bussey⁵³, J.M. Butler²², A.I. Butt³, C.M. Buttar⁵³, J.M. Butterworth⁷⁸, P. Butti¹⁰⁷, W. Buttinger²⁵, A. Buzatu⁵³, A.R. Buzykaev^{109,c}, S. Cabrera Urbán¹⁶⁷, D. Caforio¹²⁸, V.M. Cairo^{37a,37b}, O. Cakir^{4a}, N. Calace⁴⁹, P. Calafiura¹⁵, A. Calandri¹³⁶, G. Calderini⁸⁰, P. Calfayan¹⁰⁰, L.P. Caloba^{24a}, D. Calvet³⁴, S. Calvet³⁴, R. Camacho Toro³¹, S. Camarda⁴², P. Camarri^{133a,133b}, D. Cameron¹¹⁹, R. Caminal Armadans¹⁶⁵, S. Campana³⁰, M. Campanelli⁷⁸, A. Campoverde¹⁴⁸, V. Canale^{104a,104b}, A. Canepa^{159a}, M. Cano Bret^{33e}, J. Cantero⁸², R. Cantrill^{126a}, T. Cao⁴⁰, M.D.M. Capeans Garrido³⁰, I. Caprini^{26a}, M. Caprini^{26a}, M. Capua^{37a,37b}, R. Caputo⁸³, R. Cardarelli^{133a}, F. Cardillo⁴⁸, T. Carli³⁰, G. Carlino^{104a}, L. Carminati^{91a,91b}, S. Caron¹⁰⁶, E. Carquin^{32a}, G.D. Carrillo-Montoya³⁰, J.R. Carter²⁸, J. Carvalho^{126a,126c}, D. Casadei⁷⁸, M.P. Casado¹², M. Casolino¹², E. Castaneda-Miranda^{145a}, A. Castelli¹⁰⁷, V. Castillo Gimenez¹⁶⁷, N.F. Castro^{126a,g}, P. Catastini⁵⁷, A. Catinaccio³⁰, J.R. Catmore¹¹⁹, A. Cattai³⁰, J. Caudron⁸³, V. Cavaliere¹⁶⁵, D. Cavalli^{91a}, M. Cavalli-Sforza¹², V. Cavasinni^{124a,124b}, F. Ceradini^{134a,134b}, B.C. Cerio⁴⁵, K. Cerny¹²⁹, A.S. Cerqueira^{24b}, A. Cerri¹⁴⁹, L. Cerrito⁷⁶, F. Cerutti¹⁵, M. Cerv³⁰, A. Cervelli¹⁷, S.A. Cetin^{19c}, A. Chafaq^{135a}, D. Chakraborty¹⁰⁸, I. Chalupkova¹²⁹, P. Chang¹⁶⁵, J.D. Chapman²⁸, D.G. Charlton¹⁸, C.C. Chau¹⁵⁸, C.A. Chavez Barajas¹⁴⁹, S. Cheatham¹⁵², A. Chegwidden⁹⁰, S. Chekanov⁶, S.V. Chekulaev^{159a}, G.A. Chelkov^{65,h}, M.A. Chelstowska⁸⁹, C. Chen⁶⁴, H. Chen²⁵, K. Chen¹⁴⁸, L. Chen^{33d,i}, S. Chen^{33c}, X. Chen^{33f}, Y. Chen⁶⁷, H.C. Cheng⁸⁹, Y. Cheng³¹, A. Cheplakov⁶⁵, E. Cheremushkina¹³⁰, R. Cherkaoui El Moursli^{135e}, V. Chernyatin^{25,*}, E. Cheu⁷, L. Chevalier¹³⁶, V. Chiarella⁴⁷, G. Chiarelli^{124a,124b}, G. Chiodini^{73a}, A.S. Chisholm¹⁸, R.T. Chislett⁷⁸, A. Chitan^{26a}, M.V. Chizhov⁶⁵, K. Choi⁶¹, S. Chouridou⁹, B.K.B. Chow¹⁰⁰, V. Christodoulou⁷⁸, D. Chromek-Burckhart³⁰, J. Chudoba¹²⁷, A.J. Chuinard⁸⁷, J.J. Chwastowski³⁹, L. Chytka¹¹⁵, G. Ciapetti^{132a,132b}, A.K. Ciftci^{4a}, D. Cinca⁵³, V. Cindro⁷⁵, I.A. Cioara²¹, A. Ciocio¹⁵, F. Ciroto^{104a,104b}, Z.H. Citron¹⁷², M. Ciubancan^{26a}, A. Clark⁴⁹, B.L. Clark⁵⁷, P.J. Clark⁴⁶, R.N. Clarke¹⁵, W. Cleland¹²⁵, C. Clement^{146a,146b}, Y. Coadou⁸⁵, M. Cokal^{164a,164c}, A. Coccaro⁴⁹, J. Cochran⁶⁴, L. Coffey²³, J.G. Cogan¹⁴³, L. Colasurdo¹⁰⁶, B. Cole³⁵, S. Cole¹⁰⁸, A.P. Colijn¹⁰⁷, J. Collot⁵⁵, T. Colombo^{58c}, G. Compostella¹⁰¹, P. Conde Muiño^{126a,126b}, E. Coniavitis⁴⁸, S.H. Connell^{145b}, I.A. Connelly⁷⁷, V. Consorti⁴⁸, S. Constantinescu^{26a}, C. Conta^{121a,121b}, G. Conti³⁰, F. Conventi^{104a,j}, M. Cooke¹⁵, B.D. Cooper⁷⁸, A.M. Cooper-Sarkar¹²⁰, T. Cornelissen¹⁷⁵, M. Corradi^{20a}, F. Corriqueau^{87,k}, A. Corso-Radu¹⁶³, A. Cortes-Gonzalez¹², G. Cortiana¹⁰¹, G. Costa^{91a}, M.J. Costa¹⁶⁷, D. Costanzo¹³⁹, D. Côté⁸, G. Cottin²⁸, G. Cowan⁷⁷, B.E. Cox⁸⁴, K. Cranmer¹¹⁰, G. Cree²⁹,

S. Crépé-Renaudin⁵⁵, F. Crescioli⁸⁰, W.A. Cribbs^{146a,146b}, M. Crispin Ortuzar¹²⁰,
 M. Cristinziani²¹, V. Croft¹⁰⁶, G. Crosetti^{37a,37b}, T. Cuhadar Donszelmann¹³⁹, J. Cummings¹⁷⁶,
 M. Curatolo⁴⁷, C. Cuthbert¹⁵⁰, H. Cziri¹⁴¹, P. Czodrowski³, S. D'Auria⁵³, M. D'Onofrio⁷⁴,
 M.J. Da Cunha Sargedas De Sousa^{126a,126b}, C. Da Via⁸⁴, W. Dabrowski^{38a}, A. Dainca¹²⁰,
 T. Dai⁸⁹, O. Dale¹⁴, F. Dallaire⁹⁵, C. Dallapiccola⁸⁶, M. Dam³⁶, J.R. Dandoy³¹, N.P. Dang⁴⁸,
 A.C. Daniells¹⁸, M. Danninger¹⁶⁸, M. Dano Hoffmann¹³⁶, V. Dao⁴⁸, G. Darbo^{50a}, S. Darmora⁸,
 J. Dassoulas³, A. Dattagupta⁶¹, W. Davey²¹, C. David¹⁶⁹, T. Davidek¹²⁹, E. Davies^{120,l},
 M. Davies¹⁵³, P. Davison⁷⁸, Y. Davygora^{58a}, E. Dawe⁸⁸, I. Dawson¹³⁹,
 R.K. Daya-Ishmukhametova⁸⁶, K. De⁸, R. de Asmundis^{104a}, A. De Benedetti¹¹³,
 S. De Castro^{20a,20b}, S. De Cecco⁸⁰, N. De Groot¹⁰⁶, P. de Jong¹⁰⁷, H. De la Torre⁸²,
 F. De Lorenzi⁶⁴, D. De Pedis^{132a}, A. De Salvo^{132a}, U. De Sanctis¹⁴⁹, A. De Santo¹⁴⁹,
 J.B. De Vivie De Regie¹¹⁷, W.J. Dearnaley⁷², R. Debbe²⁵, C. Debenedetti¹³⁷, D.V. Dedovich⁶⁵,
 I. Deigaard¹⁰⁷, J. Del Peso⁸², T. Del Prete^{124a,124b}, D. Delgove¹¹⁷, F. Deliot¹³⁶, C.M. Delitzsch⁴⁹,
 M. Deliyergiyev⁷⁵, A. Dell'Acqua³⁰, L. Dell'Asta²², M. Dell'Orso^{124a,124b}, M. Della Pietra^{104a,j},
 D. della Volpe⁴⁹, M. Delmastro⁵, P.A. Delsart⁵⁵, C. Deluca¹⁰⁷, D.A. DeMarco¹⁵⁸, S. Demers¹⁷⁶,
 M. Demichev⁶⁵, A. Demilly⁸⁰, S.P. Denisov¹³⁰, D. Derendarz³⁹, J.E. Derkaoui^{135d}, F. Derue⁸⁰,
 P. Dervan⁷⁴, K. Desch²¹, C. Deterre⁴², P.O. Deviveiros³⁰, A. Dewhurst¹³¹, S. Dhaliwal²³,
 A. Di Ciaccio^{133a,133b}, L. Di Ciaccio⁵, A. Di Domenico^{132a,132b}, C. Di Donato^{104a,104b},
 A. Di Girolamo³⁰, B. Di Girolamo³⁰, A. Di Mattia¹⁵², B. Di Micco^{134a,134b}, R. Di Nardo⁴⁷,
 A. Di Simone⁴⁸, R. Di Sipio¹⁵⁸, D. Di Valentino²⁹, C. Diaconu⁸⁵, M. Diamond¹⁵⁸, F.A. Dias⁴⁶,
 M.A. Diaz^{32a}, E.B. Diehl⁸⁹, J. Dietrich¹⁶, S. Diglio⁸⁵, A. Dimitrievska¹³, J. Dingfelder²¹,
 P. Dita^{26a}, S. Dita^{26a}, F. Dittus³⁰, F. Djama⁸⁵, T. Djobava^{51b}, J.I. Djuvsland^{58a},
 M.A.B. do Vale^{24c}, D. Dobos³⁰, M. Dobre^{26a}, C. Doglioni⁸¹, T. Dohmae¹⁵⁵, J. Dolejsi¹²⁹,
 Z. Dolezal¹²⁹, B.A. Dolgoshein^{98,*}, M. Donadelli^{24d}, S. Donati^{124a,124b}, P. Dondero^{121a,121b},
 J. Donini³⁴, J. Dopke¹³¹, A. Doria^{104a}, M.T. Dova⁷¹, A.T. Doyle⁵³, E. Drechsler⁵⁴, M. Dris¹⁰,
 E. Dubreuil³⁴, E. Duchovni¹⁷², G. Duckeck¹⁰⁰, O.A. Ducu^{26a,85}, D. Duda¹⁰⁷, A. Dudarev³⁰,
 L. Duflot¹¹⁷, L. Duguid⁷⁷, M. Dührssen³⁰, M. Dunford^{58a}, H. Duran Yildiz^{4a}, M. Düren⁵²,
 A. Durglishvili^{51b}, D. Duschinger⁴⁴, M. Dyndal^{38a}, C. Eckardt⁴², K.M. Ecker¹⁰¹, R.C. Edgar⁸⁹,
 W. Edson², N.C. Edwards⁴⁶, W. Ehrenfeld²¹, T. Eifert³⁰, G. Eigen¹⁴, K. Einsweiler¹⁵,
 T. Ekelof¹⁶⁶, M. El Kacimi^{135c}, M. Ellert¹⁶⁶, S. Elles⁵, F. Ellinghaus¹⁷⁵, A.A. Elliot¹⁶⁹, N. Ellis³⁰,
 J. Elmsheuser¹⁰⁰, M. Elsing³⁰, D. Emelianov¹³¹, Y. Enari¹⁵⁵, O.C. Endner⁸³, M. Endo¹¹⁸,
 J. Erdmann⁴³, A. Ereditato¹⁷, G. Ernis¹⁷⁵, J. Ernst², M. Ernst²⁵, S. Errede¹⁶⁵, E. Ertel⁸³,
 M. Escalier¹¹⁷, H. Esch⁴³, C. Escobar¹²⁵, B. Esposito⁴⁷, A.I. Etienvre¹³⁶, E. Etzion¹⁵³,
 H. Evans⁶¹, A. Ezhilov¹²³, L. Fabbri^{20a,20b}, G. Facini³¹, R.M. Fakhrutdinov¹³⁰, S. Falciano^{132a},
 R.J. Falla⁷⁸, J. Faltova¹²⁹, Y. Fang^{33a}, M. Fanti^{91a,91b}, A. Farbin⁸, A. Farilla^{134a}, T. Farooque¹²,
 S. Farrell¹⁵, S.M. Farrington¹⁷⁰, P. Farthouat³⁰, F. Fassi^{135e}, P. Fassnacht³⁰, D. Fassouliotis⁹,
 M. Fauci Giannelli⁷⁷, A. Favareto^{50a,50b}, L. Fayard¹¹⁷, P. Federic^{144a}, O.L. Fedin^{123,m},
 W. Fedorko¹⁶⁸, S. Feigl³⁰, L. Felgioni⁸⁵, C. Feng^{33d}, E.J. Feng⁶, H. Feng⁸⁹, A.B. Fenyuk¹³⁰,
 L. Feremenga⁸, P. Fernandez Martinez¹⁶⁷, S. Fernandez Perez³⁰, J. Ferrando⁵³, A. Ferrari¹⁶⁶,
 P. Ferrari¹⁰⁷, R. Ferrari^{121a}, D.E. Ferreira de Lima⁵³, A. Ferrer¹⁶⁷, D. Ferrere⁴⁹, C. Ferretti⁸⁹,
 A. Ferretto Parodi^{50a,50b}, M. Fiascaris³¹, F. Fiedler⁸³, A. Filipčić⁷⁵, M. Filipuzzi⁴², F. Filthaut¹⁰⁶,
 M. Fincke-Keeler¹⁶⁹, K.D. Finelli¹⁵⁰, M.C.N. Fiolhais^{126a,126c}, L. Fiorini¹⁶⁷, A. Firan⁴⁰,
 A. Fischer², C. Fischer¹², J. Fischer¹⁷⁵, W.C. Fisher⁹⁰, E.A. Fitzgerald²³, N. Flaschel⁴²,
 I. Fleck¹⁴¹, P. Fleischmann⁸⁹, S. Fleischmann¹⁷⁵, G.T. Fletcher¹³⁹, G. Fletcher⁷⁶,
 R.R.M. Fletcher¹²², T. Flick¹⁷⁵, A. Floderus⁸¹, L.R. Flores Castillo^{60a}, M.J. Flowerdew¹⁰¹,
 A. Formica¹³⁶, A. Forti⁸⁴, D. Fournier¹¹⁷, H. Fox⁷², S. Fracchia¹², P. Francavilla⁸⁰,
 M. Franchini^{20a,20b}, D. Francis³⁰, L. Franconi¹¹⁹, M. Franklin⁵⁷, M. Frate¹⁶³,
 M. Fraternali^{121a,121b}, D. Freeborn⁷⁸, S.T. French²⁸, F. Friedrich⁴⁴, D. Froidevaux³⁰,

J.A. Frost¹²⁰, C. Fukunaga¹⁵⁶, E. Fullana Torregrosa⁸³, B.G. Fulson¹⁴³, T. Fusayasu¹⁰²,
 J. Fuster¹⁶⁷, C. Gabaldon⁵⁵, O. Gabizon¹⁷⁵, A. Gabrielli^{20a,20b}, A. Gabrielli^{132a,132b},
 G.P. Gach^{38a}, S. Gadatsch³⁰, S. Gadomski⁴⁹, G. Gagliardi^{50a,50b}, P. Gagnon⁶¹, C. Galea¹⁰⁶,
 B. Galhardo^{126a,126c}, E.J. Gallas¹²⁰, B.J. Gallop¹³¹, P. Gallus¹²⁸, G. Galster³⁶, K.K. Gan¹¹¹,
 J. Gao^{33b,85}, Y. Gao⁴⁶, Y.S. Gao^{143,e}, F.M. Garay Walls⁴⁶, F. Garberson¹⁷⁶, C. García¹⁶⁷,
 J.E. García Navarro¹⁶⁷, M. Garcia-Sciveres¹⁵, R.W. Gardner³¹, N. Garelli¹⁴³, V. Garonne¹¹⁹,
 C. Gatti⁴⁷, A. Gaudiello^{50a,50b}, G. Gaudio^{121a}, B. Gaur¹⁴¹, L. Gauthier⁹⁵, P. Gauzzi^{132a,132b},
 I.L. Gavrilenko⁹⁶, C. Gay¹⁶⁸, G. Gaycken²¹, E.N. Gazis¹⁰, P. Ge^{33d}, Z. Gecse¹⁶⁸, C.N.P. Gee¹³¹,
 Ch. Geich-Gimbel²¹, M.P. Geisler^{58a}, C. Gemme^{50a}, M.H. Genest⁵⁵, S. Gentile^{132a,132b},
 M. George⁵⁴, S. George⁷⁷, D. Gerbaudo¹⁶³, A. Gershon¹⁵³, S. Ghasemi¹⁴¹, H. Ghazlane^{135b},
 B. Giacobbe^{20a}, S. Giagu^{132a,132b}, V.angiobbe¹², P. Giannetti^{124a,124b}, B. Gibbard²⁵,
 S.M. Gibson⁷⁷, M. Gilchriese¹⁵, T.P.S. Gillam²⁸, D. Gillberg³⁰, G. Gilles³⁴, D.M. Gingrich^{3,d},
 N. Giokaris⁹, M.P. Giordani^{164a,164c}, F.M. Giorgi^{20a}, F.M. Giorgi¹⁶, P.F. Giraud¹³⁶, P. Giromini⁴⁷,
 D. Giugni^{91a}, C. Giuliani⁴⁸, M. Giulini^{58b}, B.K. Gjelsten¹¹⁹, S. Gkaitatzis¹⁵⁴, I. Gkialas¹⁵⁴,
 E.L. Gkougkousis¹¹⁷, L.K. Gladilin⁹⁹, C. Glasman⁸², J. Glatzer³⁰, P.C.F. Glaysheer⁴⁶, A. Glazov⁴²,
 M. Goblirsch-Kolb¹⁰¹, J.R. Goddard⁷⁶, J. Godlewski³⁹, S. Goldfarb⁸⁹, T. Golling⁴⁹,
 D. Golubkov¹³⁰, A. Gomes^{126a,126b,126d}, R. Gonçalo^{126a}, J. Goncalves Pinto Firmino Da Costa¹³⁶,
 L. Gonella²¹, S. González de la Hoz¹⁶⁷, G. Gonzalez Parra¹², S. Gonzalez-Sevilla⁴⁹, L. Goossens³⁰,
 P.A. Gorbounov⁹⁷, H.A. Gordon²⁵, I. Gorelov¹⁰⁵, B. Gorini³⁰, E. Gorini^{73a,73b}, A. Gorišek⁷⁵,
 E. Gornicki³⁹, A.T. Goshaw⁴⁵, C. Gössling⁴³, M.I. Gostkin⁶⁵, D. Goujdami^{135c}, A.G. Goussiou¹³⁸,
 N. Govender^{145b}, E. Gozani¹⁵², H.M.X. Grabas¹³⁷, L. Graber⁵⁴, I. Grabowska-Bold^{38a},
 P.O.J. Gradin¹⁶⁶, P. Grafström^{20a,20b}, K.-J. Grahn⁴², J. Gramling⁴⁹, E. Gramstad¹¹⁹,
 S. Grancagnolo¹⁶, V. Gratchev¹²³, H.M. Gray³⁰, E. Graziani^{134a}, Z.D. Greenwood^{79,n}, C. Grefe²¹,
 K. Gregersen⁷⁸, I.M. Gregor⁴², P. Grenier¹⁴³, J. Griffiths⁸, A.A. Grillo¹³⁷, K. Grimm⁷²,
 S. Grinstein^{12,o}, Ph. Gris³⁴, J.-F. Grivaz¹¹⁷, J.P. Grohs⁴⁴, A. Grohsjean⁴², E. Gross¹⁷²,
 J. Grosse-Knetter⁵⁴, G.C. Grossi⁷⁹, Z.J. Grout¹⁴⁹, L. Guan⁸⁹, J. Guenther¹²⁸, F. Guescini⁴⁹,
 D. Guest¹⁷⁶, O. Gueta¹⁵³, E. Guido^{50a,50b}, T. Guillemin¹¹⁷, S. Guindon², U. Gul⁵³,
 C. Gumpert⁴⁴, J. Guo^{33e}, Y. Guo^{33b}, S. Gupta¹²⁰, G. Gustavino^{132a,132b}, P. Gutierrez¹¹³,
 N.G. Gutierrez Ortiz⁷⁸, C. Gutsche⁴⁴, C. Guyot¹³⁶, C. Gwenlan¹²⁰, C.B. Gwilliam⁷⁴,
 A. Haas¹¹⁰, C. Haber¹⁵, H.K. Hadavand⁸, N. Haddad^{135e}, P. Haefner²¹, S. Hageböck²¹,
 Z. Hajduk³⁹, H. Hakobyan¹⁷⁷, M. Haleem⁴², J. Haley¹¹⁴, D. Hall¹²⁰, G. Halladjian⁹⁰,
 G.D. Hallewell⁸⁵, K. Hamacher¹⁷⁵, P. Hamal¹¹⁵, K. Hamano¹⁶⁹, A. Hamilton^{145a}, G.N. Hamity¹³⁹,
 P.G. Hamnett⁴², L. Han^{33b}, K. Hanagaki^{66,p}, K. Hanawa¹⁵⁵, M. Hance¹⁵, P. Hanke^{58a},
 R. Hanna¹³⁶, J.B. Hansen³⁶, J.D. Hansen³⁶, M.C. Hansen²¹, P.H. Hansen³⁶, K. Hara¹⁶⁰,
 A.S. Hard¹⁷³, T. Harenberg¹⁷⁵, F. Hariri¹¹⁷, S. Harkusha⁹², R.D. Harrington⁴⁶, P.F. Harrison¹⁷⁰,
 F. Hartjes¹⁰⁷, M. Hasegawa⁶⁷, Y. Hasegawa¹⁴⁰, A. Hasib¹¹³, S. Hassani¹³⁶, S. Haug¹⁷,
 R. Hauser⁹⁰, L. Hauswald⁴⁴, M. Havranek¹²⁷, C.M. Hawkes¹⁸, R.J. Hawkins³⁰, A.D. Hawkins⁸¹,
 T. Hayashi¹⁶⁰, D. Hayden⁹⁰, C.P. Hays¹²⁰, J.M. Hays⁷⁶, H.S. Hayward⁷⁴, S.J. Haywood¹³¹,
 S.J. Head¹⁸, T. Heck⁸³, V. Hedberg⁸¹, L. Heelan⁸, S. Heim¹²², T. Heim¹⁷⁵, B. Heinemann¹⁵,
 L. Heinrich¹¹⁰, J. Hejbal¹²⁷, L. Helary²², S. Hellman^{146a,146b}, D. Hellmich²¹, C. Hensens¹²,
 J. Henderson¹²⁰, R.C.W. Henderson⁷², Y. Heng¹⁷³, C. Hengler⁴², S. Henkelmann¹⁶⁸,
 A. Henrichs¹⁷⁶, A.M. Henriques Correia³⁰, S. Henrot-Versille¹¹⁷, G.H. Herbert¹⁶,
 Y. Hernández Jiménez¹⁶⁷, R. Herrberg-Schubert¹⁶, G. Herten⁴⁸, R. Hertenberger¹⁰⁰, L. Hervas³⁰,
 G.G. Hesketh⁷⁸, N.P. Hessey¹⁰⁷, J.W. Hetherly⁴⁰, R. Hickling⁷⁶, E. Higón-Rodríguez¹⁶⁷,
 E. Hill¹⁶⁹, J.C. Hill²⁸, K.H. Hiller⁴², S.J. Hillier¹⁸, I. Hinchliffe¹⁵, E. Hines¹²², R.R. Hinman¹⁵,
 M. Hirose¹⁵⁷, D. Hirschbuehl¹⁷⁵, J. Hobbs¹⁴⁸, N. Hod¹⁰⁷, M.C. Hodgkinson¹³⁹, P. Hodgson¹³⁹,
 A. Hoecker³⁰, M.R. Hoferkamp¹⁰⁵, F. Hoenig¹⁰⁰, M. Hohlfeld⁸³, D. Hohn²¹, T.R. Holmes¹⁵,
 M. Homann⁴³, T.M. Hong¹²⁵, L. Hooft van Huysduynen¹¹⁰, W.H. Hopkins¹¹⁶, Y. Horii¹⁰³,

A.J. Horton¹⁴², J.-Y. Hostachy⁵⁵, S. Hou¹⁵¹, A. Hoummada^{135a}, J. Howard¹²⁰, J. Howarth⁴²,
 M. Hrabovsky¹¹⁵, I. Hristova¹⁶, J. Hrivnac¹¹⁷, T. Hryn'ova⁵, A. Hrynevich⁹³, C. Hsu^{145c},
 P.J. Hsu^{151,q}, S.-C. Hsu¹³⁸, D. Hu³⁵, Q. Hu^{33b}, X. Hu⁸⁹, Y. Huang⁴², Z. Hubacek¹²⁸,
 F. Hubaut⁸⁵, F. Huegging²¹, T.B. Huffman¹²⁰, E.W. Hughes³⁵, G. Hughes⁷², M. Huhtinen³⁰,
 T.A. Hülsing⁸³, N. Huseynov^{65,b}, J. Huston⁹⁰, J. Huth⁵⁷, G. Iacobucci⁴⁹, G. Iakovidis²⁵,
 I. Ibragimov¹⁴¹, L. Iconomidou-Fayard¹¹⁷, E. Ideal¹⁷⁶, Z. Idrissi^{135e}, P. Iengo³⁰, O. Igonkina¹⁰⁷,
 T. Iizawa¹⁷¹, Y. Ikegami⁶⁶, K. Ikematsu¹⁴¹, M. Ikeno⁶⁶, Y. Ilchenko^{31,r}, D. Iliadis¹⁵⁴, N. Ilic¹⁴³,
 T. Ince¹⁰¹, G. Introzzi^{121a,121b}, P. Ioannou⁹, M. Iodice^{134a}, K. Iordanidou³⁵, V. Ippolito⁵⁷,
 A. Irles Quiles¹⁶⁷, C. Isaksson¹⁶⁶, M. Ishino⁶⁸, M. Ishitsuka¹⁵⁷, R. Ishmukhametov¹¹¹,
 C. Issever¹²⁰, S. Istin^{19a}, J.M. Iturbe Ponce⁸⁴, R. Iuppa^{133a,133b}, J. Ivarsson⁸¹, W. Iwanski³⁹,
 H. Iwasaki⁶⁶, J.M. Izen⁴¹, V. Izzo^{104a}, S. Jabbar³, B. Jackson¹²², M. Jackson⁷⁴, P. Jackson¹,
 M.R. Jaekel³⁰, V. Jain², K. Jakobs⁴⁸, S. Jakobsen³⁰, T. Jakoubek¹²⁷, J. Jakubek¹²⁸,
 D.O. Jamin¹¹⁴, D.K. Jana⁷⁹, E. Jansen⁷⁸, R. Jansky⁶², J. Janssen²¹, M. Janus⁵⁴, G. Jarlskog⁸¹,
 N. Javadov^{65,b}, T. Javůrek⁴⁸, L. Jeanty¹⁵, J. Jejelava^{51a,s}, G.-Y. Jeng¹⁵⁰, D. Jennens⁸⁸,
 P. Jenni^{48,t}, J. Jentzsch⁴³, C. Jeske¹⁷⁰, S. Jézéquel⁵, H. Ji¹⁷³, J. Jia¹⁴⁸, Y. Jiang^{33b}, S. Jiggins⁷⁸,
 J. Jimenez Pena¹⁶⁷, S. Jin^{33a}, A. Jinaru^{26a}, O. Jinnouchi¹⁵⁷, M.D. Joergensen³⁶, P. Johansson¹³⁹,
 K.A. Johns⁷, K. Jon-And^{146a,146b}, G. Jones¹⁷⁰, R.W.L. Jones⁷², T.J. Jones⁷⁴, J. Jongmanns^{58a},
 P.M. Jorge^{126a,126b}, K.D. Joshi⁸⁴, J. Jovicevic^{159a}, X. Ju¹⁷³, C.A. Jung⁴³, P. Jussel⁶²,
 A. Juste Rozas^{12,o}, M. Kaci¹⁶⁷, A. Kaczmarek³⁹, M. Kado¹¹⁷, H. Kagan¹¹¹, M. Kagan¹⁴³,
 S.J. Kahn⁸⁵, E. Kajomovitz⁴⁵, C.W. Kalderon¹²⁰, S. Kama⁴⁰, A. Kamenshchikov¹³⁰,
 N. Kanaya¹⁵⁵, S. Kaneti²⁸, V.A. Kantserov⁹⁸, J. Kanzaki⁶⁶, B. Kaplan¹¹⁰, L.S. Kaplan¹⁷³,
 A. Kapliy³¹, D. Kar^{145c}, K. Karakostas¹⁰, A. Karamaoun³, N. Karastathis^{10,107}, M.J. Kareem⁵⁴,
 E. Karentzos¹⁰, M. Karnevskiy⁸³, S.N. Karpov⁶⁵, Z.M. Karpova⁶⁵, K. Karthik¹¹⁰,
 V. Kartvelishvili⁷², A.N. Karyukhin¹³⁰, L. Kashif¹⁷³, R.D. Kass¹¹¹, A. Kastanas¹⁴, Y. Kataoka¹⁵⁵,
 C. Kato¹⁵⁵, A. Katre⁴⁹, J. Katzy⁴², K. Kawagoe⁷⁰, T. Kawamoto¹⁵⁵, G. Kawamura⁵⁴,
 S. Kazama¹⁵⁵, V.F. Kazanin^{109,c}, R. Keeler¹⁶⁹, R. Kehoe⁴⁰, J.S. Keller⁴², J.J. Kempster⁷⁷,
 H. Keoshkerian⁸⁴, O. Kepka¹²⁷, B.P. Kerševan⁷⁵, S. Kersten¹⁷⁵, R.A. Keyes⁸⁷, F. Khalil-zada¹¹,
 H. Khandanyan^{146a,146b}, A. Khanov¹¹⁴, A.G. Kharlamov^{109,c}, T.J. Khoo²⁸, V. Khovanskiy⁹⁷,
 E. Khramov⁶⁵, J. Khubua^{51b,u}, S. Kido⁶⁷, H.Y. Kim⁸, S.H. Kim¹⁶⁰, Y.K. Kim³¹, N. Kimura¹⁵⁴,
 O.M. Kind¹⁶, B.T. King⁷⁴, M. King¹⁶⁷, S.B. King¹⁶⁸, J. Kirk¹³¹, A.E. Kiryunin¹⁰¹,
 T. Kishimoto⁶⁷, D. Kisielewska^{38a}, F. Kiss⁴⁸, K. Kiuchi¹⁶⁰, O. Kivernyk¹³⁶, E. Kladiva^{144b},
 M.H. Klein³⁵, M. Klein⁷⁴, U. Klein⁷⁴, K. Kleinknecht⁸³, P. Klimek^{146a,146b}, A. Klimentov²⁵,
 R. Klingenberg⁴³, J.A. Klinger¹³⁹, T. Klioutchnikova³⁰, E.-E. Kluge^{58a}, P. Kluit¹⁰⁷, S. Kluth¹⁰¹,
 J. Knapik³⁹, E. Kneringer⁶², E.B.F.G. Knoops⁸⁵, A. Knue⁵³, A. Kobayashi¹⁵⁵, D. Kobayashi¹⁵⁷,
 T. Kobayashi¹⁵⁵, M. Kobel⁴⁴, M. Kocian¹⁴³, P. Kodys¹²⁹, T. Koffas²⁹, E. Koffeman¹⁰⁷,
 L.A. Kogan¹²⁰, S. Kohlmann¹⁷⁵, Z. Kohout¹²⁸, T. Kohriki⁶⁶, T. Koi¹⁴³, H. Kolanoski¹⁶,
 I. Koletsou⁵, A.A. Komar^{96,*}, Y. Komori¹⁵⁵, T. Kondo⁶⁶, N. Kondrashova⁴², K. Köneke⁴⁸,
 A.C. König¹⁰⁶, T. Kono⁶⁶, R. Konoplich^{110,v}, N. Konstantinidis⁷⁸, R. Kopeliansky¹⁵²,
 S. Koperny^{38a}, L. Köpke⁸³, A.K. Kopp⁴⁸, K. Korcyl³⁹, K. Kordas¹⁵⁴, A. Korn⁷⁸, A.A. Korol^{109,c},
 I. Korolkov¹², E.V. Korolkova¹³⁹, O. Kortner¹⁰¹, S. Kortner¹⁰¹, T. Kosek¹²⁹, V.V. Kostyukhin²¹,
 V.M. Kotov⁶⁵, A. Kotwal⁴⁵, A. Kourkouveli-Charalampidi¹⁵⁴, C. Kourkouvelis⁹,
 V. Kouskoura²⁵, A. Koutsman^{159a}, R. Kowalewski¹⁶⁹, T.Z. Kowalski^{38a}, W. Kozanecki¹³⁶,
 A.S. Kozhin¹³⁰, V.A. Kramarenko⁹⁹, G. Kramberger⁷⁵, D. Krasnopevtsev⁹⁸, M.W. Krasny⁸⁰,
 A. Krasznahorkay³⁰, J.K. Kraus²¹, A. Kravchenko²⁵, S. Kreiss¹¹⁰, M. Kretz^{58c}, J. Kretzschmar⁷⁴,
 K. Kreutzfeldt⁵², P. Krieger¹⁵⁸, K. Krizka³¹, K. Kroeninger⁴³, H. Kroha¹⁰¹, J. Kroll¹²²,
 J. Kroseberg²¹, J. Krstic¹³, U. Kruchonak⁶⁵, H. Krüger²¹, N. Krumnack⁶⁴, A. Kruse¹⁷³,
 M.C. Kruse⁴⁵, M. Kruskal²², T. Kubota⁸⁸, H. Kucuk⁷⁸, S. Kудay^{4b}, S. Kuehn⁴⁸, A. Kugel^{58c},
 F. Kuger¹⁷⁴, A. Kuhl¹³⁷, T. Kuhl⁴², V. Kukhtin⁶⁵, R. Kukla¹³⁶, Y. Kulchitsky⁹², S. Kuleshov^{32b},

M. Kuna^{132a,132b}, T. Kunigo⁶⁸, A. Kupco¹²⁷, H. Kurashige⁶⁷, Y.A. Kurochkin⁹², V. Kus¹²⁷,
 E.S. Kuwertz¹⁶⁹, M. Kuze¹⁵⁷, J. Kvita¹¹⁵, T. Kwan¹⁶⁹, D. Kyriazopoulos¹³⁹, A. La Rosa¹³⁷,
 J.L. La Rosa Navarro^{24d}, L. La Rotonda^{37a,37b}, C. Lacasta¹⁶⁷, F. Lacava^{132a,132b}, J. Lacey²⁹,
 H. Lacker¹⁶, D. Lacour⁸⁰, V.R. Lacuesta¹⁶⁷, E. Ladygin⁶⁵, R. Lafaye⁵, B. Laforge⁸⁰,
 T. Lagouri¹⁷⁶, S. Lai⁵⁴, L. Lambourne⁷⁸, S. Lammers⁶¹, C.L. Lampen⁷, W. Lampl⁷, E. Lançon¹³⁶,
 U. Landgraf⁴⁸, M.P.J. Landon⁷⁶, V.S. Lang^{58a}, J.C. Lange¹², A.J. Lankford¹⁶³, F. Lanni²⁵,
 K. Lantzsch²¹, A. Lanza^{121a}, S. Laplace⁸⁰, C. Lapoire³⁰, J.F. Laporte¹³⁶, T. Lari^{91a},
 F. Lasagni Manghi^{20a,20b}, M. Lassnig³⁰, P. Laurelli⁴⁷, W. Lavrijsen¹⁵, A.T. Law¹³⁷, P. Laycock⁷⁴,
 T. Lazovich⁵⁷, O. Le Dortz⁸⁰, E. Le Guirriec⁸⁵, E. Le Menedeu¹², M. LeBlanc¹⁶⁹, T. LeCompte⁶,
 F. Ledroit-Guillon⁵⁵, C.A. Lee^{145b}, S.C. Lee¹⁵¹, L. Lee¹, G. Lefebvre⁸⁰, M. Lefebvre¹⁶⁹,
 F. Legger¹⁰⁰, C. Leggett¹⁵, A. Lehan⁷⁴, G. Lehmann Miotto³⁰, X. Lei⁷, W.A. Leight²⁹,
 A. Leisos^{154,w}, A.G. Leister¹⁷⁶, M.A.L. Leite^{24d}, R. Leitner¹²⁹, D. Lellouch¹⁷², B. Lemmer⁵⁴,
 K.J.C. Leney⁷⁸, T. Lenz²¹, B. Lenzi³⁰, R. Leone⁷, S. Leone^{124a,124b}, C. Leonidopoulos⁴⁶,
 S. Leontsinis¹⁰, C. Leroy⁹⁵, C.G. Lester²⁸, M. Levchenko¹²³, J. Levêque⁵, D. Levin⁸⁹,
 L.J. Levinson¹⁷², M. Levy¹⁸, A. Lewis¹²⁰, A.M. Leyko²¹, M. Leyton⁴¹, B. Li^{33b,x}, H. Li¹⁴⁸,
 H.L. Li³¹, L. Li⁴⁵, L. Li^{33e}, S. Li⁴⁵, X. Li⁸⁴, Y. Li^{33c,y}, Z. Liang¹³⁷, H. Liao³⁴, B. Liberti^{133a},
 A. Liblong¹⁵⁸, P. Lichard³⁰, K. Lie¹⁶⁵, J. Liebal²¹, W. Liebig¹⁴, C. Limbach²¹, A. Limosani¹⁵⁰,
 S.C. Lin^{151,z}, T.H. Lin⁸³, F. Linde¹⁰⁷, B.E. Lindquist¹⁴⁸, J.T. Linnemann⁹⁰, E. Lipeles¹²²,
 A. Lipniacka¹⁴, M. Lisovyi^{58b}, T.M. Liss¹⁶⁵, D. Lissauer²⁵, A. Lister¹⁶⁸, A.M. Litke¹³⁷,
 B. Liu^{151,aa}, D. Liu¹⁵¹, H. Liu⁸⁹, J. Liu⁸⁵, J.B. Liu^{33b}, K. Liu⁸⁵, L. Liu¹⁶⁵, M. Liu⁴⁵, M. Liu^{33b},
 Y. Liu^{33b}, M. Livan^{121a,121b}, A. Lleres⁵⁵, J. Llorente Merino⁸², S.L. Lloyd⁷⁶, F. Lo Sterzo¹⁵¹,
 E. Lobodzinska⁴², P. Loch⁷, W.S. Lockman¹³⁷, F.K. Loebinger⁸⁴, A.E. Loevschall-Jensen³⁶,
 A. Loginov¹⁷⁶, T. Lohse¹⁶, K. Lohwasser⁴², M. Lokajicek¹²⁷, B.A. Long²², J.D. Long⁸⁹,
 R.E. Long⁷², K.A. Looper¹¹¹, L. Lopes^{126a}, D. Lopez Mateos⁵⁷, B. Lopez Paredes¹³⁹,
 I. Lopez Paz¹², J. Lorenz¹⁰⁰, N. Lorenzo Martinez⁶¹, M. Losada¹⁶², P.J. Lösel¹⁰⁰, X. Lou^{33a},
 A. Lounis¹¹⁷, J. Love⁶, P.A. Love⁷², N. Lu⁸⁹, H.J. Lubatti¹³⁸, C. Luci^{132a,132b}, A. Lucotte⁵⁵,
 F. Luehring⁶¹, W. Lukas⁶², L. Luminari^{132a}, O. Lundberg^{146a,146b}, B. Lund-Jensen¹⁴⁷, D. Lynn²⁵,
 R. Lysak¹²⁷, E. Lytken⁸¹, H. Ma²⁵, L.L. Ma^{33d}, G. Maccarrone⁴⁷, A. Macchiolo¹⁰¹,
 C.M. Macdonald¹³⁹, B. Maček⁷⁵, J. Machado Miguens^{122,126b}, D. Macina³⁰, D. Madaffari⁸⁵,
 R. Madar³⁴, H.J. Maddocks⁷², W.F. Mader⁴⁴, A. Madsen¹⁶⁶, J. Maeda⁶⁷, S. Maeland¹⁴,
 T. Maeno²⁵, A. Maevskiy⁹⁹, E. Magradze⁵⁴, K. Mahboubi⁴⁸, J. Mahlstedt¹⁰⁷, C. Maiani¹³⁶,
 C. Maidantchik^{24a}, A.A. Maier¹⁰¹, T. Maier¹⁰⁰, A. Maio^{126a,126b,126d}, S. Majewski¹¹⁶,
 Y. Makida⁶⁶, N. Makovec¹¹⁷, B. Malaescu⁸⁰, Pa. Malecki³⁹, V.P. Maleev¹²³, F. Malek⁵⁵,
 U. Mallik⁶³, D. Malon⁶, C. Malone¹⁴³, S. Maltezos¹⁰, V.M. Malyshev¹⁰⁹, S. Malyukov³⁰,
 J. Mamuzic⁴², G. Mancini⁴⁷, B. Mandelli³⁰, L. Mandelli^{91a}, I. Mandić⁷⁵, R. Mandrysch⁶³,
 J. Maneira^{126a,126b}, A. Manfredini¹⁰¹, L. Manhaes de Andrade Filho^{24b}, J. Manjarres Ramos^{159b},
 A. Mann¹⁰⁰, A. Manousakis-Katsikakis⁹, B. Mansoulie¹³⁶, R. Mantifel⁸⁷, M. Mantoani⁵⁴,
 L. Mapelli³⁰, L. March^{145c}, G. Marchiori⁸⁰, M. Marcisovsky¹²⁷, C.P. Marino¹⁶⁹, M. Marjanovic¹³,
 D.E. Marley⁸⁹, F. Marroquim^{24a}, S.P. Marsden⁸⁴, Z. Marshall¹⁵, L.F. Marti¹⁷, S. Marti-Garcia¹⁶⁷,
 B. Martin⁹⁰, T.A. Martin¹⁷⁰, V.J. Martin⁴⁶, B. Martin dit Latour¹⁴, M. Martinez^{12,o},
 S. Martin-Haugh¹³¹, V.S. Martoiu^{26a}, A.C. Martyniuk⁷⁸, M. Marx¹³⁸, F. Marzano^{132a},
 A. Marzin³⁰, L. Masetti⁸³, T. Mashimo¹⁵⁵, R. Mashinistov⁹⁶, J. Masik⁸⁴, A.L. Maslennikov^{109,c},
 I. Massa^{20a,20b}, L. Massa^{20a,20b}, N. Massol⁵, P. Mastrandrea¹⁴⁸, A. Mastroberardino^{37a,37b},
 T. Masubuchi¹⁵⁵, P. Mättig¹⁷⁵, J. Mattmann⁸³, J. Maurer^{26a}, S.J. Maxfield⁷⁴, D.A. Maximov^{109,c},
 R. Mazini¹⁵¹, S.M. Mazza^{91a,91b}, L. Mazzaferro^{133a,133b}, G. Mc Goldrick¹⁵⁸, S.P. Mc Kee⁸⁹,
 A. McCarn⁸⁹, R.L. McCarthy¹⁴⁸, T.G. McCarthy²⁹, N.A. McCubbin¹³¹, K.W. McFarlane^{56,*},
 J.A. MCFayden⁷⁸, G. Mchedlidze⁵⁴, S.J. McMahon¹³¹, R.A. McPherson^{169,k}, M. Medinnis⁴²,
 S. Meehan^{145a}, S. Mehlhase¹⁰⁰, A. Mehta⁷⁴, K. Meier^{58a}, C. Meineck¹⁰⁰, B. Meirose⁴¹,

B.R. Mellado Garcia^{145c}, F. Meloni¹⁷, A. Mengarelli^{20a,20b}, S. Menke¹⁰¹, E. Meoni¹⁶¹,
 K.M. Mercurio⁵⁷, S. Mergelmeyer²¹, P. Mermod⁴⁹, L. Merola^{104a,104b}, C. Meroni^{91a},
 F.S. Merritt³¹, A. Messina^{132a,132b}, J. Metcalfe²⁵, A.S. Mete¹⁶³, C. Meyer⁸³, C. Meyer¹²²,
 J.-P. Meyer¹³⁶, J. Meyer¹⁰⁷, H. Meyer Zu Theenhausen^{58a}, R.P. Middleton¹³¹,
 S. Miglioranzi^{164a,164c}, L. Mijović²¹, G. Mikenberg¹⁷², M. Mikestikova¹²⁷, M. Mikuz⁷⁵, M. Milesi⁸⁸,
 A. Milic³⁰, D.W. Miller³¹, C. Mills⁴⁶, A. Milov¹⁷², D.A. Milstead^{146a,146b}, A.A. Minaenko¹³⁰,
 Y. Minami¹⁵⁵, I.A. Minashvili⁶⁵, A.I. Mincer¹¹⁰, B. Mindur^{38a}, M. Mineev⁶⁵, Y. Ming¹⁷³,
 L.M. Mir¹², T. Mitani¹⁷¹, J. Mitrevski¹⁰⁰, V.A. Mitsou¹⁶⁷, A. Miucci⁴⁹, P.S. Miyagawa¹³⁹,
 J.U. Mjörnmark⁸¹, T. Moa^{146a,146b}, K. Mochizuki⁸⁵, S. Mohapatra³⁵, W. Mohr⁴⁸,
 S. Molander^{146a,146b}, R. Moles-Valls²¹, R. Monden⁶⁸, K. Mönig⁴², C. Monini⁵⁵, J. Monk³⁶,
 E. Monnier⁸⁵, J. Montejó Berlingen¹², F. Monticelli⁷¹, S. Monzani^{132a,132b}, R.W. Moore³,
 N. Morange¹¹⁷, D. Moreno¹⁶², M. Moreno Llácer⁵⁴, P. Morettini^{50a}, D. Mori¹⁴², M. Morii⁵⁷,
 M. Morinaga¹⁵⁵, V. Morisbak¹¹⁹, S. Moritz⁸³, A.K. Morley¹⁵⁰, G. Mornacchi³⁰, J.D. Morris⁷⁶,
 S.S. Mortensen³⁶, A. Morton⁵³, L. Morvaj¹⁰³, M. Mosidze^{51b}, J. Moss¹⁴³, K. Motohashi¹⁵⁷,
 R. Mount¹⁴³, E. Mountricha²⁵, S.V. Mouraviev^{96,*}, E.J.W. Moyse⁸⁶, S. Muanza⁸⁵, R.D. Mudd¹⁸,
 F. Mueller¹⁰¹, J. Mueller¹²⁵, R.S.P. Mueller¹⁰⁰, T. Mueller²⁸, D. Muenstermann⁴⁹, P. Mullen⁵³,
 G.A. Mullier¹⁷, J.A. Murillo Quijada¹⁸, W.J. Murray^{170,131}, H. Musheghyan⁵⁴, E. Musto¹⁵²,
 A.G. Myagkov^{130,ab}, M. Myska¹²⁸, B.P. Nachman¹⁴³, O. Nackenhorst⁵⁴, J. Nadal⁵⁴, K. Nagai¹²⁰,
 R. Nagai¹⁵⁷, Y. Nagai⁸⁵, K. Nagano⁶⁶, A. Nagarkar¹¹¹, Y. Nagasaka⁵⁹, K. Nagata¹⁶⁰, M. Nagel¹⁰¹,
 E. Nagy⁸⁵, A.M. Nairz³⁰, Y. Nakahama³⁰, K. Nakamura⁶⁶, T. Nakamura¹⁵⁵, I. Nakano¹¹²,
 H. Namasivayam⁴¹, R.F. Naranjo Garcia⁴², R. Narayan³¹, D.I. Narrias Villar^{58a}, T. Naumann⁴²,
 G. Navarro¹⁶², R. Nayyar⁷, H.A. Neal⁸⁹, P.Yu. Nechaeva⁹⁶, T.J. Neep⁸⁴, P.D. Nef¹⁴³,
 A. Negri^{121a,121b}, M. Negrini^{20a}, S. Nektarijevic¹⁰⁶, C. Nellist¹¹⁷, A. Nelson¹⁶³, S. Nemecek¹²⁷,
 P. Nemethy¹¹⁰, A.A. Nepomuceno^{24a}, M. Nessi^{30,ac}, M.S. Neubauer¹⁶⁵, M. Neumann¹⁷⁵,
 R.M. Neves¹¹⁰, P. Nevski²⁵, P.R. Newman¹⁸, D.H. Nguyen⁶, R.B. Nickerson¹²⁰, R. Nicolaidou¹³⁶,
 B. Nicquevert³⁰, J. Nielsen¹³⁷, N. Nikiforou³⁵, A. Nikiforov¹⁶, V. Nikolaenko^{130,ab},
 I. Nikolic-Audit⁸⁰, K. Nikolopoulos¹⁸, J.K. Nilsen¹¹⁹, P. Nilsson²⁵, Y. Ninomiya¹⁵⁵, A. Nisati^{132a},
 R. Nisius¹⁰¹, T. Nobe¹⁵⁵, M. Nomachi¹¹⁸, I. Nomidis²⁹, T. Nooney⁷⁶, S. Norberg¹¹³,
 M. Nordberg³⁰, O. Novgorodova⁴⁴, S. Nowak¹⁰¹, M. Nozaki⁶⁶, L. Nozka¹¹⁵, K. Ntekas¹⁰,
 G. Nunes Hanninger⁸⁸, T. Nunnemann¹⁰⁰, E. Nurse⁷⁸, F. Nuti⁸⁸, B.J. O'Brien⁴⁶, F. O'grady⁷,
 D.C. O'Neil¹⁴², V. O'Shea⁵³, F.G. Oakham^{29,d}, H. Oberlack¹⁰¹, T. Obermann²¹, J. Ocariz⁸⁰,
 A. Ochi⁶⁷, I. Ochoa⁷⁸, J.P. Ochoa-Ricoux^{32a}, S. Oda⁷⁰, S. Odaka⁶⁶, H. Ogren⁶¹, A. Oh⁸⁴,
 S.H. Oh⁴⁵, C.C. Ohm¹⁵, H. Ohman¹⁶⁶, H. Oide³⁰, W. Okamura¹¹⁸, H. Okawa¹⁶⁰, Y. Okumura³¹,
 T. Okuyama⁶⁶, A. Olariu^{26a}, S.A. Olivares Pino⁴⁶, D. Oliveira Damazio²⁵, E. Oliver Garcia¹⁶⁷,
 A. Olszewski³⁹, J. Olszowska³⁹, A. Onofre^{126a,126e}, K. Onogi¹⁰³, P.U.E. Onyisi^{31,r}, C.J. Oram^{159a},
 M.J. Oreglia³¹, Y. Oren¹⁵³, D. Orestano^{134a,134b}, N. Orlando¹⁵⁴, C. Oropeza Barrera⁵³,
 R.S. Orr¹⁵⁸, B. Osculati^{50a,50b}, R. Ospanov⁸⁴, G. Otero y Garzon²⁷, H. Otono⁷⁰, M. Ouchrif^{135d},
 F. Ould-Saada¹¹⁹, A. Ouraou¹³⁶, K.P. Oussoren¹⁰⁷, Q. Ouyang^{33a}, A. Ovcharova¹⁵, M. Owen⁵³,
 R.E. Owen¹⁸, V.E. Ozcan^{19a}, N. Ozturk⁸, K. Pachal¹⁴², A. Pacheco Pages¹², C. Padilla Aranda¹²,
 M. Pagáčová⁴⁸, S. Pagan Griso¹⁵, E. Paganis¹³⁹, F. Paige²⁵, P. Pais⁸⁶, K. Pajchel¹¹⁹,
 G. Palacino^{159b}, S. Palestini³⁰, M. Palka^{38b}, D. Pallin³⁴, A. Palma^{126a,126b}, Y.B. Pan¹⁷³,
 E. Panagiotopoulou¹⁰, C.E. Pandini⁸⁰, J.G. Panduro Vazquez⁷⁷, P. Pani^{146a,146b}, S. Panitkin²⁵,
 D. Pantea^{26a}, L. Paolozzi⁴⁹, Th.D. Papadopoulou¹⁰, K. Papageorgiou¹⁵⁴, A. Paramonov⁶,
 D. Paredes Hernandez¹⁵⁴, M.A. Parker²⁸, K.A. Parker¹³⁹, F. Parodi^{50a,50b}, J.A. Parsons³⁵,
 U. Parzefall⁴⁸, E. Pasqualucci^{132a}, S. Passaggio^{50a}, F. Pastore^{134a,134b,*}, Fr. Pastore⁷⁷,
 G. Pásztor²⁹, S. Pataria¹⁷⁵, N.D. Patel¹⁵⁰, J.R. Pater⁸⁴, T. Pauly³⁰, J. Pearce¹⁶⁹, B. Pearson¹¹³,
 L.E. Pedersen³⁶, M. Pedersen¹¹⁹, S. Pedraza Lopez¹⁶⁷, R. Pedro^{126a,126b}, S.V. Peleganchuk^{109,c},
 D. Pelikan¹⁶⁶, O. Penc¹²⁷, C. Peng^{33a}, H. Peng^{33b}, B. Penning³¹, J. Penwell⁶¹, D.V. Perepelitsa²⁵,

E. Perez Codina^{159a}, M.T. Pérez García-Estañ¹⁶⁷, L. Perini^{91a,91b}, H. Pernegger³⁰,
 S. Perrella^{104a,104b}, R. Peschke⁴², V.D. Peshekhonov⁶⁵, K. Peters³⁰, R.F.Y. Peters⁸⁴,
 B.A. Petersen³⁰, T.C. Petersen³⁶, E. Petit⁴², A. Petridis¹, C. Petridou¹⁵⁴, P. Petroff¹¹⁷,
 E. Petrolu^{132a}, F. Petrucci^{134a,134b}, N.E. Pettersson¹⁵⁷, R. Pezoa^{32b}, P.W. Phillips¹³¹,
 G. Piacquadio¹⁴³, E. Pianori¹⁷⁰, A. Picazio⁴⁹, E. Piccaro⁷⁶, M. Piccinini^{20a,20b}, M.A. Pickering¹²⁰,
 R. Piegai²⁷, D.T. Pignotti¹¹¹, J.E. Pilcher³¹, A.D. Pilkington⁸⁴, J. Pina^{126a,126b,126d},
 M. Pinamonti^{164a,164c,ad}, J.L. Pinfold³, A. Pingel³⁶, S. Pires⁸⁰, H. Pirumov⁴², M. Pitt¹⁷²,
 C. Pizio^{91a,91b}, L. Plazak^{144a}, M.-A. Pleier²⁵, V. Pleskot¹²⁹, E. Plotnikova⁶⁵, P. Plucinski^{146a,146b},
 D. Pluth⁶⁴, R. Poettgen^{146a,146b}, L. Poggioli¹¹⁷, D. Pohl²¹, G. Polesello^{121a}, A. Poley⁴²,
 A. Policicchio^{37a,37b}, R. Polifka¹⁵⁸, A. Polini^{20a}, C.S. Pollard⁵³, V. Polychronakos²⁵,
 K. Pommès³⁰, L. Pontecorvo^{132a}, B.G. Pope⁹⁰, G.A. Popeneciu^{26b}, D.S. Popovic¹³,
 A. Poppleton³⁰, S. Pospisil¹²⁸, K. Potamianos¹⁵, I.N. Potrap⁶⁵, C.J. Potter¹⁴⁹, C.T. Potter¹¹⁶,
 G. Poulard³⁰, J. Poveda³⁰, V. Pozdnyakov⁶⁵, P. Pralavorio⁸⁵, A. Pranko¹⁵, S. Prasad³⁰, S. Prell⁶⁴,
 D. Price⁸⁴, L.E. Price⁶, M. Primavera^{73a}, S. Prince⁸⁷, M. Proissl⁴⁶, K. Prokofiev^{60c},
 F. Prokoshin^{32b}, E. Protopapadaki¹³⁶, S. Protopopescu²⁵, J. Proudfoot⁶, M. Przybycien^{38a},
 E. Ptacek¹¹⁶, D. Puddu^{134a,134b}, E. Pueschel⁸⁶, D. Puldon¹⁴⁸, M. Purohit^{25,ae}, P. Puzo¹¹⁷,
 J. Qian⁸⁹, G. Qin⁵³, Y. Qin⁸⁴, A. Quadt⁵⁴, D.R. Quarrie¹⁵, W.B. Quayle^{164a,164b},
 M. Queitsch-Maitland⁸⁴, D. Quilty⁵³, S. Raddum¹¹⁹, V. Radeka²⁵, V. Radescu⁴²,
 S.K. Radhakrishnan¹⁴⁸, P. Radloff¹¹⁶, P. Rados⁸⁸, F. Ragusa^{91a,91b}, G. Rahal¹⁷⁸,
 S. Rajagopalan²⁵, M. Rammensee³⁰, C. Rangel-Smith¹⁶⁶, F. Rauscher¹⁰⁰, S. Rave⁸³,
 T. Ravenscroft⁵³, M. Raymond³⁰, A.L. Read¹¹⁹, N.P. Readioff⁷⁴, D.M. Rebutzi^{121a,121b},
 A. Redelbach¹⁷⁴, G. Redlinger²⁵, R. Reece¹³⁷, K. Reeves⁴¹, L. Rehnisch¹⁶, J. Reichert¹²²,
 H. Reisin²⁷, M. Relich¹⁶³, C. Rembser³⁰, H. Ren^{33a}, A. Renaud¹¹⁷, M. Rescigno^{132a},
 S. Resconi^{91a}, O.L. Rezanova^{109,c}, P. Reznicek¹²⁹, R. Rezvani⁹⁵, R. Richter¹⁰¹, S. Richter⁷⁸,
 E. Richter-Was^{38b}, O. Ricken²¹, M. Ridel⁸⁰, P. Rieck¹⁶, C.J. Riegel¹⁷⁵, J. Rieger⁵⁴, O. Rifki¹¹³,
 M. Rijssenbeek¹⁴⁸, A. Rimoldi^{121a,121b}, L. Rinaldi^{20a}, B. Ristić⁴⁹, E. Ritsch³⁰, I. Riu¹²,
 F. Rizatdinova¹¹⁴, E. Rizvi⁷⁶, S.H. Robertson^{87,k}, A. Robichaud-Veronneau⁸⁷, D. Robinson²⁸,
 J.E.M. Robinson⁴², A. Robson⁵³, C. Roda^{124a,124b}, S. Roe³⁰, O. Röhne¹¹⁹, S. Rolli¹⁶¹,
 A. Romaniouk⁹⁸, M. Romano^{20a,20b}, S.M. Romano Saez³⁴, E. Romero Adam¹⁶⁷, N. Rompotis¹³⁸,
 M. Ronzani⁴⁸, L. Roos⁸⁰, E. Ros¹⁶⁷, S. Rosati^{132a}, K. Rosbach⁴⁸, P. Rose¹³⁷, P.L. Rosendahl¹⁴,
 O. Rosenthal¹⁴¹, V. Rossetti^{146a,146b}, E. Rossi^{104a,104b}, L.P. Rossi^{50a}, J.H.N. Rosten²⁸,
 R. Rosten¹³⁸, M. Rotaru^{26a}, I. Roth¹⁷², J. Rothberg¹³⁸, D. Rousseau¹¹⁷, C.R. Royon¹³⁶,
 A. Rozanov⁸⁵, Y. Rozen¹⁵², X. Ruan^{145c}, F. Rubbo¹⁴³, I. Rubinskiy⁴², V.I. Rud⁹⁹, C. Rudolph⁴⁴,
 M.S. Rudolph¹⁵⁸, F. Rühr⁴⁸, A. Ruiz-Martinez³⁰, Z. Rurikova⁴⁸, N.A. Rusakovich⁶⁵,
 A. Ruschke¹⁰⁰, H.L. Russell¹³⁸, J.P. Rutherford⁷, N. Ruthmann⁴⁸, Y.F. Ryabov¹²³, M. Rybar¹⁶⁵,
 G. Rybkin¹¹⁷, N.C. Ryder¹²⁰, A.F. Saavedra¹⁵⁰, G. Sabato¹⁰⁷, S. Sacerdoti²⁷, A. Saddique³,
 H.F.-W. Sadrozinski¹³⁷, R. Sadykov⁶⁵, F. Safai Tehrani^{132a}, M. Sahinsoy^{58a}, M. Saimpert¹³⁶,
 T. Saito¹⁵⁵, H. Sakamoto¹⁵⁵, Y. Sakurai¹⁷¹, G. Salamanna^{134a,134b}, A. Salamon^{133a},
 J.E. Salazar Loyola^{32b}, M. Saleem¹¹³, D. Salek¹⁰⁷, P.H. Sales De Bruin¹³⁸, D. Salihagic¹⁰¹,
 A. Salmikov¹⁴³, J. Salt¹⁶⁷, D. Salvatore^{37a,37b}, F. Salvatore¹⁴⁹, A. Salvucci^{60a}, A. Salzburger³⁰,
 D. Sammel⁴⁸, D. Sampsonidis¹⁵⁴, A. Sanchez^{104a,104b}, J. Sánchez¹⁶⁷, V. Sanchez Martinez¹⁶⁷,
 H. Sandaker¹¹⁹, R.L. Sandbach⁷⁶, H.G. Sander⁸³, M.P. Sanders¹⁰⁰, M. Sandhoff¹⁷⁵,
 C. Sandoval¹⁶², R. Sandstroem¹⁰¹, D.P.C. Sankey¹³¹, M. Sannino^{50a,50b}, A. Sansoni⁴⁷,
 C. Santoni³⁴, R. Santonico^{133a,133b}, H. Santos^{126a}, I. Santoyo Castillo¹⁴⁹, K. Sapp¹²⁵,
 A. Sapronov⁶⁵, J.G. Saraiva^{126a,126d}, B. Sarrazin²¹, O. Sasaki⁶⁶, Y. Sasaki¹⁵⁵, K. Sato¹⁶⁰,
 G. Sauvage^{5,*}, E. Sauvan⁵, G. Savage⁷⁷, P. Savard^{158,d}, C. Sawyer¹³¹, L. Sawyer^{79,n}, J. Saxon³¹,
 C. Sbarra^{20a}, A. Sbrizzi^{20a,20b}, T. Scanlon⁷⁸, D.A. Scannicchio¹⁶³, M. Scarcella¹⁵⁰,
 V. Scarfone^{37a,37b}, J. Schaarschmidt¹⁷², P. Schacht¹⁰¹, D. Schaefer³⁰, R. Schaefer⁴², J. Schaeffer⁸³,

S. Schaepe²¹, S. Schaezel^{58b}, U. Schäfer⁸³, A.C. Schaffer¹¹⁷, D. Schaile¹⁰⁰, R.D. Schamberger¹⁴⁸, V. Scharf^{58a}, V.A. Schegelsky¹²³, D. Scheirich¹²⁹, M. Schernau¹⁶³, C. Schiavi^{50a,50b}, C. Schillo⁴⁸, M. Schioppa^{37a,37b}, S. Schlenker³⁰, K. Schmieden³⁰, C. Schmitt⁸³, S. Schmitt^{58b}, S. Schmitt⁴², B. Schneider^{159a}, Y.J. Schnellbach⁷⁴, U. Schnoor⁴⁴, L. Schoeffel¹³⁶, A. Schoening^{58b}, B.D. Schoenrock⁹⁰, E. Schopf²¹, A.L.S. Schorlemmer⁵⁴, M. Schott⁸³, D. Schouten^{159a}, J. Schovancova⁸, S. Schramm⁴⁹, M. Schreyer¹⁷⁴, C. Schroeder⁸³, N. Schuh⁸³, M.J. Schultens²¹, H.-C. Schultz-Coulon^{58a}, H. Schulz¹⁶, M. Schumacher⁴⁸, B.A. Schumm¹³⁷, Ph. Schune¹³⁶, C. Schwanenberger⁸⁴, A. Schwartzman¹⁴³, T.A. Schwarz⁸⁹, Ph. Schwegler¹⁰¹, H. Schweiger⁸⁴, Ph. Schwemling¹³⁶, R. Schwienhorst⁹⁰, J. Schwindling¹³⁶, T. Schwindt²¹, F.G. Sciaccia¹⁷, E. Scifo¹¹⁷, G. Sciolla²³, F. Scuri^{124a,124b}, F. Scutti²¹, J. Searcy⁸⁹, G. Sedov⁴², E. Sedykh¹²³, P. Seema²¹, S.C. Seidel¹⁰⁵, A. Seiden¹³⁷, F. Seifert¹²⁸, J.M. Seixas^{24a}, G. Sekhniaidze^{104a}, K. Sekhon⁸⁹, S.J. Sekula⁴⁰, D.M. Seliverstov^{123,*}, N. Semprini-Cesari^{20a,20b}, C. Serfon³⁰, L. Serin¹¹⁷, L. Serkin^{164a,164b}, T. Serre⁸⁵, M. Sessa^{134a,134b}, R. Seuster^{159a}, H. Severini¹¹³, T. Sfiligoj⁷⁵, F. Sforza³⁰, A. Sfyrila³⁰, E. Shabalina⁵⁴, M. Shamim¹¹⁶, L.Y. Shan^{33a}, R. Shang¹⁶⁵, J.T. Shank²², M. Shapiro¹⁵, P.B. Shatalov⁹⁷, K. Shaw^{164a,164b}, S.M. Shaw⁸⁴, A. Shcherbakova^{146a,146b}, C.Y. Shehu¹⁴⁹, P. Sherwood⁷⁸, L. Shi^{151,af}, S. Shimizu⁶⁷, C.O. Shimmin¹⁶³, M. Shimojima¹⁰², M. Shiyakova⁶⁵, A. Shmeleva⁹⁶, D. Shoaleh Saadi⁹⁵, M.J. Shochet³¹, S. Shojaii^{91a,91b}, S. Shrestha¹¹¹, E. Shulga⁹⁸, M.A. Shupe⁷, S. Shushkevich⁴², P. Sicho¹²⁷, P.E. Sidebo¹⁴⁷, O. Sidiropoulou¹⁷⁴, D. Sidorov¹¹⁴, A. Sidoti^{20a,20b}, F. Siegert⁴⁴, Dj. Sijacki¹³, J. Silva^{126a,126d}, Y. Silver¹⁵³, S.B. Silverstein^{146a}, V. Simak¹²⁸, O. Simard⁵, Lj. Simic¹³, S. Simion¹¹⁷, E. Simioni⁸³, B. Simmons⁷⁸, D. Simon³⁴, P. Sinervo¹⁵⁸, N.B. Sinev¹¹⁶, M. Sioli^{20a,20b}, G. Siragusa¹⁷⁴, A.N. Sisakyan^{65,*}, S.Yu. Sivoklov⁹⁹, J. Sjölin^{146a,146b}, T.B. Sjurson¹⁴, M.B. Skinner⁷², H.P. Skottowe⁵⁷, P. Skubic¹¹³, M. Slater¹⁸, T. Slavicek¹²⁸, M. Slawinska¹⁰⁷, K. Sliwa¹⁶¹, V. Smakhtin¹⁷², B.H. Smart⁴⁶, L. Smestad¹⁴, S.Yu. Smirnov⁹⁸, Y. Smirnov⁹⁸, L.N. Smirnova^{99,ag}, O. Smirnova⁸¹, M.N.K. Smith³⁵, R.W. Smith³⁵, M. Smizanska⁷², K. Smolek¹²⁸, A.A. Snesarev⁹⁶, G. Snidero⁷⁶, S. Snyder²⁵, R. Sobie^{169,k}, F. Socher⁴⁴, A. Soffer¹⁵³, D.A. Soh^{151,af}, G. Sokhrannyi⁷⁵, C.A. Solans³⁰, M. Solar¹²⁸, J. Solc¹²⁸, E.Yu. Soldatov⁹⁸, U. Soldevila¹⁶⁷, A.A. Solodkov¹³⁰, A. Soloshenko⁶⁵, O.V. Solovyanov¹³⁰, V. Solovyev¹²³, P. Sommer⁴⁸, H.Y. Song^{33b}, N. Soni¹, A. Sood¹⁵, A. Sopczak¹²⁸, B. Sopko¹²⁸, V. Sopko¹²⁸, V. Sorin¹², D. Sosa^{58b}, M. Sosebee⁸, C.L. Sotiropoulou^{124a,124b}, R. Soualah^{164a,164c}, A.M. Soukharev^{109,c}, D. South⁴², B.C. Sowden⁷⁷, S. Spagnolo^{73a,73b}, M. Spalla^{124a,124b}, M. Spangenberg¹⁷⁰, F. Spanò⁷⁷, W.R. Spearman⁵⁷, D. Sperlich¹⁶, F. Spettel¹⁰¹, R. Spighi^{20a}, G. Spigo³⁰, L.A. Spiller⁸⁸, M. Spousta¹²⁹, T. Spreitzer¹⁵⁸, R.D. St. Denis^{53,*}, A. Stabile^{91a}, S. Staerz⁴⁴, J. Stahlman¹²², R. Stamen^{58a}, S. Stamm¹⁶, E. Stanecka³⁹, C. Stanescu^{134a}, M. Stanescu-Bellu⁴², M.M. Stanitzki⁴², S. Stapnes¹¹⁹, E.A. Starchenko¹³⁰, J. Stark⁵⁵, P. Staroba¹²⁷, P. Starovoitov^{58a}, R. Staszewski³⁹, P. Steinberg²⁵, B. Stelzer¹⁴², H.J. Stelzer³⁰, O. Stelzer-Chilton^{159a}, H. Stenzel⁵², G.A. Stewart⁵³, J.A. Stillings²¹, M.C. Stockton⁸⁷, M. Stoebe⁸⁷, G. Stoicea^{26a}, P. Stolte⁵⁴, S. Stonjek¹⁰¹, A.R. Stradling⁸, A. Straessner⁴⁴, M.E. Stramaglia¹⁷, J. Strandberg¹⁴⁷, S. Strandberg^{146a,146b}, A. Strandlie¹¹⁹, E. Strauss¹⁴³, M. Strauss¹¹³, P. Striznec^{144b}, R. Ströhmer¹⁷⁴, D.M. Strom¹¹⁶, R. Stroynowski⁴⁰, A. Strubig¹⁰⁶, S.A. Stucci¹⁷, B. Stugu¹⁴, N.A. Styles⁴², D. Su¹⁴³, J. Su¹²⁵, R. Subramaniam⁷⁹, A. Succurro¹², Y. Sugaya¹¹⁸, M. Suk¹²⁸, V.V. Sulin⁹⁶, S. Sultansoy^{4c}, T. Sumida⁶⁸, S. Sun⁵⁷, X. Sun^{33a}, J.E. Sundermann⁴⁸, K. Suruliz¹⁴⁹, G. Susinno^{37a,37b}, M.R. Sutton¹⁴⁹, S. Suzuki⁶⁶, M. Svatos¹²⁷, M. Swiatlowski¹⁴³, I. Sykora^{144a}, T. Sykora¹²⁹, D. Ta⁴⁸, C. Taccini^{134a,134b}, K. Tackmann⁴², J. Taenzer¹⁵⁸, A. Taffard¹⁶³, R. Tafirout^{159a}, N. Taiblum¹⁵³, H. Takai²⁵, R. Takashima⁶⁹, H. Takeda⁶⁷, T. Takeshita¹⁴⁰, Y. Takubo⁶⁶, M. Talby⁸⁵, A.A. Talyshv^{109,c}, J.Y.C. Tam¹⁷⁴, K.G. Tan⁸⁸, J. Tanaka¹⁵⁵, R. Tanaka¹¹⁷, S. Tanaka⁶⁶, B.B. Tannenwald¹¹¹, N. Tannoury²¹, S. Tapprogge⁸³, S. Tarem¹⁵², F. Tarrade²⁹, G.F. Tartarelli^{91a}, P. Tas¹²⁹, M. Tasevsky¹²⁷,

T. Tashiro⁶⁸, E. Tassi^{37a,37b}, A. Tavares Delgado^{126a,126b}, Y. Tayalati^{135d}, F.E. Taylor⁹⁴, G.N. Taylor⁸⁸, P.T.E. Taylor⁸⁸, W. Taylor^{159b}, F.A. Teischinger³⁰, M. Teixeira Dias Castanheira⁷⁶, P. Teixeira-Dias⁷⁷, K.K. Temming⁴⁸, D. Temple¹⁴², H. Ten Kate³⁰, P.K. Teng¹⁵¹, J.J. Teoh¹¹⁸, F. Tepel¹⁷⁵, S. Terada⁶⁶, K. Terashi¹⁵⁵, J. Terron⁸², S. Terzo¹⁰¹, M. Testa⁴⁷, R.J. Teuscher^{158,k}, T. Theveneaux-Pelzer³⁴, J.P. Thomas¹⁸, J. Thomas-Wilsker⁷⁷, E.N. Thompson³⁵, P.D. Thompson¹⁸, R.J. Thompson⁸⁴, A.S. Thompson⁵³, L.A. Thomsen¹⁷⁶, E. Thomson¹²², M. Thomson²⁸, R.P. Thun^{89,*}, M.J. Tibbetts¹⁵, R.E. Ticse Torres⁸⁵, V.O. Tikhomirov^{96,ah}, Yu.A. Tikhonov^{109,c}, S. Timoshenko⁹⁸, E. Tiouchichine⁸⁵, P. Tipton¹⁷⁶, S. Tisserant⁸⁵, K. Todome¹⁵⁷, T. Todorov^{5,*}, S. Todorova-Nova¹²⁹, J. Tojo⁷⁰, S. Tokár^{144a}, K. Tokushuku⁶⁶, K. Tollefson⁹⁰, E. Tolley⁵⁷, L. Tomlinson⁸⁴, M. Tomoto¹⁰³, L. Tompkins^{143,ai}, K. Toms¹⁰⁵, E. Torrence¹¹⁶, H. Torres¹⁴², E. Torró Pastor¹³⁸, J. Toth^{85,aj}, F. Touchard⁸⁵, D.R. Tovey¹³⁹, T. Trefzger¹⁷⁴, L. Tremblet³⁰, A. Tricoli³⁰, I.M. Trigger^{159a}, S. Trincaz-Duvold⁸⁰, M.F. Tripiana¹², W. Trischuk¹⁵⁸, B. Trocme⁵⁵, C. Troncon^{91a}, M. Trottier-McDonald¹⁵, M. Trovatelli¹⁶⁹, P. True⁹⁰, L. Truong^{164a,164c}, M. Trzebinski³⁹, A. Trzupek³⁹, C. Tsarouchas³⁰, J.C-L. Tseng¹²⁰, P.V. Tsiareshka⁹², D. Tsionou¹⁵⁴, G. Tsipolitis¹⁰, N. Tsirintanis⁹, S. Tsiskaridze¹², V. Tsiskaridze⁴⁸, E.G. Tskhadadze^{51a}, I.I. Tsukerman⁹⁷, V. Tsulaia¹⁵, S. Tsuno⁶⁶, D. Tsybychev¹⁴⁸, A. Tudorache^{26a}, V. Tudorache^{26a}, A.N. Tuna⁵⁷, S.A. Tuppiti^{20a,20b}, S. Turchikhin^{99,ag}, D. Turecek¹²⁸, R. Turra^{91a,91b}, A.J. Turvey⁴⁰, P.M. Tuts³⁵, A. Tykhonov⁴⁹, M. Tylmad^{146a,146b}, M. Tyndel¹³¹, I. Ueda¹⁵⁵, R. Ueno²⁹, M. Ughetto^{146a,146b}, M. Ugland¹⁴, F. Ukegawa¹⁶⁰, G. Unal³⁰, A. Undrus²⁵, G. Unel¹⁶³, F.C. Ungaro⁴⁸, Y. Unno⁶⁶, C. Unverdorben¹⁰⁰, J. Urban^{144b}, P. Urquijo⁸⁸, P. Urrejola⁸³, G. Usai⁸, A. Usanova⁶², L. Vacavant⁸⁵, V. Vacek¹²⁸, B. Vachon⁸⁷, C. Valderanis⁸³, N. Valencic¹⁰⁷, S. Valentineti^{20a,20b}, A. Valero¹⁶⁷, L. Valery¹², S. Valkar¹²⁹, E. Valladolid Gallego¹⁶⁷, S. Vallecorsa⁴⁹, J.A. Valls Ferrer¹⁶⁷, W. Van Den Wollenberg¹⁰⁷, P.C. Van Der Deijl¹⁰⁷, R. van der Geer¹⁰⁷, H. van der Graaf¹⁰⁷, N. van Eldik¹⁵², P. van Gemmeren⁶, J. Van Nieuwkoop¹⁴², I. van Vulpen¹⁰⁷, M.C. van Woerden³⁰, M. Vanadia^{132a,132b}, W. Vandelli³⁰, R. Vanguri¹²², A. Vaniachine⁶, F. Vannucci⁸⁰, G. Vardanyan¹⁷⁷, R. Vari^{132a}, E.W. Varnes⁷, T. Varol⁴⁰, D. Varouchas⁸⁰, A. Vartapetian⁸, K.E. Varvell¹⁵⁰, F. Vazeille³⁴, T. Vazquez Schroeder⁸⁷, J. Veatch⁷, L.M. Veloce¹⁵⁸, F. Veloso^{126a,126c}, T. Velz²¹, S. Veneziano^{132a}, A. Ventura^{73a,73b}, D. Ventura⁸⁶, M. Venturi¹⁶⁹, N. Venturi¹⁵⁸, A. Venturini²³, V. Vercesi^{121a}, M. Verducci^{132a,132b}, W. Verkerke¹⁰⁷, J.C. Vermeulen¹⁰⁷, A. Vest⁴⁴, M.C. Vetterli^{142,d}, O. Viazlo⁸¹, I. Vichou¹⁶⁵, T. Vickey¹³⁹, O.E. Vickey Boeriu¹³⁹, G.H.A. Viehhauser¹²⁰, S. Viel¹⁵, R. Vigne⁶², M. Villa^{20a,20b}, M. Villaplana Perez^{91a,91b}, E. Vilucchi⁴⁷, M.G. Vincter²⁹, V.B. Vinogradov⁶⁵, I. Vivarelli¹⁴⁹, F. Vives Vague³, S. Vlachos¹⁰, D. Vladoiu¹⁰⁰, M. Vlasak¹²⁸, M. Vogel^{32a}, P. Vokac¹²⁸, G. Volpi^{124a,124b}, M. Volpi⁸⁸, H. von der Schmitt¹⁰¹, H. von Radziewski⁴⁸, E. von Toerne²¹, V. Vorobel¹²⁹, K. Vorobev⁹⁸, M. Vos¹⁶⁷, R. Voss³⁰, J.H. Vossebeld⁷⁴, N. Vranjes¹³, M. Vranjes Milosavljevic¹³, V. Vrba¹²⁷, M. Vreeswijk¹⁰⁷, R. Vuillermet³⁰, I. Vukotic³¹, Z. Vykydal¹²⁸, P. Wagner²¹, W. Wagner¹⁷⁵, H. Wahlberg⁷¹, S. Wahrenmund⁴⁴, J. Wakabayashi¹⁰³, J. Walder⁷², R. Walker¹⁰⁰, W. Walkowiak¹⁴¹, C. Wang¹⁵¹, F. Wang¹⁷³, H. Wang¹⁵, H. Wang⁴⁰, J. Wang⁴², J. Wang^{33a}, K. Wang⁸⁷, R. Wang⁶, S.M. Wang¹⁵¹, T. Wang²¹, T. Wang³⁵, X. Wang¹⁷⁶, C. Wanotayaroj¹¹⁶, A. Warburton⁸⁷, C.P. Ward²⁸, D.R. Wardrope⁷⁸, A. Washbrook⁴⁶, C. Wasicki⁴², P.M. Watkins¹⁸, A.T. Watson¹⁸, I.J. Watson¹⁵⁰, M.F. Watson¹⁸, G. Watts¹³⁸, S. Watts⁸⁴, B.M. Waugh⁷⁸, S. Webb⁸⁴, M.S. Weber¹⁷, S.W. Weber¹⁷⁴, J.S. Webster³¹, A.R. Weidberg¹²⁰, B. Weinert⁶¹, J. Weingarten⁵⁴, C. Weiser⁴⁸, H. Weits¹⁰⁷, P.S. Wells³⁰, T. Wenaus²⁵, T. Wengler³⁰, S. Wenig³⁰, N. Wermes²¹, M. Werner⁴⁸, P. Werner³⁰, M. Wessels^{58a}, J. Wetter¹⁶¹, K. Whalen¹¹⁶, A.M. Wharton⁷², A. White⁸, M.J. White¹, R. White^{32b}, S. White^{124a,124b}, D. Whiteson¹⁶³, F.J. Wickens¹³¹, W. Wiedenmann¹⁷³,

M. Wielers¹³¹, P. Wienemann²¹, C. Wigglesworth³⁶, L.A.M. Wiik-Fuchs²¹, A. Wildauer¹⁰¹, H.G. Wilkens³⁰, H.H. Williams¹²², S. Williams¹⁰⁷, C. Willis⁹⁰, S. Willocq⁸⁶, A. Wilson⁸⁹, J.A. Wilson¹⁸, I. Wingerter-Seez⁵, F. Winklmeier¹¹⁶, B.T. Winter²¹, M. Wittgen¹⁴³, J. Wittkowski¹⁰⁰, S.J. Wollstadt⁸³, M.W. Wolter³⁹, H. Wolters^{126a,126c}, B.K. Wosiek³⁹, J. Wotschack³⁰, M.J. Woudstra⁸⁴, K.W. Wozniak³⁹, M. Wu⁵⁵, M. Wu³¹, S.L. Wu¹⁷³, X. Wu⁴⁹, Y. Wu⁸⁹, T.R. Wyatt⁸⁴, B.M. Wynne⁴⁶, S. Xella³⁶, D. Xu^{33a}, L. Xu²⁵, B. Yabsley¹⁵⁰, S. Yacoub^{145a}, R. Yakabe⁶⁷, M. Yamada⁶⁶, D. Yamaguchi¹⁵⁷, Y. Yamaguchi¹¹⁸, A. Yamamoto⁶⁶, S. Yamamoto¹⁵⁵, T. Yamanaka¹⁵⁵, K. Yamauchi¹⁰³, Y. Yamazaki⁶⁷, Z. Yan²², H. Yang^{33e}, H. Yang¹⁷³, Y. Yang¹⁵¹, W.-M. Yao¹⁵, Y. Yasu⁶⁶, E. Yatsenko⁵, K.H. Yau Wong²¹, J. Ye⁴⁰, S. Ye²⁵, I. Yeletsikh⁶⁵, A.L. Yen⁵⁷, E. Yildirim⁴², K. Yorita¹⁷¹, R. Yoshida⁶, K. Yoshihara¹²², C. Young¹⁴³, C.J.S. Young³⁰, S. Youssef²², D.R. Yu¹⁵, J. Yu⁸, J.M. Yu⁸⁹, J. Yu¹¹⁴, L. Yuan⁶⁷, S.P.Y. Yuen²¹, A. Yurkewicz¹⁰⁸, I. Yusuff^{28.ak}, B. Zabinski³⁹, R. Zaidan⁶³, A.M. Zaitsev^{130.ab}, J. Zalieckas¹⁴, A. Zaman¹⁴⁸, S. Zambito⁵⁷, L. Zanello^{132a,132b}, D. Zanzi⁸⁸, C. Zeitnitz¹⁷⁵, M. Zeman¹²⁸, A. Zemla^{38a}, Q. Zeng¹⁴³, K. Zengel²³, O. Zenin¹³⁰, T. Ženiš^{144a}, D. Zerwas¹¹⁷, D. Zhang⁸⁹, F. Zhang¹⁷³, H. Zhang^{33c}, J. Zhang⁶, L. Zhang⁴⁸, R. Zhang^{33b}, X. Zhang^{33d}, Z. Zhang¹¹⁷, X. Zhao⁴⁰, Y. Zhao^{33d,117}, Z. Zhao^{33b}, A. Zhemchugov⁶⁵, J. Zhong¹²⁰, B. Zhou⁸⁹, C. Zhou⁴⁵, L. Zhou³⁵, L. Zhou⁴⁰, M. Zhou¹⁴⁸, N. Zhou^{33f}, C.G. Zhu^{33d}, H. Zhu^{33a}, J. Zhu⁸⁹, Y. Zhu^{33b}, X. Zhuang^{33a}, K. Zhukov⁹⁶, A. Zibell¹⁷⁴, D. Zieminska⁶¹, N.I. Zimine⁶⁵, C. Zimmermann⁸³, S. Zimmermann⁴⁸, Z. Zinonos⁵⁴, M. Zinser⁸³, M. Ziolkowski¹⁴¹, L. Živković¹³, G. Zobernig¹⁷³, A. Zoccoli^{20a,20b}, M. zur Nedden¹⁶, G. Zurzolo^{104a,104b}, L. Zwalinski³⁰.

¹ Department of Physics, University of Adelaide, Adelaide, Australia

² Physics Department, SUNY Albany, Albany NY, United States of America

³ Department of Physics, University of Alberta, Edmonton AB, Canada

⁴ (a) Department of Physics, Ankara University, Ankara; (b) Istanbul Aydin University, Istanbul; (c) Division of Physics, TOBB University of Economics and Technology, Ankara, Turkey

⁵ LAPP, CNRS/IN2P3 and Université Savoie Mont Blanc, Annecy-le-Vieux, France

⁶ High Energy Physics Division, Argonne National Laboratory, Argonne IL, United States of America

⁷ Department of Physics, University of Arizona, Tucson AZ, United States of America

⁸ Department of Physics, The University of Texas at Arlington, Arlington TX, United States of America

⁹ Physics Department, University of Athens, Athens, Greece

¹⁰ Physics Department, National Technical University of Athens, Zografou, Greece

¹¹ Institute of Physics, Azerbaijan Academy of Sciences, Baku, Azerbaijan

¹² Institut de Física d'Altes Energies and Departament de Física de la Universitat Autònoma de Barcelona, Barcelona, Spain

¹³ Institute of Physics, University of Belgrade, Belgrade, Serbia

¹⁴ Department for Physics and Technology, University of Bergen, Bergen, Norway

¹⁵ Physics Division, Lawrence Berkeley National Laboratory and University of California, Berkeley CA, United States of America

¹⁶ Department of Physics, Humboldt University, Berlin, Germany

¹⁷ Albert Einstein Center for Fundamental Physics and Laboratory for High Energy Physics, University of Bern, Bern, Switzerland

¹⁸ School of Physics and Astronomy, University of Birmingham, Birmingham, United Kingdom

¹⁹ (a) Department of Physics, Bogazici University, Istanbul; (b) Department of Physics Engineering, Gaziantep University, Gaziantep; (c) Department of Physics, Dogus University, Istanbul, Turkey

²⁰ (a) INFN Sezione di Bologna; (b) Dipartimento di Fisica e Astronomia, Università di Bologna, Bologna, Italy

²¹ Physikalisches Institut, University of Bonn, Bonn, Germany

²² Department of Physics, Boston University, Boston MA, United States of America

²³ Department of Physics, Brandeis University, Waltham MA, United States of America

- 24 (a) *Universidade Federal do Rio De Janeiro COPPE/EE/IF, Rio de Janeiro*; (b) *Electrical Circuits Department, Federal University of Juiz de Fora (UFJF), Juiz de Fora*; (c) *Federal University of Sao Joao del Rei (UFSJ), Sao Joao del Rei*; (d) *Instituto de Física, Universidade de Sao Paulo, Sao Paulo, Brazil*
- 25 *Physics Department, Brookhaven National Laboratory, Upton NY, United States of America*
- 26 (a) *National Institute of Physics and Nuclear Engineering, Bucharest*; (b) *National Institute for Research and Development of Isotopic and Molecular Technologies, Physics Department, Cluj Napoca*; (c) *University Politehnica Bucharest, Bucharest*; (d) *West University in Timisoara, Timisoara, Romania*
- 27 *Departamento de Física, Universidad de Buenos Aires, Buenos Aires, Argentina*
- 28 *Cavendish Laboratory, University of Cambridge, Cambridge, United Kingdom*
- 29 *Department of Physics, Carleton University, Ottawa ON, Canada*
- 30 *CERN, Geneva, Switzerland*
- 31 *Enrico Fermi Institute, University of Chicago, Chicago IL, United States of America*
- 32 (a) *Departamento de Física, Pontificia Universidad Católica de Chile, Santiago*; (b) *Departamento de Física, Universidad Técnica Federico Santa María, Valparaíso, Chile*
- 33 (a) *Institute of High Energy Physics, Chinese Academy of Sciences, Beijing*; (b) *Department of Modern Physics, University of Science and Technology of China, Anhui*; (c) *Department of Physics, Nanjing University, Jiangsu*; (d) *School of Physics, Shandong University, Shandong*; (e) *Department of Physics and Astronomy, Shanghai Key Laboratory for Particle Physics and Cosmology, Shanghai Jiao Tong University, Shanghai*; (f) *Physics Department, Tsinghua University, Beijing 100084, China*
- 34 *Laboratoire de Physique Corpusculaire, Clermont Université and Université Blaise Pascal and CNRS/IN2P3, Clermont-Ferrand, France*
- 35 *Nevis Laboratory, Columbia University, Irvington NY, United States of America*
- 36 *Niels Bohr Institute, University of Copenhagen, Kobenhavn, Denmark*
- 37 (a) *INFN Gruppo Collegato di Cosenza, Laboratori Nazionali di Frascati*; (b) *Dipartimento di Fisica, Università della Calabria, Rende, Italy*
- 38 (a) *AGH University of Science and Technology, Faculty of Physics and Applied Computer Science, Krakow*; (b) *Marian Smoluchowski Institute of Physics, Jagiellonian University, Krakow, Poland*
- 39 *Institute of Nuclear Physics Polish Academy of Sciences, Krakow, Poland*
- 40 *Physics Department, Southern Methodist University, Dallas TX, United States of America*
- 41 *Physics Department, University of Texas at Dallas, Richardson TX, United States of America*
- 42 *DESY, Hamburg and Zeuthen, Germany*
- 43 *Institut für Experimentelle Physik IV, Technische Universität Dortmund, Dortmund, Germany*
- 44 *Institut für Kern- und Teilchenphysik, Technische Universität Dresden, Dresden, Germany*
- 45 *Department of Physics, Duke University, Durham NC, United States of America*
- 46 *SUPA - School of Physics and Astronomy, University of Edinburgh, Edinburgh, United Kingdom*
- 47 *INFN Laboratori Nazionali di Frascati, Frascati, Italy*
- 48 *Fakultät für Mathematik und Physik, Albert-Ludwigs-Universität, Freiburg, Germany*
- 49 *Section de Physique, Université de Genève, Geneva, Switzerland*
- 50 (a) *INFN Sezione di Genova*; (b) *Dipartimento di Fisica, Università di Genova, Genova, Italy*
- 51 (a) *E. Andronikashvili Institute of Physics, Iv. Javakishvili Tbilisi State University, Tbilisi*; (b) *High Energy Physics Institute, Tbilisi State University, Tbilisi, Georgia*
- 52 *II Physikalisches Institut, Justus-Liebig-Universität Giessen, Giessen, Germany*
- 53 *SUPA - School of Physics and Astronomy, University of Glasgow, Glasgow, United Kingdom*
- 54 *II Physikalisches Institut, Georg-August-Universität, Göttingen, Germany*
- 55 *Laboratoire de Physique Subatomique et de Cosmologie, Université Grenoble-Alpes, CNRS/IN2P3, Grenoble, France*
- 56 *Department of Physics, Hampton University, Hampton VA, United States of America*
- 57 *Laboratory for Particle Physics and Cosmology, Harvard University, Cambridge MA, United States of America*

- 58 ^(a) *Kirchhoff-Institut für Physik, Ruprecht-Karls-Universität Heidelberg, Heidelberg;* ^(b)
Physikalisches Institut, Ruprecht-Karls-Universität Heidelberg, Heidelberg; ^(c) *ZITI Institut für*
technische Informatik, Ruprecht-Karls-Universität Heidelberg, Mannheim, Germany
- 59 *Faculty of Applied Information Science, Hiroshima Institute of Technology, Hiroshima, Japan*
- 60 ^(a) *Department of Physics, The Chinese University of Hong Kong, Shatin, N.T., Hong Kong;* ^(b)
Department of Physics, The University of Hong Kong, Hong Kong; ^(c) *Department of Physics, The*
Hong Kong University of Science and Technology, Clear Water Bay, Kowloon, Hong Kong, China
- 61 *Department of Physics, Indiana University, Bloomington IN, United States of America*
- 62 *Institut für Astro- und Teilchenphysik, Leopold-Franzens-Universität, Innsbruck, Austria*
- 63 *University of Iowa, Iowa City IA, United States of America*
- 64 *Department of Physics and Astronomy, Iowa State University, Ames IA, United States of America*
- 65 *Joint Institute for Nuclear Research, JINR Dubna, Dubna, Russia*
- 66 *KEK, High Energy Accelerator Research Organization, Tsukuba, Japan*
- 67 *Graduate School of Science, Kobe University, Kobe, Japan*
- 68 *Faculty of Science, Kyoto University, Kyoto, Japan*
- 69 *Kyoto University of Education, Kyoto, Japan*
- 70 *Department of Physics, Kyushu University, Fukuoka, Japan*
- 71 *Instituto de Física La Plata, Universidad Nacional de La Plata and CONICET, La Plata, Argentina*
- 72 *Physics Department, Lancaster University, Lancaster, United Kingdom*
- 73 ^(a) *INFN Sezione di Lecce;* ^(b) *Dipartimento di Matematica e Fisica, Università del Salento, Lecce,*
Italy
- 74 *Oliver Lodge Laboratory, University of Liverpool, Liverpool, United Kingdom*
- 75 *Department of Physics, Jožef Stefan Institute and University of Ljubljana, Ljubljana, Slovenia*
- 76 *School of Physics and Astronomy, Queen Mary University of London, London, United Kingdom*
- 77 *Department of Physics, Royal Holloway University of London, Surrey, United Kingdom*
- 78 *Department of Physics and Astronomy, University College London, London, United Kingdom*
- 79 *Louisiana Tech University, Ruston LA, United States of America*
- 80 *Laboratoire de Physique Nucléaire et de Hautes Energies, UPMC and Université Paris-Diderot and*
CNRS/IN2P3, Paris, France
- 81 *Fysiska institutionen, Lunds universitet, Lund, Sweden*
- 82 *Departamento de Física Teórica C-15, Universidad Autónoma de Madrid, Madrid, Spain*
- 83 *Institut für Physik, Universität Mainz, Mainz, Germany*
- 84 *School of Physics and Astronomy, University of Manchester, Manchester, United Kingdom*
- 85 *CPPM, Aix-Marseille Université and CNRS/IN2P3, Marseille, France*
- 86 *Department of Physics, University of Massachusetts, Amherst MA, United States of America*
- 87 *Department of Physics, McGill University, Montreal QC, Canada*
- 88 *School of Physics, University of Melbourne, Victoria, Australia*
- 89 *Department of Physics, The University of Michigan, Ann Arbor MI, United States of America*
- 90 *Department of Physics and Astronomy, Michigan State University, East Lansing MI, United States*
of America
- 91 ^(a) *INFN Sezione di Milano;* ^(b) *Dipartimento di Fisica, Università di Milano, Milano, Italy*
- 92 *B.I. Stepanov Institute of Physics, National Academy of Sciences of Belarus, Minsk, Republic of*
Belarus
- 93 *National Scientific and Educational Centre for Particle and High Energy Physics, Minsk, Republic*
of Belarus
- 94 *Department of Physics, Massachusetts Institute of Technology, Cambridge MA, United States of*
America
- 95 *Group of Particle Physics, University of Montreal, Montreal QC, Canada*
- 96 *P.N. Lebedev Institute of Physics, Academy of Sciences, Moscow, Russia*
- 97 *Institute for Theoretical and Experimental Physics (ITEP), Moscow, Russia*
- 98 *National Research Nuclear University MEPhI, Moscow, Russia*
- 99 *D.V. Skobeltsyn Institute of Nuclear Physics, M.V. Lomonosov Moscow State University, Moscow,*

- Russia
- 100 Fakultät für Physik, Ludwig-Maximilians-Universität München, München, Germany
- 101 Max-Planck-Institut für Physik (Werner-Heisenberg-Institut), München, Germany
- 102 Nagasaki Institute of Applied Science, Nagasaki, Japan
- 103 Graduate School of Science and Kobayashi-Maskawa Institute, Nagoya University, Nagoya, Japan
- 104 ^(a) INFN Sezione di Napoli; ^(b) Dipartimento di Fisica, Università di Napoli, Napoli, Italy
- 105 Department of Physics and Astronomy, University of New Mexico, Albuquerque NM, United States of America
- 106 Institute for Mathematics, Astrophysics and Particle Physics, Radboud University Nijmegen/Nikhef, Nijmegen, Netherlands
- 107 Nikhef National Institute for Subatomic Physics and University of Amsterdam, Amsterdam, Netherlands
- 108 Department of Physics, Northern Illinois University, DeKalb IL, United States of America
- 109 Budker Institute of Nuclear Physics, SB RAS, Novosibirsk, Russia
- 110 Department of Physics, New York University, New York NY, United States of America
- 111 Ohio State University, Columbus OH, United States of America
- 112 Faculty of Science, Okayama University, Okayama, Japan
- 113 Homer L. Dodge Department of Physics and Astronomy, University of Oklahoma, Norman OK, United States of America
- 114 Department of Physics, Oklahoma State University, Stillwater OK, United States of America
- 115 Palacký University, RCPTM, Olomouc, Czech Republic
- 116 Center for High Energy Physics, University of Oregon, Eugene OR, United States of America
- 117 LAL, Université Paris-Sud and CNRS/IN2P3, Orsay, France
- 118 Graduate School of Science, Osaka University, Osaka, Japan
- 119 Department of Physics, University of Oslo, Oslo, Norway
- 120 Department of Physics, Oxford University, Oxford, United Kingdom
- 121 ^(a) INFN Sezione di Pavia; ^(b) Dipartimento di Fisica, Università di Pavia, Pavia, Italy
- 122 Department of Physics, University of Pennsylvania, Philadelphia PA, United States of America
- 123 National Research Centre “Kurchatov Institute” B.P.Konstantinov Petersburg Nuclear Physics Institute, St. Petersburg, Russia
- 124 ^(a) INFN Sezione di Pisa; ^(b) Dipartimento di Fisica E. Fermi, Università di Pisa, Pisa, Italy
- 125 Department of Physics and Astronomy, University of Pittsburgh, Pittsburgh PA, United States of America
- 126 ^(a) Laboratório de Instrumentação e Física Experimental de Partículas - LIP, Lisboa; ^(b) Faculdade de Ciências, Universidade de Lisboa, Lisboa; ^(c) Department of Physics, University of Coimbra, Coimbra; ^(d) Centro de Física Nuclear da Universidade de Lisboa, Lisboa; ^(e) Departamento de Física, Universidade do Minho, Braga; ^(f) Departamento de Física Teórica y del Cosmos and CAFPE, Universidad de Granada, Granada (Spain); ^(g) Dep Física and CEFITEC of Faculdade de Ciências e Tecnologia, Universidade Nova de Lisboa, Caparica, Portugal
- 127 Institute of Physics, Academy of Sciences of the Czech Republic, Praha, Czech Republic
- 128 Czech Technical University in Prague, Praha, Czech Republic
- 129 Faculty of Mathematics and Physics, Charles University in Prague, Praha, Czech Republic
- 130 State Research Center Institute for High Energy Physics, Protvino, Russia
- 131 Particle Physics Department, Rutherford Appleton Laboratory, Didcot, United Kingdom
- 132 ^(a) INFN Sezione di Roma; ^(b) Dipartimento di Fisica, Sapienza Università di Roma, Roma, Italy
- 133 ^(a) INFN Sezione di Roma Tor Vergata; ^(b) Dipartimento di Fisica, Università di Roma Tor Vergata, Roma, Italy
- 134 ^(a) INFN Sezione di Roma Tre; ^(b) Dipartimento di Matematica e Fisica, Università Roma Tre, Roma, Italy
- 135 ^(a) Faculté des Sciences Ain Chock, Réseau Universitaire de Physique des Hautes Energies - Université Hassan II, Casablanca; ^(b) Centre National de l’Energie des Sciences Techniques Nucleaires, Rabat; ^(c) Faculté des Sciences Semlalia, Université Cadi Ayyad, LPHEA-Marrakech;

- (d) *Faculté des Sciences, Université Mohamed Premier and LPTPM, Oujda;* (e) *Faculté des sciences, Université Mohammed V, Rabat, Morocco*
- 136 *DSM/IRFU (Institut de Recherches sur les Lois Fondamentales de l'Univers), CEA Saclay (Commissariat à l'Energie Atomique et aux Energies Alternatives), Gif-sur-Yvette, France*
- 137 *Santa Cruz Institute for Particle Physics, University of California Santa Cruz, Santa Cruz CA, United States of America*
- 138 *Department of Physics, University of Washington, Seattle WA, United States of America*
- 139 *Department of Physics and Astronomy, University of Sheffield, Sheffield, United Kingdom*
- 140 *Department of Physics, Shinshu University, Nagano, Japan*
- 141 *Fachbereich Physik, Universität Siegen, Siegen, Germany*
- 142 *Department of Physics, Simon Fraser University, Burnaby BC, Canada*
- 143 *SLAC National Accelerator Laboratory, Stanford CA, United States of America*
- 144 (a) *Faculty of Mathematics, Physics & Informatics, Comenius University, Bratislava;* (b) *Department of Subnuclear Physics, Institute of Experimental Physics of the Slovak Academy of Sciences, Kosice, Slovak Republic*
- 145 (a) *Department of Physics, University of Cape Town, Cape Town;* (b) *Department of Physics, University of Johannesburg, Johannesburg;* (c) *School of Physics, University of the Witwatersrand, Johannesburg, South Africa*
- 146 (a) *Department of Physics, Stockholm University;* (b) *The Oskar Klein Centre, Stockholm, Sweden*
- 147 *Physics Department, Royal Institute of Technology, Stockholm, Sweden*
- 148 *Departments of Physics & Astronomy and Chemistry, Stony Brook University, Stony Brook NY, United States of America*
- 149 *Department of Physics and Astronomy, University of Sussex, Brighton, United Kingdom*
- 150 *School of Physics, University of Sydney, Sydney, Australia*
- 151 *Institute of Physics, Academia Sinica, Taipei, Taiwan*
- 152 *Department of Physics, Technion: Israel Institute of Technology, Haifa, Israel*
- 153 *Raymond and Beverly Sackler School of Physics and Astronomy, Tel Aviv University, Tel Aviv, Israel*
- 154 *Department of Physics, Aristotle University of Thessaloniki, Thessaloniki, Greece*
- 155 *International Center for Elementary Particle Physics and Department of Physics, The University of Tokyo, Tokyo, Japan*
- 156 *Graduate School of Science and Technology, Tokyo Metropolitan University, Tokyo, Japan*
- 157 *Department of Physics, Tokyo Institute of Technology, Tokyo, Japan*
- 158 *Department of Physics, University of Toronto, Toronto ON, Canada*
- 159 (a) *TRIUMF, Vancouver BC;* (b) *Department of Physics and Astronomy, York University, Toronto ON, Canada*
- 160 *Faculty of Pure and Applied Sciences, University of Tsukuba, Tsukuba, Japan*
- 161 *Department of Physics and Astronomy, Tufts University, Medford MA, United States of America*
- 162 *Centro de Investigaciones, Universidad Antonio Narino, Bogota, Colombia*
- 163 *Department of Physics and Astronomy, University of California Irvine, Irvine CA, United States of America*
- 164 (a) *INFN Gruppo Collegato di Udine, Sezione di Trieste, Udine;* (b) *ICTP, Trieste;* (c) *Dipartimento di Chimica, Fisica e Ambiente, Università di Udine, Udine, Italy*
- 165 *Department of Physics, University of Illinois, Urbana IL, United States of America*
- 166 *Department of Physics and Astronomy, University of Uppsala, Uppsala, Sweden*
- 167 *Instituto de Física Corpuscular (IFIC) and Departamento de Física Atómica, Molecular y Nuclear and Departamento de Ingeniería Electrónica and Instituto de Microelectrónica de Barcelona (IMB-CNM), University of Valencia and CSIC, Valencia, Spain*
- 168 *Department of Physics, University of British Columbia, Vancouver BC, Canada*
- 169 *Department of Physics and Astronomy, University of Victoria, Victoria BC, Canada*
- 170 *Department of Physics, University of Warwick, Coventry, United Kingdom*
- 171 *Waseda University, Tokyo, Japan*

- ¹⁷² *Department of Particle Physics, The Weizmann Institute of Science, Rehovot, Israel*
- ¹⁷³ *Department of Physics, University of Wisconsin, Madison WI, United States of America*
- ¹⁷⁴ *Fakultät für Physik und Astronomie, Julius-Maximilians-Universität, Würzburg, Germany*
- ¹⁷⁵ *Fachbereich C Physik, Bergische Universität Wuppertal, Wuppertal, Germany*
- ¹⁷⁶ *Department of Physics, Yale University, New Haven CT, United States of America*
- ¹⁷⁷ *Yerevan Physics Institute, Yerevan, Armenia*
- ¹⁷⁸ *Centre de Calcul de l'Institut National de Physique Nucléaire et de Physique des Particules (IN2P3), Villeurbanne, France*
- ^a *Also at Department of Physics, King's College London, London, United Kingdom*
- ^b *Also at Institute of Physics, Azerbaijan Academy of Sciences, Baku, Azerbaijan*
- ^c *Also at Novosibirsk State University, Novosibirsk, Russia*
- ^d *Also at TRIUMF, Vancouver BC, Canada*
- ^e *Also at Department of Physics, California State University, Fresno CA, United States of America*
- ^f *Also at Department of Physics, University of Fribourg, Fribourg, Switzerland*
- ^g *Also at Departamento de Física e Astronomia, Faculdade de Ciências, Universidade do Porto, Portugal*
- ^h *Also at Tomsk State University, Tomsk, Russia*
- ⁱ *Also at CPPM, Aix-Marseille Université and CNRS/IN2P3, Marseille, France*
- ^j *Also at Università di Napoli Parthenope, Napoli, Italy*
- ^k *Also at Institute of Particle Physics (IPP), Canada*
- ^l *Also at Particle Physics Department, Rutherford Appleton Laboratory, Didcot, United Kingdom*
- ^m *Also at Department of Physics, St. Petersburg State Polytechnical University, St. Petersburg, Russia*
- ⁿ *Also at Louisiana Tech University, Ruston LA, United States of America*
- ^o *Also at Institutio Catalana de Recerca i Estudis Avancats, ICREA, Barcelona, Spain*
- ^p *Also at Graduate School of Science, Osaka University, Osaka, Japan*
- ^q *Also at Department of Physics, National Tsing Hua University, Taiwan*
- ^r *Also at Department of Physics, The University of Texas at Austin, Austin TX, United States of America*
- ^s *Also at Institute of Theoretical Physics, Ilia State University, Tbilisi, Georgia*
- ^t *Also at CERN, Geneva, Switzerland*
- ^u *Also at Georgian Technical University (GTU), Tbilisi, Georgia*
- ^v *Also at Manhattan College, New York NY, United States of America*
- ^w *Also at Hellenic Open University, Patras, Greece*
- ^x *Also at Institute of Physics, Academia Sinica, Taipei, Taiwan*
- ^y *Also at LAL, Université Paris-Sud and CNRS/IN2P3, Orsay, France*
- ^z *Also at Academia Sinica Grid Computing, Institute of Physics, Academia Sinica, Taipei, Taiwan*
- ^{aa} *Also at School of Physics, Shandong University, Shandong, China*
- ^{ab} *Also at Moscow Institute of Physics and Technology State University, Dolgoprudny, Russia*
- ^{ac} *Also at Section de Physique, Université de Genève, Geneva, Switzerland*
- ^{ad} *Also at International School for Advanced Studies (SISSA), Trieste, Italy*
- ^{ae} *Also at Department of Physics and Astronomy, University of South Carolina, Columbia SC, United States of America*
- ^{af} *Also at School of Physics and Engineering, Sun Yat-sen University, Guangzhou, China*
- ^{ag} *Also at Faculty of Physics, M.V.Lomonosov Moscow State University, Moscow, Russia*
- ^{ah} *Also at National Research Nuclear University MEPhI, Moscow, Russia*
- ^{ai} *Also at Department of Physics, Stanford University, Stanford CA, United States of America*
- ^{aj} *Also at Institute for Particle and Nuclear Physics, Wigner Research Centre for Physics, Budapest, Hungary*
- ^{ak} *Also at University of Malaya, Department of Physics, Kuala Lumpur, Malaysia*
- ^{*} *Deceased*